

Copyright
By
Thomas Henry Anderson
2007

**Fatigue Life Investigation of
Traffic Signal Mast-Arm Connection Details**

by

Thomas Henry Anderson, B.S.

Thesis

Presented to the Faculty of the Graduate School of
The University of Texas at Austin
in Partial Fulfillment
of the Requirements
for the Degree of

Master of Science in Engineering

The University of Texas at Austin

August 2007

**Fatigue Life Investigation of
Traffic Signal Mast-Arm Connection Details**

**APPROVED BY
SUPERVISING COMMITTEE:**

Karl H. Frank, Supervisor

Lance Manuel

Dedication

To my family.
Your support, prayers and encouragement made this possible.

Tot U Eer

Acknowledgements

I would like to acknowledge the following Departments of Transportation for funding this study and providing me with an opportunity to pursue my graduate education at the University of Texas: Texas, California, Pennsylvania, Wyoming, Iowa, Colorado, Minnesota, North Carolina, Wisconsin, and South Dakota.

To Dr. Karl Frank, thank you for your patience, guidance and mentoring throughout the course of my graduate education. The lessons learned from your experience are invaluable.

To Blake Stasney, Dennis Phillip, Barbara Howard and the rest of the FSEL staff, thank you for your dedication to the Ferguson family. Without your help, the research performed at this facility would not be possible.

To Craig Rios, thank you for your friendship. You were always willing to help when help was needed. I trust that your life and career will be a resounding success.

To Dr. Charles Bowen, thank you for your guidance. Without it, I would not have been here.

August 9, 2007

Abstract

Fatigue Life Investigation of Traffic Signal Mast-Arm Connection Details

Thomas Henry Anderson, M.S.E
The University of Texas at Austin, 2007

Supervisor: Karl H. Frank

This study investigated the fatigue performance of commonly used traffic signal mast-arm details. Prior research indicated that certain variables such as base plate thickness, connection weld type, external collars, and galvanizing had significant effects on the fatigue performance of traffic signal mast-arms. This study was initiated to investigate further the influence of these variables identified by previous researchers as being critical to the fatigue performance of traffic signal mast-arms as well as to investigate the fatigue performance of certain traffic signal mast-arms currently in use. A total of 20 full-size mast-arm specimens were tested for fatigue performance over the course of this project. The results indicate that increasing the base plate thickness as well as using full-penetration welded connections significantly improves the fatigue performance while galvanizing significantly decreases the fatigue performance. By using the Value Based Design Analysis Method, the external collars are also shown to improve the fatigue performance of traffic signal mast-arms. A numerical evaluation of the test data indicates that increased base plate rotational stiffness also improves the fatigue performance of traffic signal mast-arms.

Table of Contents

CHAPTER 1 INTRODUCTION	1
1.1 Background Information.....	1
1.2 Motivation for Research	2
1.3 Scope and Objectives.....	3
CHAPTER 2 TEST SETUP	5
2.1 Test Assumptions and Design.....	5
2.2 Description of Test Setup.....	7
CHAPTER 3 TRAFFIC SIGNAL MAST-ARM TEST SPECIMEN DESIGN	13
3.1 Design Variables.....	13
3.1.1 Base Plate Thickness.....	13
3.1.2 Weld Type.....	15
3.1.3 External Stiffeners	19
3.1.4 Galvanizing.....	21
3.1.5 Pole Wall Thickness	23
3.2 Traffic Signal Mast-Arm Test Specimens	23
3.2.1 Basic Test Specimen	23
3.2.2 Socketed Specimens.....	25
3.2.2.1 Standard Socketed Connection	25
3.2.2.2 California Weld Profile.....	27
3.2.3 External Collar Specimens.....	28
3.2.4 Full-Penetration Welded Specimens.....	31
3.3 Specimen Labels	33
CHAPTER 4 TESTING PROCEDURE	35
4.1 Specimen Measurement	35
4.2 Specimen Installation.....	36
4.3 Load Calculation.....	37
4.3.1 Selection of Stresses	37
4.3.2 Determining Loads.....	37

4.4	Setting Deflections.....	41
4.4.1	Static Loading	41
4.5	Dynamic Fatigue Testing.....	41
4.5.1	Testing Frequency.....	41
4.5.2	Dynamic Loading Effects	42
4.5.3	Failure	42
4.5.4	Repair of Failed Specimen.....	43
CHAPTER 5 RESULTS OF TENSILE TESTS AND CHEMISTRY ANALYSES		46
5.1	Tensile Testing.....	46
5.1.1	Testing Process	46
5.1.2	Testing Results.....	47
5.2	Chemistry Analysis.....	50
5.2.1	Analysis Procedure	50
5.2.2	Analysis Results.....	51
CHAPTER 6 FATIGUE TEST RESULTS		53
6.1	Testing Program Overview.....	53
6.2	Calculation of Reported Stresses	55
6.3	Fatigue Test Results.....	56
6.3.1	Socketed Specimens.....	56
6.3.1.1	Standard Socketed Connection	56
6.3.1.2	California Weld Profile.....	61
6.3.2	External Collar Specimens.....	63
6.3.2.1	Typical Failure of External Collar Specimens.....	64
6.3.2.2	Exception to Typical Failure of External Collar Specimens	67
6.3.3	Full-Penetration Welded Specimens.....	74
6.3.4	Run-Out Specimens	77
6.3.4.1	Standard Socketed Connection Run-Out Specimens...	78
6.3.4.2	External Collar Run-Out Specimens.....	79

CHAPTER 7 DISCUSSION OF FATIGUE TEST RESULTS	80
7.1 Influence of Design Variables	80
7.1.1 Base Plate Thickness.....	80
7.1.1.1 Standard Socketed Connection Specimens.....	80
7.1.1.2 External Collar Specimens.....	84
7.1.2 Weld Type.....	88
7.1.3 External Stiffeners	91
7.1.3.1 External Collar Specimens.....	91
7.1.3.2 Fully Effective Behavior of External Collar.....	94
CHAPTER 8 BASE PLATE STIFFNESS	98
8.1 Motivation for Numerical Evaluation.....	98
8.2 Numerical Evaluation	100
8.2.1 Further Refinement of Numerical Evaluation.....	101
8.2.2 Determination of Base Plate Rotational Stiffness.....	101
8.2.3 Base Plate Rotational Stiffness Normalization	103
8.3 Comparison with Existing Data.....	104
CHAPTER 9 CONCLUSIONS AND RECOMMENDED RESEARCH	109
9.1 Conclusions.....	109
9.2 Recommended Research.....	112
APPENDIX A MAST-ARM DEFLECTION CALCULATION EXAMPLE	114
APPENDIX B MEASURED DIMENSIONS OF TEST SPECIMENS	118
REFERENCES	123
VITA	125

List of Tables

Table 5.1 Tensile Coupon Testing Results	49
Table 5.2 Comparison of the Tensile Coupon Testing Results and the Fatigue Testing Limits	50
Table 5.3 Chemistry Analyses Results	52
Table 6.1 Fatigue Test Results.....	54
Table 7.1 Average Number of Cycles to Failure (Standard Socketed Connection Specimens)	82
Table 7.2 Average Number of Cycles to Failure (External Collar Specimens).....	86
Table 7.3 Average Number of Cycles to Failure (Different Weld Types).....	88
Table 7.4 Average Number of Cycle to Failure (External Collar Contribution).....	92
Table 8.1 High-Mast Paired Specimen Stiffness (Courtesy of Craig Rios)	99
Table 8.2 Base Plate Rotational Stiffness	102
Table 8.3 Normalized Base Plate Rotational Stiffness Data Including Concurrent High-Mast Research	106
Table 8.4 Normalized Base Plate Rotational Stiffness Data from Previous Research (Phases 1 and 2)	107
Table B.1 General Dimensions – Socketed Connections and Full-Penetration Welded Connections	118
Table B.2 General Dimensions – External Collar Connections	120

List of Figures

Figure 1.1 Type “M-2” Traffic Signal Pole with Mast-Arm (Courtesy of New York City Department of Transportation).....	2
Figure 2.1 Typical Traffic Signal Mast-Arm (Koenigs et al., 2003)	6
Figure 2.2 Simply Supported Beam Model	7
Figure 2.3 Test Setup	8
Figure 2.4 Pinned End Reaction	9
Figure 2.5 Roller End Reaction	10
Figure 3.1 Effect of Base Plate Thickness (Koenigs et al., 2003)	14
Figure 3.2 Standard Socket Welded Connection (Koenigs et al., 2003)	16
Figure 3.3 Full-Penetration Welded Connection (Koenigs et al., 2003)	17
Figure 3.4 Effect of Weld Type (Koenigs et al, 2003)	18
Figure 3.5 External Collar Connection Detail (Koenigs et al., 2003).....	20
Figure 3.6 Effect of External Collar (Koenigs et al., 2003).....	21
Figure 3.7 Effect of Galvanizing (Koenigs et al., 2003).....	22
Figure 3.8 Typical Traffic Signal Mast-Arm Test Specimen	24
Figure 3.9 End Plate Detail.....	25
Figure 3.10 Standard Socketed Connection Detail (Reproduced From Valmont Industries Manufacturing Drawings).....	26
Figure 3.11 California Weld Profile (Reproduced From Valmont Industries Manufacturing Drawings).....	28
Figure 3.12 External Collar Connection Detail (Reproduced From Valmont Industries Manufacturing Drawings).....	29
Figure 3.13 Full-Penetration Weld Detail (Reproduced From Valmont Industries Manufacturing Drawings).....	32
Figure 3.14 Full-Penetration Welded Connection (Reproduced From Valmont Industries Manufacturing Drawings).....	33
Figure 3.15 Sample Test Specimen Label	34
Figure 4.1 Determination of Moment at Critical Location	38
Figure 4.2 Calculation of Testing Loads.....	40
Figure 4.3 Fatigue Crack Propagation at Specified Point of Failure	43
Figure 4.4 Repair of Failed Specimen	44
Figure 5.1 Tensile Coupon Testing Results.....	47
Figure 5.2 Yield Strength Determination by 0.2 % Offset Method.....	48
Figure 6.1 Typical Failure of the Standard Socketed Connection	57
Figure 6.2 Detailed View of Failure Location	58
Figure 6.3 Etched Cross Section of a Standard Socketed Connection	59
Figure 6.4 Detailed View of Etched Failure Location.....	60
Figure 6.5 Standard Socketed Connection Fatigue Test Results	61
Figure 6.6 Typical Failure of the California Weld Profile Socketed Connection .62	
Figure 6.7 California Weld Profile Socketed Connection Fatigue Test Results....	63
Figure 6.8 Typical Failure of the External Collar Specimens	64
Figure 6.9 Detailed View of Failure Location	65
Figure 6.10 Etched Cross Section of an External Collar Specimen	66

Figure 6.11 Detailed View of Etched Failure Location	67
Figure 6.12 Exception to Typical Failure	68
Figure 6.13 Fatigue Crack at External Collar Maximum Dimension	69
Figure 6.14 Fatigue Crack at External Collar Minimum Dimension.....	70
Figure 6.15 Etched Cross Section of an External Collar Specimen	71
Figure 6.16 Fatigue Crack at Top of External Collar	72
Figure 6.17 Fatigue Crack Through Pole Wall.....	72
Figure 6.18 External Collar Specimens Fatigue Test Results.....	73
Figure 6.19 Typical Failure of the Full-Penetration Welded Specimens.....	74
Figure 6.20 Etched Cross Section of a Full-Penetration Welded Specimen.....	75
Figure 6.21 Detailed View of Etched Failure Location	76
Figure 6.22 Full-Penetration Welded Specimens Fatigue Test Results.....	77
Figure 6.23 Base Plate to Pole Wall Fillet Weld on Run-Out Specimen	78
Figure 6.24 Detailed View of Base Plate to Pole Wall Fillet Weld.....	79
Figure 7.1 Standard Socketed Connection Fatigue Test Results	81
Figure 7.2 Influence of Base Plate Thickness on Fatigue Performance (Standard Connection Specimens).....	84
Figure 7.3 External Collar Specimens Fatigue Test Results.....	85
Figure 7.4 Influence of Base Plate Thickness on Fatigue Performance (External Collar Specimens).....	87
Figure 7.5 Influence of Weld Type on Fatigue Performance	90
Figure 7.6 Contribution of the External Collar to Fatigue Performance	93
Figure 7.7 Additional Locations for Stress Range Calculation	95
Figure 7.8 Influence of Stress Range Calculation Location on Fatigue Category.	96
Figure 8.1 High-Mast Paired Specimen Stiffness (Courtesy of Craig Rios).....	99
Figure 8.2 High-Mast Paired Specimen Stiffness [Logarithmic Scale] (Courtesy of Craig Rios).....	100
Figure 8.3 Normalized Base Plate Rotational Stiffness.....	104
Figure 8.4 Normalized Base Plate Rotational Stiffness Including Concurrent High-Mast Research and Previous Research	108

CHAPTER 1

Introduction

This study, conducted by researchers at the University of Texas, investigated the fatigue performance of traffic signal mast-arms commonly used by Departments of Transportation throughout the United States.

1.1 BACKGROUND INFORMATION

Traffic signal mast-arms are the horizontal members of cantilevered signal support structures used extensively throughout the United States as methods of traffic control (Kaczinski et al., 1998). These types of cantilevered signal structures have been in use since the early part of the twentieth century with Union Metal supplying the first traffic mast-arm pole to Atlantic City, NJ in 1923 (Union Metal Website). New York City soon followed by installing traffic signals suspended from mast-arms, as shown in Figure 1.1, on Broadway in 1924 and 1925, soon thereafter becoming common throughout the city (New York City Website). The use of suspended traffic signals over the roadway increased after a 1960 Federal Highway Administration traffic code revision required more than one stoplight at each signaled intersection (Williams, 1995). This requirement was intended to increase safety at signaled intersections by providing at least two stoplights, thereby providing cover in the event that one of the two would stop working. More recently, the cantilevered mast-arm has become more attractive because of lower cost and increased safety on the roadway (Dexter, 2002). The single vertical supporting member increases the safety of the roadway's users by reducing the probability of collision. The overall cantilevered mast-arm structure is also more aesthetically pleasing than a cable structure or truss cantilever structure (Koenigs et al., 2003).

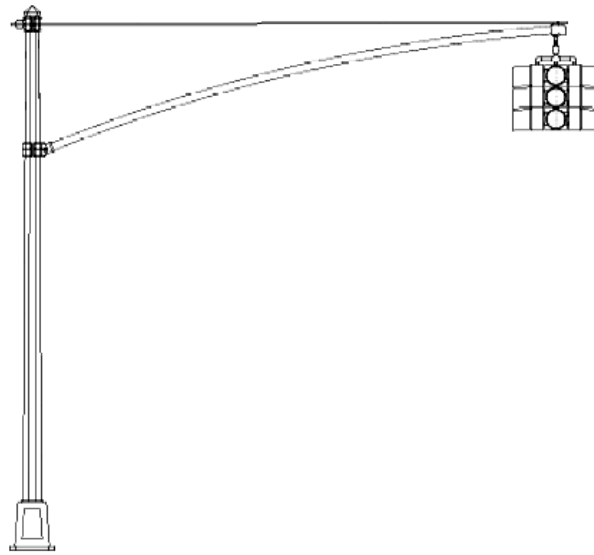


**Figure 1.1 Type “M-2” Traffic Signal Pole with Mast-Arm
(Courtesy of New York City Department of Transportation)**

1.2 MOTIVATION FOR RESEARCH

Unfortunately, the characteristics that make cantilevered mast-arms a popular choice for traffic signal supports also contributes to their susceptibility to fatigue failures. The flexibility of cantilevered mast-arm structures is quite high when compared to sign bridge support structures because of the single vertical support (Dexter, 2002). The increased flexibility combined with the low mass associated with these types of structures results in low resonant frequencies of about 1 Hz, the frequency at which the wind gust velocities often fluctuate. The damping itself is usually far less than one percent of the critical damping. The combined conditions of increased flexibility and very low damping make cantilevered mast-arm structures susceptible to large-amplitude vibration due to various wind loading phenomena (Dexter, 2002). The four types of wind loading which the cantilevered mast-arm structures are particularly susceptible to are galloping, vortex shedding, natural wind gusts, and, truck-induced wind gusts (Kaczinski et al., 1998).

Recent research conducted at the University of Texas where the effects of truck-induced wind gusts on cantilevered traffic signal mast-arm structures was evaluated, concluded that natural wind gusts were more critical than truck-induced wind gusts (Albert, 2006).

Recently, the flexibility of cantilevered mast-arm structures has been increasing due to increasing spans (Dexter, 2002). The spans have been increasing due to (1) increased setbacks of the vertical supports from the roadway for safety, and, (2) widening of roadways due to increased traffic volume. It is, therefore, not surprising that cantilevered mast-arm structures occur at nearly every modern urban intersection with three or more lanes (South, 1994). Union Metal even advertises cantilevered mast-arms of up to 85-ft in length (Union Metal Website). The increasing spans have coincided with increased instances of vibration and fatigue problems.

Even though instances of fatigue failure are relatively low when considering the number of cantilevered mast-arm structures in use across the United States, the unexpected failure of such a structure could still cause serious injury or at the very least traffic congestion. The fact that typical failures have occurred in relatively normal weather, the hazard is unexpected (Dexter, 2002). The conditions surrounding typical failures combined with the costs associated with inspection or replacement of these types of structures warrants further study to decrease the instances of fatigue failure.

1.3 SCOPE AND OBJECTIVES

This thesis presents the results of fatigue testing on traffic signal mast-arm test specimens conducted at the University of Texas at Austin. It is part of a pooled-fund sponsored study, Research Project No. 9-1526, "Investigation of the Fatigue Life of Steel Base Plate to Pole Connections for Traffic Structures." The following Departments of Transportation were the sponsors: Texas, California, Pennsylvania, Wyoming, Iowa, Colorado, Minnesota, North Carolina, Wisconsin, and South Dakota. Previous related

research upon which this project builds can be found in the Master's thesis titled "Fatigue Resistance of Traffic Signal Mast-Arm Connection Details" (Koenigs, 2003).

The primary objective of this research project is to further evaluate the fatigue performance of the connection details identified in the previous testing program conducted at the University of Texas as being improved fatigue connection details. In doing so, certain recommendations will be followed such as galvanizing all test specimens as this was identified as having a negative impact on general fatigue performance. A secondary objective is to evaluate the fatigue performance of connection details currently in use by two of the sponsoring Departments of Transportation, California and Wyoming.

The following chapters present and discuss the results of this testing program. Chapter 2 presents the test setup as well as discussing the assumptions behind the test setup. Chapter 3 discusses the mast-arm test specimen design by first presenting the variables that motivated the designs and then describing the designs. The testing procedure is described in Chapter 4. Material testing in the form of tensile tests and chemistry analyses is presented in Chapter 5. The fatigue test results are presented in Chapter 6 and discussed in detail in Chapter 7. Chapter 8 introduces a relationship between base plate connection stiffness and fatigue life while Chapter 9, the final chapter, presents the general conclusions from the test results as well as further recommended research.

CHAPTER 2

Test Setup

The testing was accomplished using a test setup developed in previous research on the fatigue of mast-arms. Minor adjustments were made to enhance the performance and operation of the test.

2.1 TEST ASSUMPTIONS AND DESIGN

A traffic signal mast-arm is essentially a cantilevered beam with a tapered cross-section. Several point and distributed loads (traffic signals and signs) are applied along the length. A typical traffic signal mast-arm with varied loading is shown in Figure 2.1. Regardless of the exact position and magnitude of the applied loads, the moment diagram for the traffic signal mast-arm can be approximated as increasing from zero at the free-end to its maximum value at the fixed-end. This is similar to the moment diagram for a cantilevered beam with a point load applied at the free-end. The assumption that typical traffic signal mast-arm loading can be approximated as a cantilevered beam with a point load applied at the free-end was used by previous researchers to transform the service loading into a simple testing apparatus. The decision was made to place two traffic signal mast-arm specimens with the critical connections back to back and model the resulting structure as a simply supported beam. The simply supported beam model is shown in Figure 2.2. The load would be applied at the center of the structure and the resulting moment diagram for each individual traffic signal mast-arm specimen would resemble that of the cantilevered beam with a point load applied at the free-end. This simply supported beam analogy allowed for a very simple test setup design.



Figure 2.1 Typical Traffic Signal Mast-Arm (Koenigs et al., 2003)

The test setup was designed so that the end reactions would remain in tension for all tests. This decision was made by the previous researchers to ensure that the test setup simulated in-service conditions with a nominal dead load stress of approximately 20 ksi at the top of the connection of the mast-arm to the vertical mast and the live load stress producing fluctuation about the dead load stress. Also, having the test setup in tension eliminates the need for lateral stability as the loading would occur in a single vertical plane.

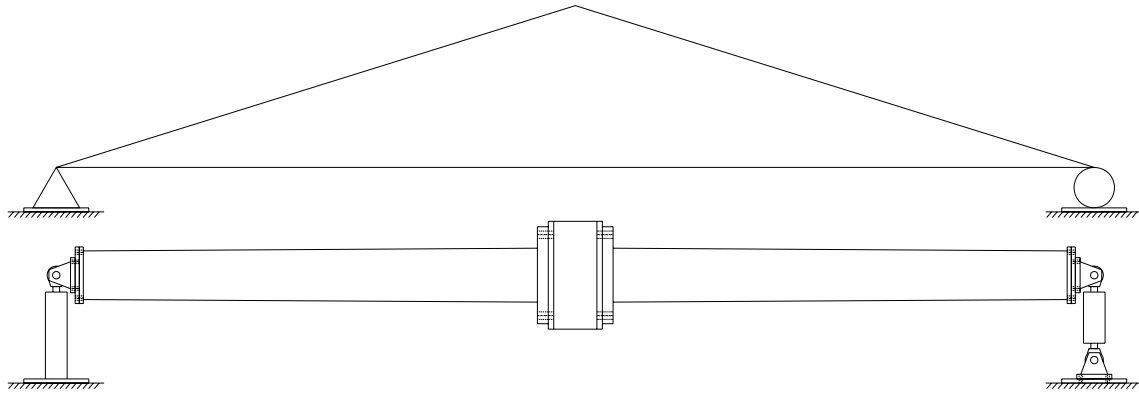


Figure 2.2 Simply Supported Beam Model

The previous researchers chose the total length of the test setup to be 16-ft to fit the test floor hole spacing of 4-ft on center. This set the individual specimen length to approximately 87-in. The total test setup length was chosen to both align the test setup end reactions with the available anchorage points on the laboratory reaction floor and to ensure that the desired stress levels and stress ranges, which depend on the force applied, could be achieved without exceeding the capabilities of the MTS hydraulic actuator.

2.2 DESCRIPTION OF TEST SETUP

The test setup used for testing can be seen in Figure 2.3. At the center of the figure, the yellow loading box can be seen. The loading box was used to connect the traffic signal mast-arm specimens to each other to form the simply supported beam and also to connect the beam to the MTS hydraulic actuator which applied the load. The MTS hydraulic actuator was hung vertically from a standard test frame and connected to the top side of the loading box. The MTS hydraulic actuator was connected to both the standard test frame and the loading box by means of spherical ball joint clevises. This allowed for slight imperfections in alignment and irregularities, if any, in the straightness of the traffic signal mast-arm specimens.



Figure 2.3 Test Setup

At either end of the traffic signal mast-arm specimens in the figure, the red end reactions can be seen. These end reactions represent the simply supported conditions of the simply supported beam analogy and can be seen in more detail in Figure 2.4 and Figure 2.5.

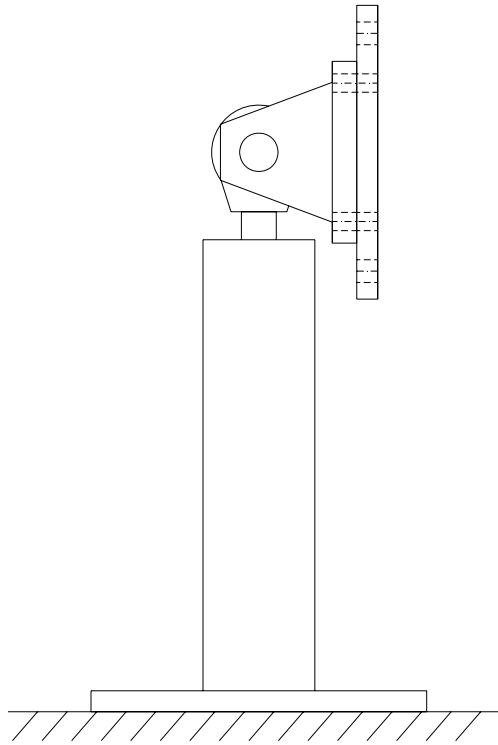


Figure 2.4 Pinned End Reaction

The end reaction in Figure 2.4 reproduced the behavior of a pinned end connection and consisted of a single spherical rod eye and clevis fixture connecting the top end of the end reaction to the traffic signal mast-arm specimen and a solid tubular section connecting the bottom end of the end reaction to the laboratory reaction floor.

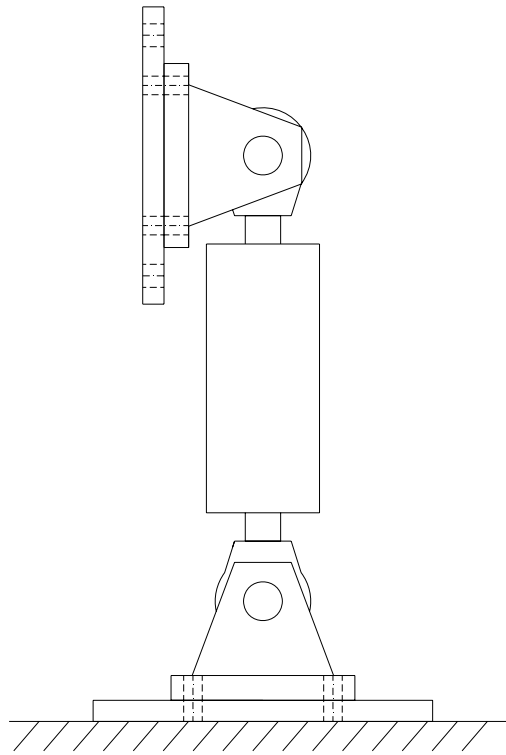


Figure 2.5 Roller End Reaction

The end reaction in Figure 2.5 reproduced the behavior of a roller connection and consisted of two spherical rod eye and clevis fixtures connecting both the top and bottom ends of the end reaction to the traffic signal mast-arm specimen and the laboratory reaction floor respectively. The spherical rod eye and clevis fixtures allowed for slight imperfections in alignment as the spherical ball joint clevises had done for the MTS hydraulic actuator connections. The end reaction that reproduced the behavior of a roller connection allowed for displacements along the longitudinal axis of the test setup, which eliminated potential axial loads in the traffic signal mast-arm test specimens as well as facilitated in their installation during testing.

Hydraulic pressure was supplied by an external pump supplying a constant pressure of 3000 psi. A MTS 293 Hydraulic Service Manifold was used to control the

hydraulic oil supply, filter the oil, and through the use of accumulators reduce the pressure pulses in the oil supply. The MTS hydraulic actuator was controlled by an MTS FlexTest SE Controller.

Each traffic signal mast-arm specimen was connected to the loading box by four 1.5-in diameter threaded rods. The threaded rod was sized to replicate the bolt size typically used by the Texas Department of Transportation (TXDOT). The choice was made to deviate from what was done by previous researchers and forgo extending the threaded rods through the loading box. Instead, each traffic signal mast-arm specimen was individually attached to the loading box. This was done to ease the process of installing the traffic signal mast-arm test specimens as well as allowing for one traffic signal mast-arm specimen to be removed without having to loosen both. The issue of pretensioning the loading box by extending the threaded rods through the loading box was not considered as being critical. Also, since the level of tightening of the threaded rods would not significantly vary from having shorter threaded rods, the fatigue of the threaded rods themselves was not considered to be critical since the threaded rods used by previous researchers performed well. This was again verified as the same eight threaded rods were used throughout the duration of this project without any fatigue failure.

As was done by the previous researchers, washers were placed on the threaded rods between the loading box and the base plates of the traffic signal mast-arm specimens. This was done to provide known locations of fixity and force transfer between the loading box and the traffic signal mast-arm specimens. Additionally, this prevented any prying of the traffic signal mast-arm specimens' base plates onto the loading box by allowing for any out of flatness of the plates. To allow for variable lengths in the traffic

signal mast-arm specimens, washers would be added as needed between the traffic signal mast-arm specimen end reaction plate and the top end of the end reaction.

CHAPTER 3

Traffic Signal Mast-Arm Test Specimen Design

The designs of the traffic signal mast-arm specimens tested over the course of this project were guided by the need to, (1) investigate further the influence of certain variables identified by previous research as being critical to improving the fatigue performance of traffic signal mast-arm structures, and, (2) to investigate the fatigue performance of certain traffic signal mast-arm structures currently in use. In doing so, the designs of the traffic signal mast-arm test specimens followed what was being done in current practice.

3.1 DESIGN VARIABLES

3.1.1 Base Plate Thickness

During the first phase of testing of an earlier study conducted by researchers at the University of Texas, it was noticed that the traffic signal mast-arm specimens tested exhibited noticeably poorer fatigue performance than specimens previously tested under other studies (Koenigs et al., 2003). In comparing the specimens from the first phase of testing to those of the other studies, one noticeable difference was observed; the thickness of the base plates being used varied. This observation motivated the researchers to further investigate the influence of the thickness of the base plate on the fatigue performance of traffic signal mast-arm structures by including specimens with thicker base plates in a second phase of testing. The traffic signal mast-arm test specimens tested in the first phase all had a uniform base plate thickness of 1.5-in. In order to examine the influence of base plate thickness in the second phase of testing, two traffic signal mast-arm specimens with 2-in thick base plates were included.

The two traffic signal mast-arm specimens with 2-in thick base plates exhibited a dramatic improvement in fatigue performance over those with 1.5-in thick base plates. This improvement is shown graphically in Figure 3.1. This was surprising as the base plate thickness was not recognized in the fatigue design provisions as a variable that affected the fatigue performance of traffic signal mast-arm structures. As a result, the researchers suggested that further research be done to attempt to fully understand the significance of minor geometrical changes such as the base plate thickness.

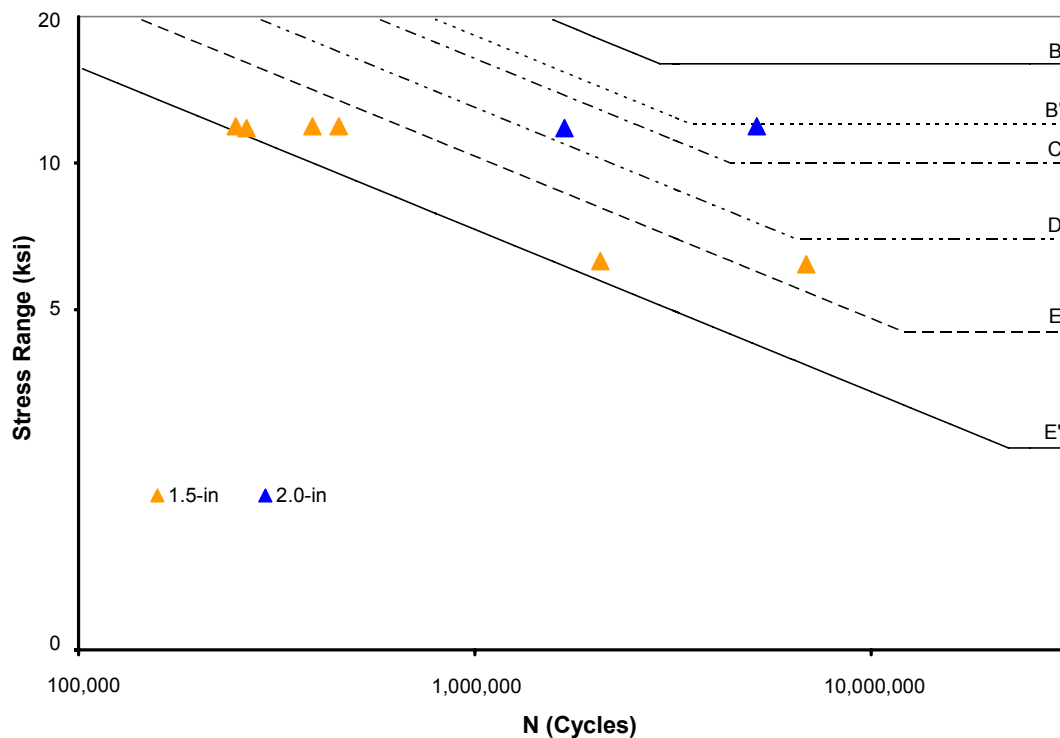


Figure 3.1 Effect of Base Plate Thickness (Koenigs et al., 2003)

In an attempt to determine the effect that varying the base plate thickness had on the fatigue performance of traffic signal mast-arm structures, a parametric finite element study was undertaken by researchers at the University of Texas. Geometric variables

considered in the parametric finite element study included: (1) base plate thickness, (2) mast-arm diameter, (3) mast-arm wall thickness, and, (4) weld geometry. It was decided to investigate what effect, if any, these geometric variables had on the stress concentration factor (SCF) at the weld toe, the location of where failures were typically observed both in the laboratory and in service. For a traffic signal mast-arm specimen with an 11-in outside diameter and a wall thickness of 0.239-in, the base plate thickness was varied from 1-in to 3-in. It was determined that increasing the base plate thickness from 1-in to 1.5-in reduced the SCF by 20% while increasing the base plate thickness from 1-in to 3-in reduced the SCF by 35% (Koenigs et al., 2003). These results obtained by the parametric finite element study provided an explanation for the fatigue behavior observed.

It was with these observations and results in mind that the decision was made to vary the base plate thicknesses of the traffic signal mast-arm specimens being tested over the course of this project. In order to compare the results that would be obtained over the course of this project with the results obtained in the earlier study conducted at the University of Texas, it was decided that three different base plate thicknesses would be used. The three different base plate thicknesses were specified as 1.75-in, 2-in, and, 3-in.

3.1.2 Weld Type

A variation of weld types was not included in the first phase of testing of the earlier study at the University of Texas. This was done because the type of weld used to attach the pole section to the base plate of a traffic signal mast-arm structure was not initially considered as being critical to the fatigue performance of those types of structures. A socket welded connection was therefore used on all the traffic signal mast-arm specimens tested in the first phase. The socket welded connection used was based on a standard design provided by Valmont Industries and can be seen in Figure 3.2.

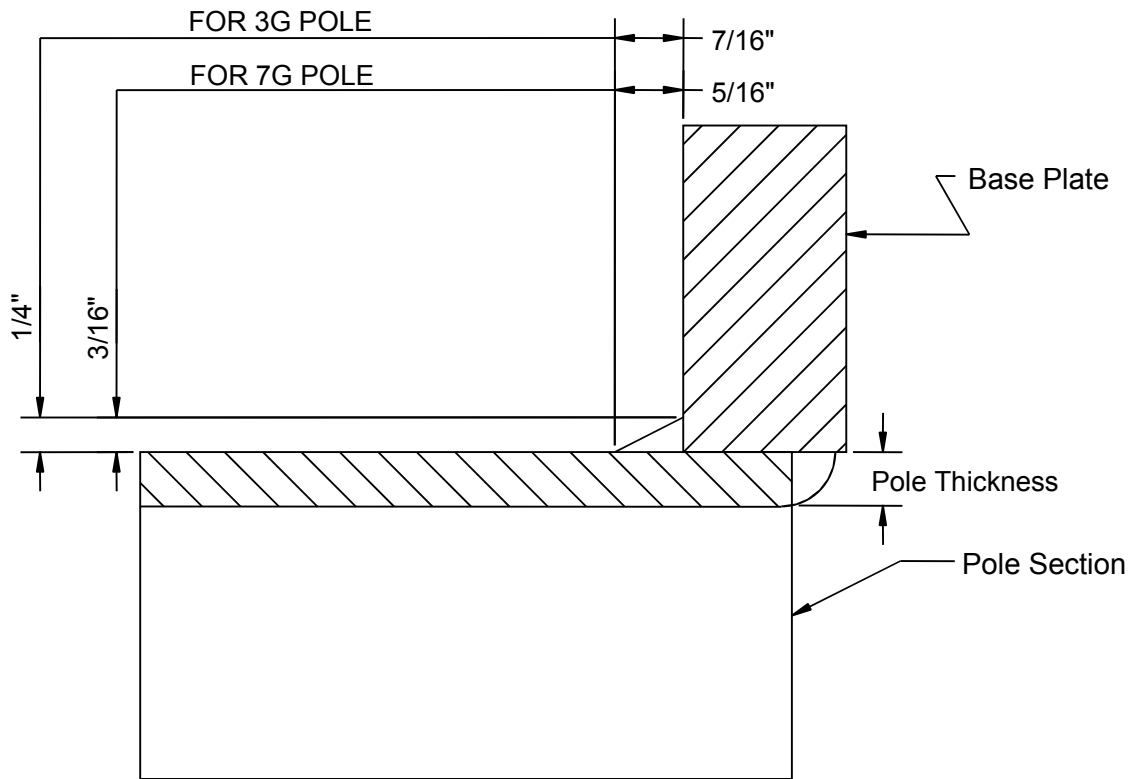


Figure 3.2 Standard Socket Welded Connection (Koenigs et al., 2003)

In the second phase of testing of the earlier study conducted by researchers at the University of Texas, it was suggested that it might be useful to test a full-penetration welded connection. This was done to verify that the extra cost and labor associated with utilizing a full-penetration welded connection was in fact unnecessary since the fatigue provisions of the 2001 AASHTO Highway Signs, Luminaires and Traffic Signal Specifications classified the full-penetration welded connection as a category E' detail, the same category used to classify the socket welded connection. The design for the full-penetration welded connection used for the two traffic signal mast-arm test specimens tested in the second phase is shown in Figure 3.3

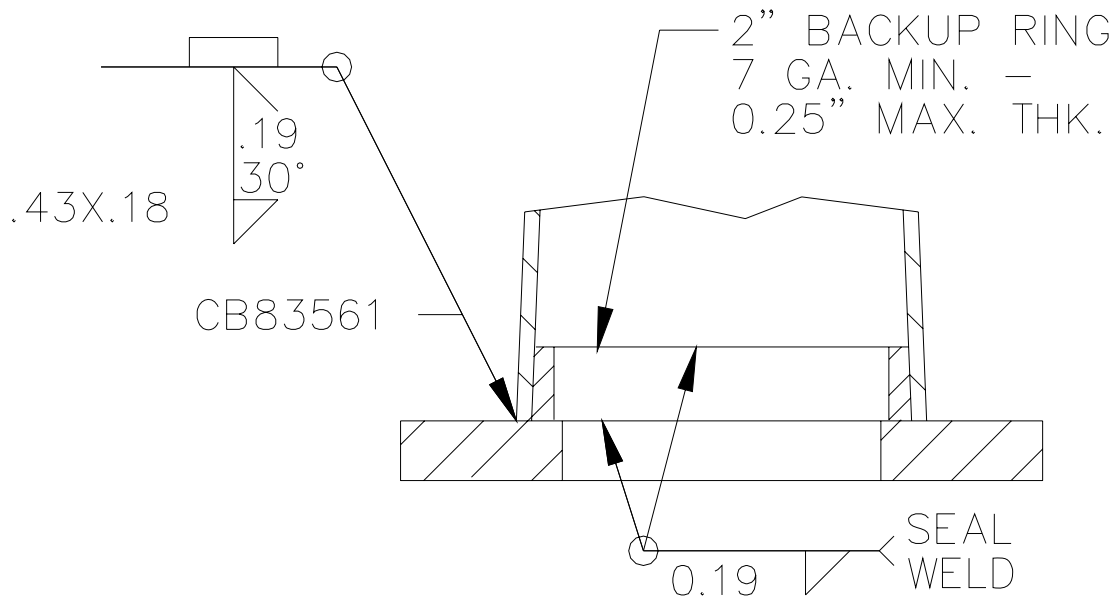


Figure 3.3 Full-Penetration Welded Connection (Koenigs et al., 2003)

The two traffic signal mast-arm specimens with the full-penetration welded connection tested exhibited a dramatic improvement in fatigue performance over those with the standard socket welded connection. This improvement is shown graphically in Figure 3.4. The two full-penetration welded specimens reached fatigue category D. This was very surprising as the fatigue design provisions classified the full-penetration welded connection in the same category used to classify the socket welded connection, category E'.

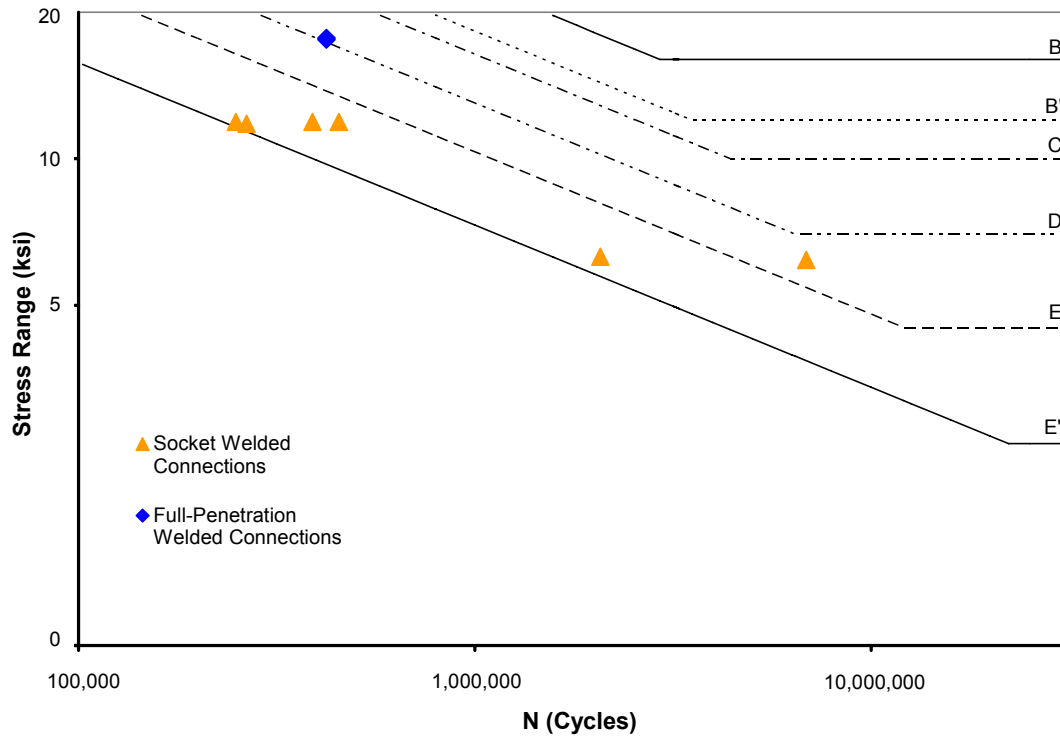


Figure 3.4 Effect of Weld Type (Koenigs et al, 2003)

Based on the results obtained by researchers at the University of Texas, three weld types were chosen for comparison over the course of this project. The three weld types were, (1) a standard socket welded connection, (2) a full-penetration welded connection, and, (3) a California socket welded connection. It was decided to specify the standard socket welded connection on a number of traffic signal mast-arm specimens. This provided a control connection detail for this project, allowed for direct comparison with the results obtained in the earlier study by researchers at the University of Texas, and provided a constant variable when other geometric properties were being studied. The full-penetration welded connection was specified to accomplish two objectives; (1) to confirm that a full-penetration welded connection would improve the fatigue performance of traffic signal mast-arm structures, as was shown by the earlier study, and,

(2) to provide an opportunity to investigate the fatigue performance of traffic signal mast-arm connections currently being used in the state of Wyoming. The California socket welded connection was also specified to accomplish two objectives; (1) to investigate whether or not a different weld profile on a socket welded connection would influence the fatigue performance of that type of connection, and, (2) to provide an opportunity to investigate the fatigue performance of traffic signal mast-arm connections currently being used in the state of California.

3.1.3 External Stiffeners

The influence that the use of external stiffeners had on the fatigue performance of traffic signal mast-arm structures was extensively studied during both phases of testing of the earlier study conducted by researchers at the University of Texas. In order to investigate the case of having a large number of stiffeners evenly distributed around the circumference of the traffic signal mast-arm, an external collar detail was tested. The external collar detail tested is shown in Figure 3.5.

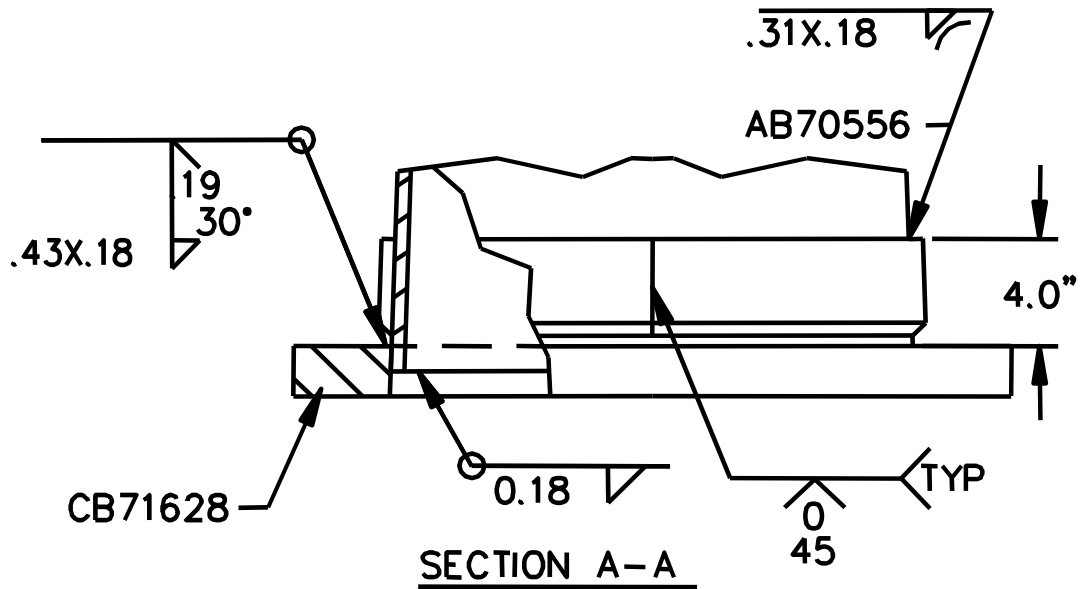


Figure 3.5 External Collar Connection Detail (Koenigs et al., 2003)

The two traffic signal mast-arm specimens with the external collar connection tested exhibited a dramatic improvement in fatigue performance over those with the standard socket welded connection (Koenigs et al., 2003). This became particularly evident when the Value Based Design Analysis Method was used to compare the fatigue performance of the external collar specimens to that of the standard socket welded specimens. The improvement in fatigue performance is shown in Figure 3.6.

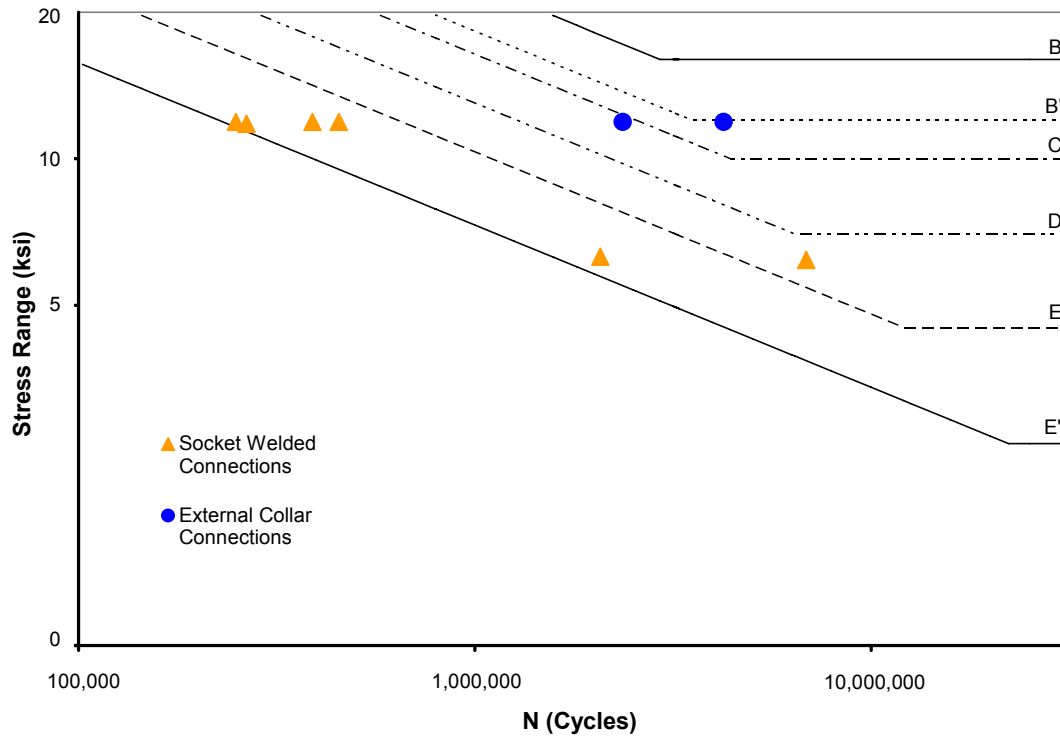


Figure 3.6 Effect of External Collar (Koenigs et al., 2003)

Based on the improvement in fatigue performance exhibited by the two traffic signal mast-arm specimens with the external collar connection, it was decided that further study was warranted. Two pairs of traffic signal mast-arm specimens with an external collar connection were specified for testing over the course of this project.

3.1.4 Galvanizing

During the first phase of testing by researchers at the University of Texas, the question of whether or not galvanizing had an effect on the fatigue performance of traffic signal mast-arm structures was raised. The issue of galvanizing was considered because the majority of traffic signal structures in use were galvanized and all the traffic signal

mast-arm specimens tested in phase one were not galvanized. The decision was made to include galvanizing as a variable in the second phase of testing.

The fatigue performance of the galvanized traffic signal mast-arm socket welded specimens tested in the second phase was exceptionally poor (Koenigs et al., 2003). This indicated that galvanizing had a negative effect on the fatigue performance of traffic signal mast-arm structures. This negative effect can be seen in Figure 3.7.

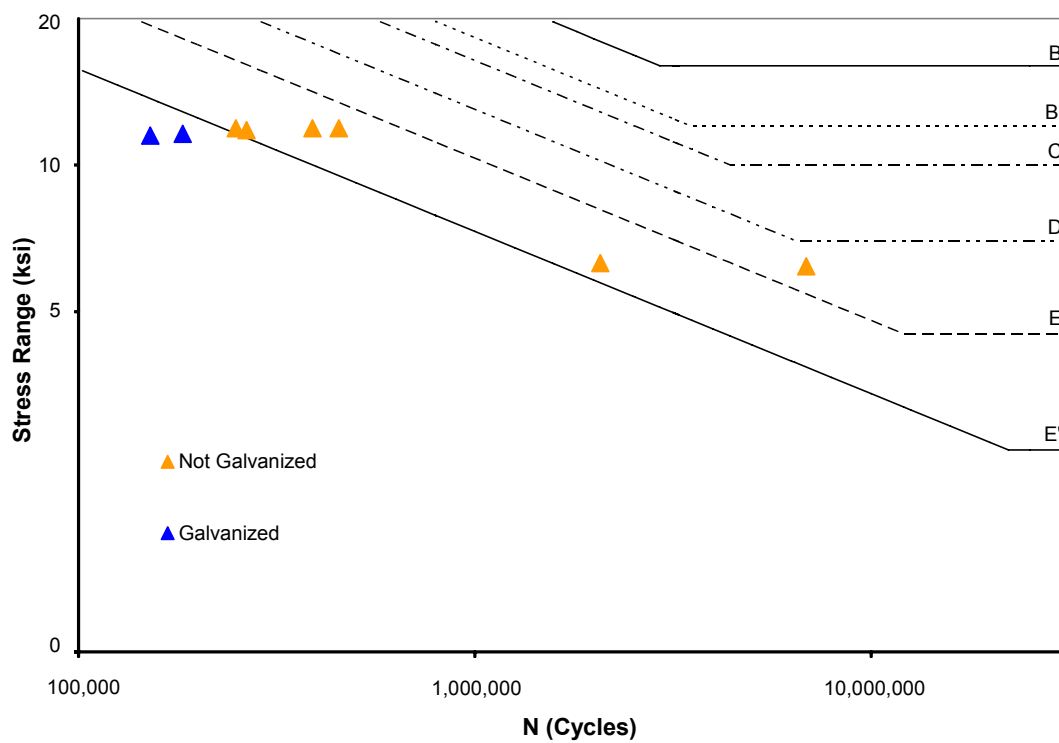


Figure 3.7 Effect of Galvanizing (Koenigs et al., 2003)

As a result of the poor fatigue performance of the galvanized traffic signal mast-arm specimens tested by researchers at the University of Texas, it was decided that all traffic signal mast-arm specimens tested over the course of this project should be

galvanized. This was done to better simulate the fatigue performance of traffic signal structures currently in use and to provide more conservative results.

3.1.5 Pole Wall Thickness

Pole wall thickness was introduced as a variable in the earlier study conducted at the University of Texas. Several specimens were replicated with pole wall thicknesses of 0.1793-in (7 gauge) and 0.2391-in (3 gauge). In comparing the fatigue test results of the two groups of specimens with different pole wall thicknesses, the researchers concluded that the pole wall thickness had no significant effect on the fatigue performance (Koenigs et al., 2003). It was with the results of the earlier study in mind, and, the desire to avoid introducing another geometric variable, that a constant pole wall thickness of 0.1793-in was chosen for all the traffic signal mast-arm specimens tested over the course of this project. It is also important to note that a pole wall of 0.1793-in is a typical thickness used for traffic signal mast-arms with outside diameters of 10-in or less.

3.2 TRAFFIC SIGNAL MAST-ARM TEST SPECIMENS

3.2.1 Basic Test Specimen

As was discussed in Chapter 2, the length of each individual traffic signal mast-arm test specimen was determined by the overall dimensions of the test setup. The length was chosen to enable adequate testing speed with desirable load ranges. The overall length of each traffic signal mast-arm test specimen was set at 86.75-in or 7-ft 2.75-in. A typical traffic signal mast-arm test specimen is shown in Figure 3.8. It is important to note that regardless of the base plate thickness or the base plate to pole wall connection type used, each traffic signal mast-arm specimen was specified with a 10-in outside diameter at the base plate to pole wall connection. The pole wall thickness for all specimens was set at 0.1793-in. The taper was set at 0.14-in per foot of length, which is

typical for traffic signal structures. A standard base plate and bolt detail was used for all specimens. The overall dimensions for the base plate specified were based on a typical design utilized by the Texas Department of Transportation (TXDOT). However, for some specimens, the base plate thickness was varied. The end plate used to attach the traffic signal mast-arm test specimen to each of the test setup end reactions is shown in Figure 3.9.

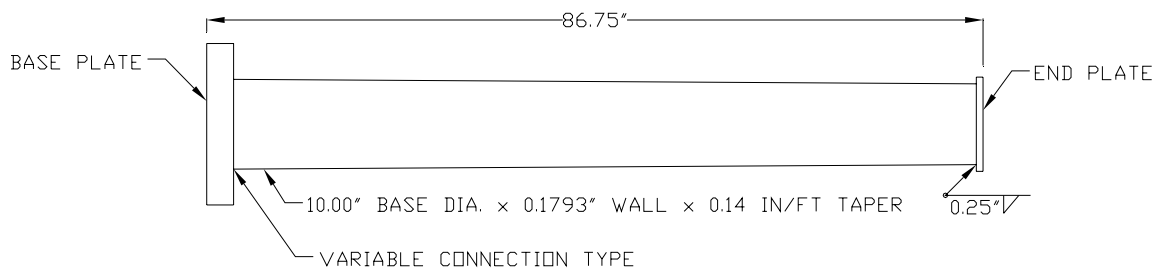


Figure 3.8 Typical Traffic Signal Mast-Arm Test Specimen

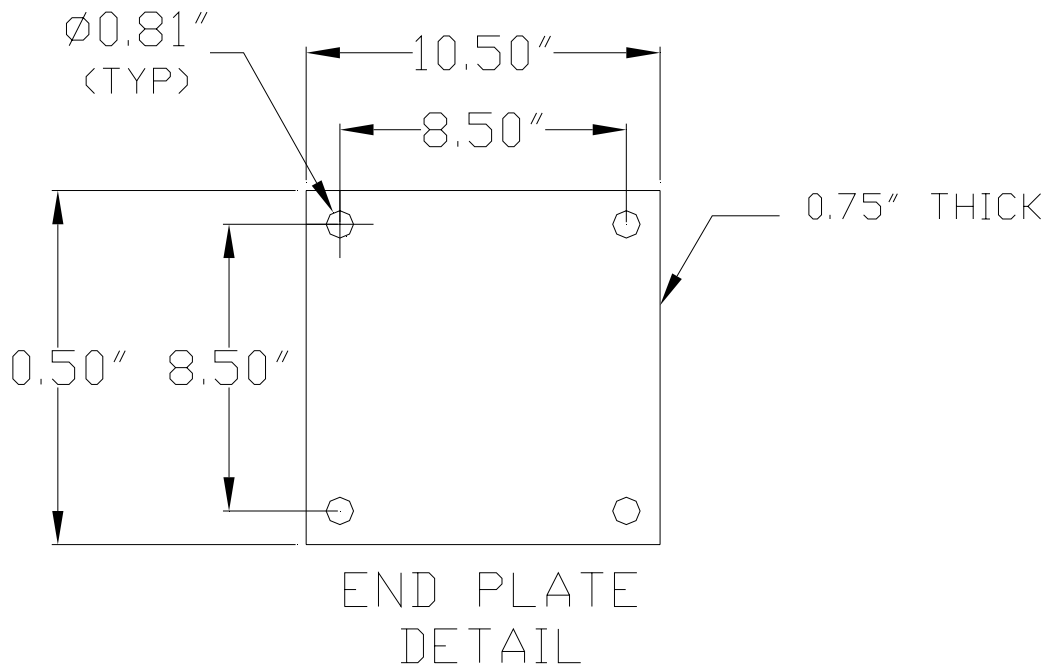


Figure 3.9 End Plate Detail

3.2.2 Socketed Specimens

A socketed connection refers to a connection type where a hole is cut into the base plate and the pole section is inserted into the hole. Fillet welds are then made around the outside of the pole where the pole intersects with the base plate and around the inside of the hole where the pole section ends. Two socketed connections were included in this testing program.

3.2.2.1 Standard Socketed Connection

The fillet weld specified for the standard socket welded traffic signal mast-arm test specimens was based on the standard Valmont Industries design utilized by TXDOT. The fillet weld utilized by Valmont Industries is an unequal leg fillet weld with the long leg along the pole wall and is sized based on the pole wall thickness of the traffic signal

mast-arm; this is shown in Figure 3.2. Three pairs of standard socket welded traffic signal mast-arm test specimens were initially specified for testing over the course of this project. Each pair had a different base plate thickness; 1.75-in, 2-in, and 3-in. A fourth pair with a base plate thickness of 2-in was later specified after the first pair with a base plate thickness of 2-in was suspected of damage before testing had taken place. The manufacturing drawing for the socket welded traffic signal mast-arm test specimens with 2-in thick base plates is shown in Figure 3.10. The other socketed specimens were identical except for the base plate thicknesses.

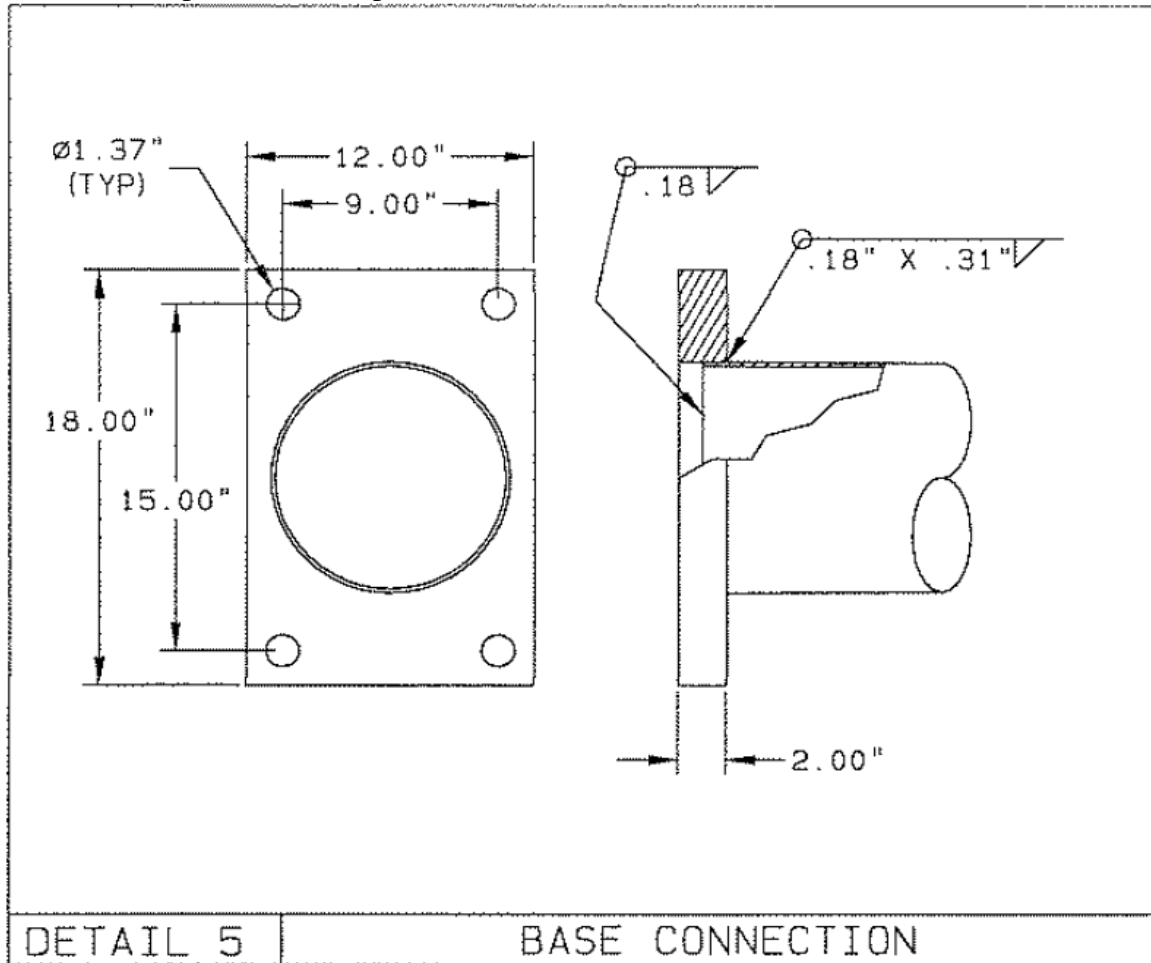


**Figure 3.10 Standard Socketed Connection Detail
(Reproduced From Valmont Industries Manufacturing Drawings)**

3.2.2.2 California Weld Profile

The fillet weld specified for the California socket welded traffic signal mast-arm test specimens was based on a standard design specified by the California Department of Transportation (CALTRANS). The fillet weld specified by CALTRANS is an unequal leg fillet weld with the long leg along the pole wall and is shown in Figure 3.11. It is important to note that both a throat dimension of 0.18-in (3/16-in) and a maximum contact angle of 30° for the long leg of the fillet weld are specified. One pair of California socket welded traffic signal mast-arm test specimens was tested with a base plate thickness of 2-in.

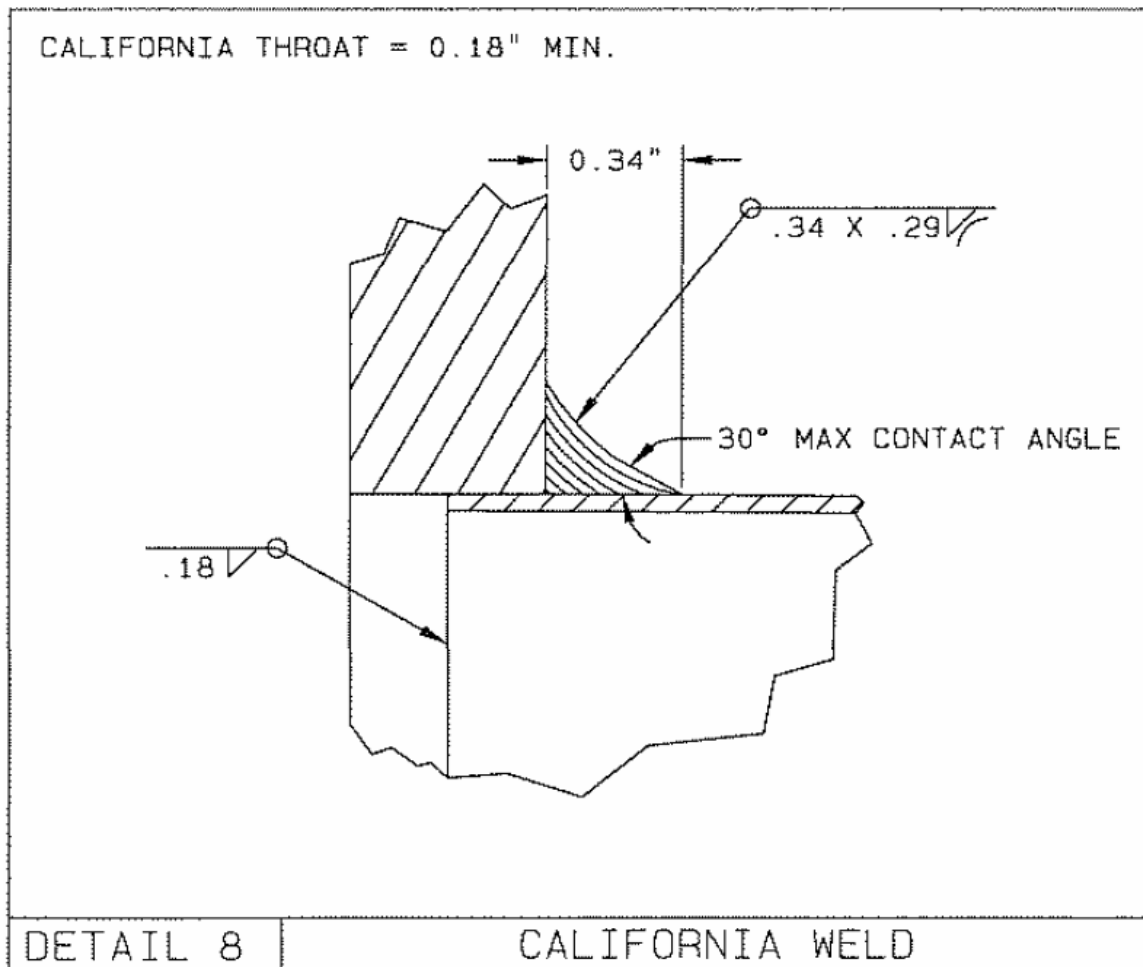
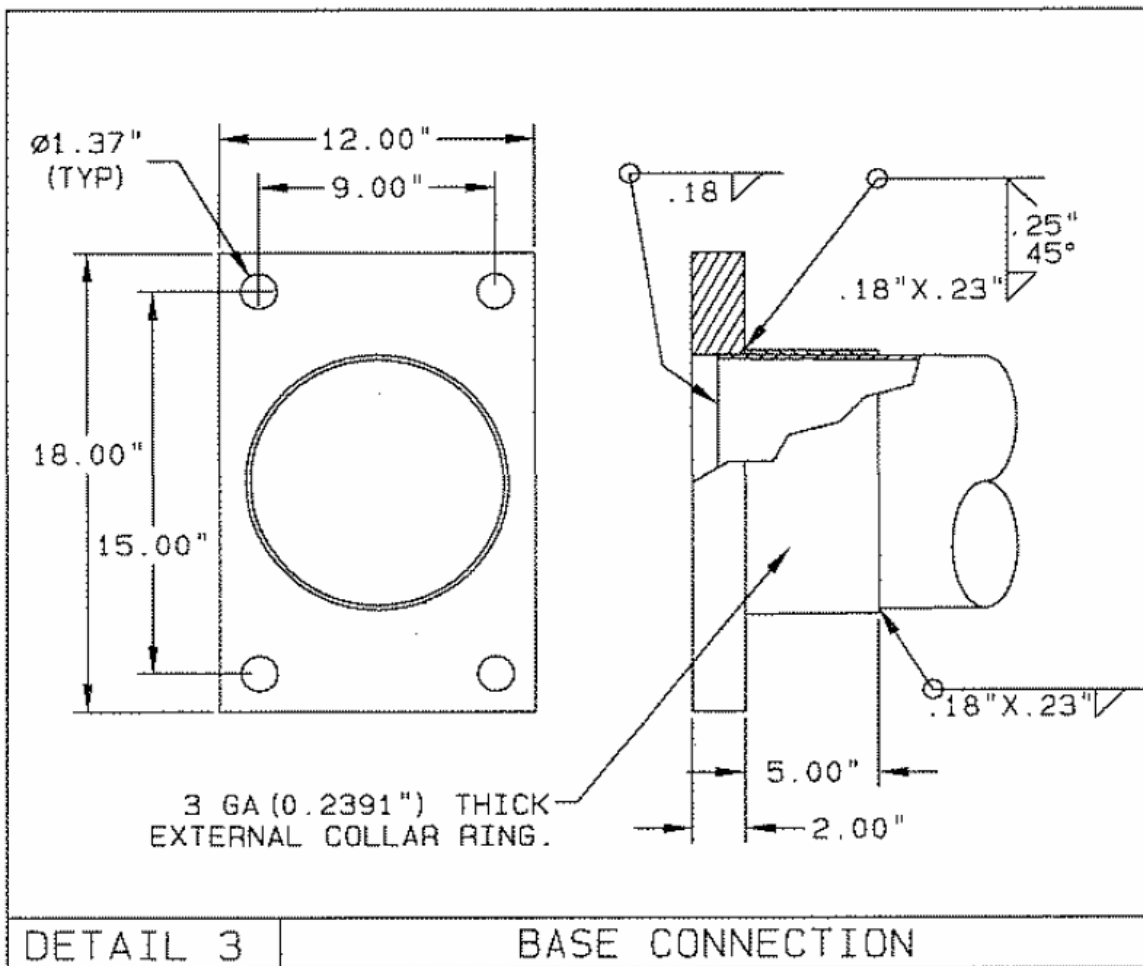


Figure 3.11 California Weld Profile
(Reproduced From Valmont Industries Manufacturing Drawings)

3.2.3 External Collar Specimens

The external collar connection is essentially a socket welded connection with an external ring around the portion of the traffic signal mast-arm pole section intersecting with the base plate. The external ring or collar is then welded to the pole section as well as to the base plate. The manufacturing drawing can be shown in Figure 3.12. The end of the external collar is welded to the traffic signal mast-arm pole section with an unequal

leg fillet weld with the long leg along the pole wall. The other end of the external collar is welded to both the base plate and the pole wall. This is achieved by beveling the external collar with a 45° bevel, making a groove weld, and then finishing with an unequal leg reinforcing weld. The long leg of the unequal leg reinforcing weld is along the external collar. The weld sizes and external collar thicknesses were determined by the manufacturer.



**Figure 3.12 External Collar Connection Detail
(Reproduced From Valmont Industries Manufacturing Drawings)**

The external collar length along the pole section was specified as half the outside diameter of the base section of the traffic signal mast-arm test specimens or 5-in. Two base plate thicknesses were specified for the two initial pairs of external collar connection traffic signal mast-arm test specimens tested over the course of this project. One pair of traffic signal mast-arm test specimens was specified with a base plate thickness of 1.75-in. The second pair of traffic signal mast-arm test specimens was specified with a base plate thickness of 2-in. The thickness of the external collar was specified by the manufacturer as 0.2391-in (3 gauge). Both sets of external collar connection traffic signal mast-arm test specimens were specified with the same weld dimensions.

In addition to the two initial pairs of external collar traffic signal mast-arm test specimens, two replicate pairs were provided by the manufacturer. The manufacturer suspected that there were possible defects in the welds of the first pair of external collar test specimens and subsequently, two additional pairs of test specimens were provided. In total, four pairs of external collar traffic signal mast-arm test specimens were tested over the course of this project.

It was initially intended that the end of the external collar that is fillet welded to the traffic signal mast-arm pole section be straight as is shown in Figure 3.12. However, Carl Macchietto from Valmont Industries suggested that instead of using a straight edge a scalloped edge should be used. A scalloped edge has a series of curved projections along the circumference of the external collar. Macchietto suggested that this change would reduce the stress concentrations at the external collar to pole wall connection and thereby improve the fatigue performance of the traffic signal mast-arm. All the external collar connection traffic signal mast-arm test specimens tested over the course of this project had external collars with scalloped edges.

3.2.4 Full-Penetration Welded Specimens

Two full-penetration welded traffic signal mast-arm test specimens were tested. The weld design was based on a standard design specified by the Wyoming Department of Transportation (WYDOT). The full-penetration weld specified by WYDOT is shown in detail in Figure 3.13. The traffic signal mast-arm pole section along with the backing bar is butted up against the base plate. A 0.25-in fillet weld attaches the backing bar to the base plate before the full-penetration weld is made to attach the pole section to the base plate. The short dimension of the full-penetration weld along the base plate is specified as being equal to the pole wall thickness, 0.1793-in, while the long dimension of the full-penetration weld along the pole wall is specified as being equal to the pole wall thickness plus 0.44-in or 0.62-in. The backing bar is specified with a maximum thickness of 0.375-in. A backing bar thickness equal to the pole wall thickness was used.

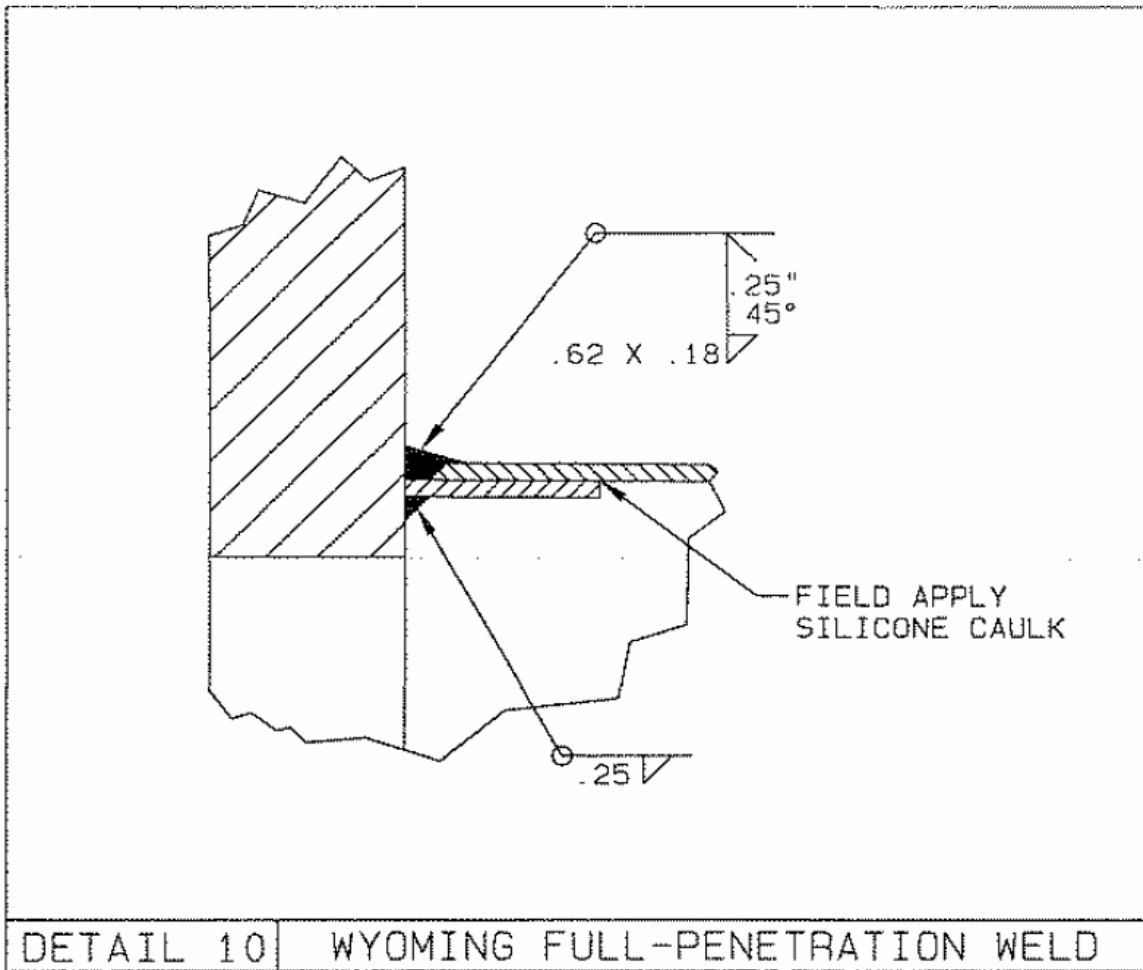


**Figure 3.13 Full-Penetration Weld Detail
(Reproduced From Valmont Industries Manufacturing Drawings)**

A base plate thickness of 2-in was chosen for the pair of full-penetration welded test specimens tested. It is important to note that the diameter of the hole in the base plate where the pole section attaches to the base plate was specified as being 2-in smaller than the inside diameter of the traffic signal mast-arm pole section at the pole wall to base plate connection. This can be seen in Figure 3.14.

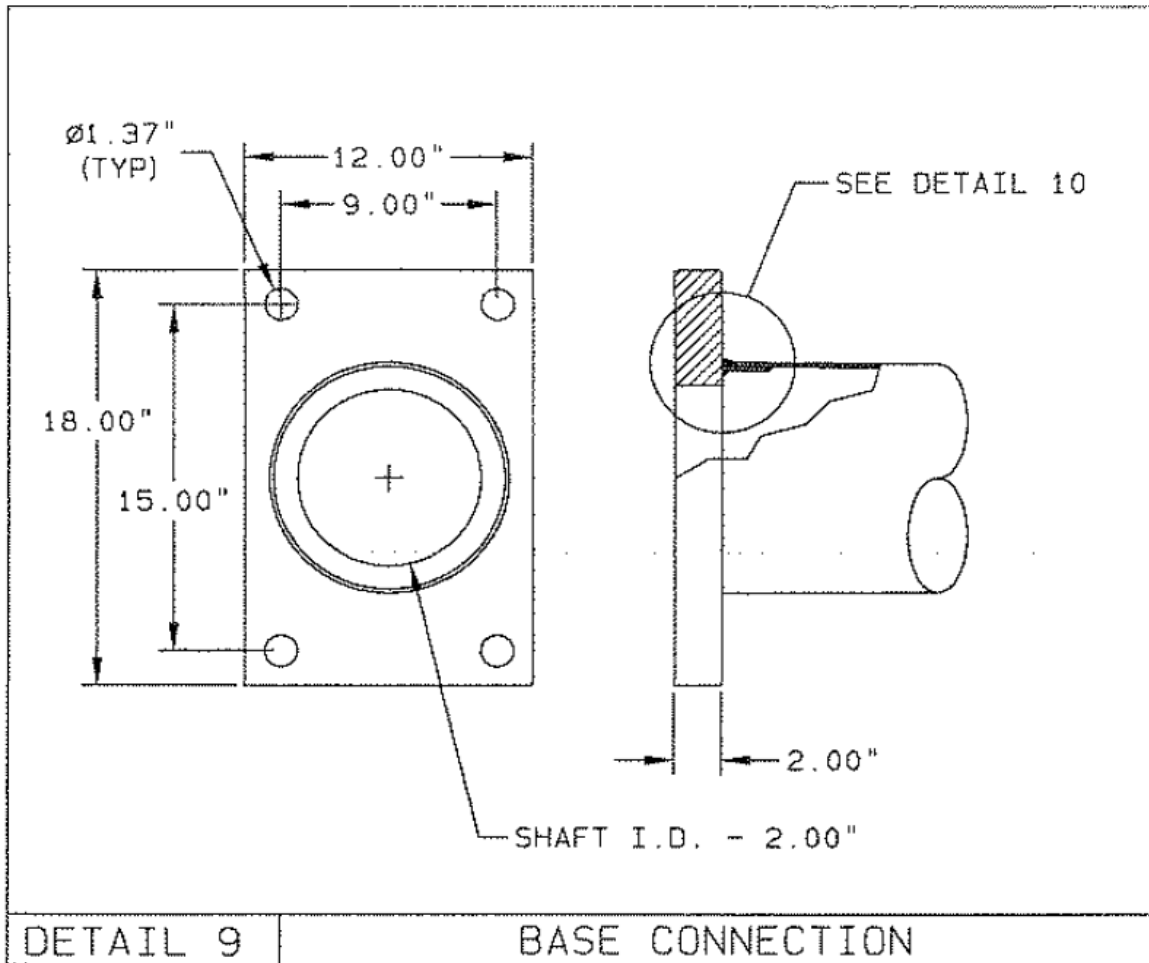


**Figure 3.14 Full-Penetration Welded Connection
 (Reproduced From Valmont Industries Manufacturing Drawings)**

3.3 SPECIMEN LABELS

In order to facilitate in the identification of the traffic signal mast-arm test specimens being tested over the course of this project, a specimen labeling system was developed. The specimen labeling system indicates the traffic signal mast-arm test specimen diameter at the pole wall to base plate connection, the base plate thickness, the connection type, and the individual specimen. A sample traffic signal mast-arm test specimen label is shown in Figure 3.15.

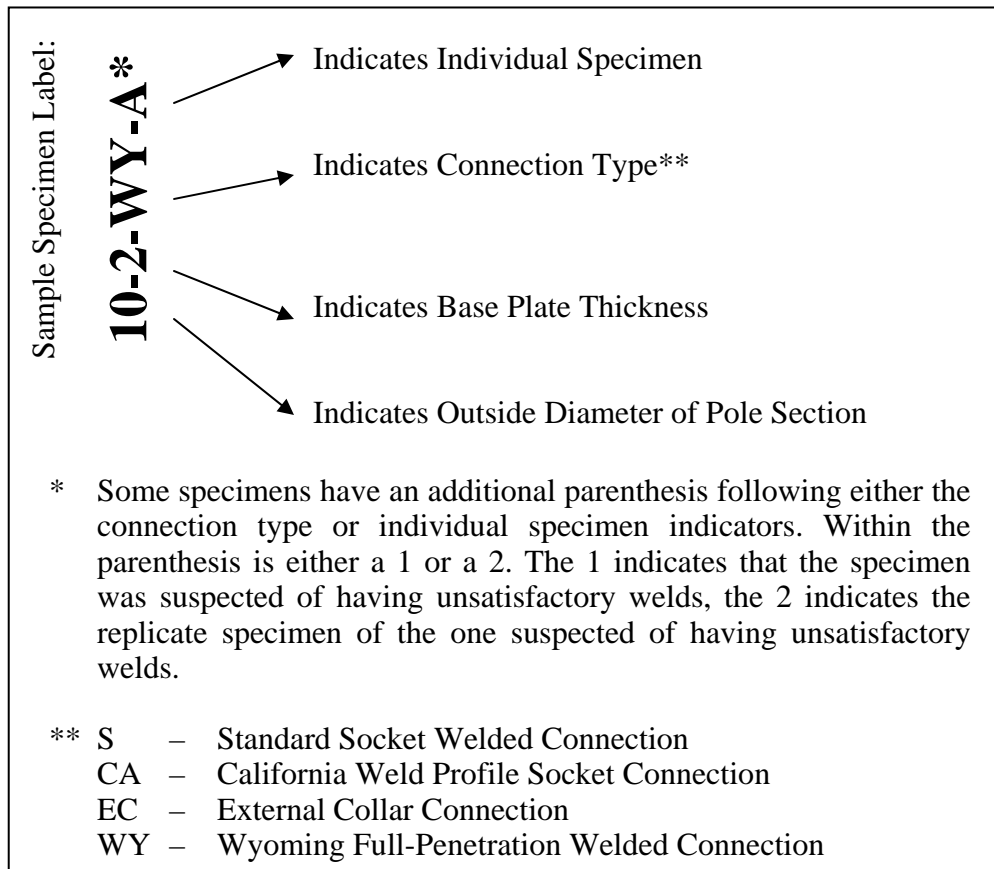


Figure 3.15 Sample Test Specimen Label

CHAPTER 4

Testing Procedure

The traffic signal mast-arm test specimens were tested following the procedures described in this chapter. The testing procedures included taking measurements of the mast-arm test specimen, installing the mast-arm test specimen into the test setup, determining the loads for fatigue testing, determining the displacements by static testing, and dynamic fatigue testing.

4.1 SPECIMEN MEASUREMENT

Measurements were taken on each mast-arm test specimen prior to testing. The measurements included: (1) specimen length, (2) base plate thickness, (3) mast-arm diameter, (4) pole wall thickness, and, (5) weld dimensions. Additional measurements were taken on the external collar mast-arm specimens. These measurements included the external collar thickness and the external collar minimum and maximum length. In general, with the exception of the mast-arm diameter, each measurement was taken at three different locations and averaged. The mast-arm diameter was measured twice at the pole wall to base plate connection; the second measurement taken 90-degrees away from the first. The outside diameter was measured for all the test specimens with the exception being the external collar specimens, where the inside diameter was measured. The pole wall thickness as well as the external collar thickness was measured using a Krautkramer USN 60 ultrasonic detector. This allowed for accurate measurement without damage to the test specimen prior to testing. Weld leg dimensions were measured using an adjustable fillet weld G.A.L. gauge.

4.2 SPECIMEN INSTALLATION

Prior to the start of testing, the loading box was positioned such that the elevation of the center of the bolt hole pattern on the loading box would correspond to the elevation of the center of the bolt hole patterns on both end reactions. Blocks of wood were positioned underneath the loading box to hold it at the correct elevation when hydraulic pressure was removed from the MTS hydraulic actuator. The first specimen was installed on the side of the pinned end reaction. The specimen was raised and positioned into place with the help of a manually operated hydraulic lift. Washers were placed in between the specimen base plate and the loading box to ensure an even bearing surface. The specimen was then connected to the loading box and end reaction, only snug tightening the bolts. The second specimen was then installed on the side of the roller end reaction in a very similar fashion, also only snug tightening the bolts. If problems arose with alignment of either test specimen, the loading box would be raised or lowered to the desired elevation by the MTS hydraulic actuator. This greatly facilitated in the ease of specimen installation. When both specimens were properly aligned, the bolts were fully tightened utilizing a criss-cross pattern to ensure even tightening.

It is important to note that only replicate specimens were tested at the same time. The use of replicates would ensure that no rotation occurred at the point of loading due to unequal stiffness of the test specimens.

In order to determine if the fatigue performance of the traffic signal mast-arm test specimens was being affected by the test setup, the decision was made to install all specimens labeled “A” on the side of the pinned end reaction and all specimens labeled “B” on the side of the roller end reaction. This would provide an avenue for comparison of the influence of the test setup upon the test results.

4.3 LOAD CALCULATION

4.3.1 Selection of Stresses

Prior researchers had performed calculations to determine the approximate mean stress due to dead load and the attached traffic signals and signs at a typical mast-arm socket connection. The mean stress for a typical 10-in outside diameter 40-ft long traffic signal mast-arm was found to vary between 14-ksi and 17-ksi depending on material and loading assumptions (Koenigs et al., 2003). The decision was made to set the minimum stress used in this testing program to 16-ksi, an approximately average value of the previously calculated dead load mean stresses. A mean stress of 22-ksi was selected in order to simulate a worst-case scenario. This was intended to produce more conservative fatigue performance values. Under typical service conditions, it is expected that any applied loading would oscillate the traffic signal mast-arm structure about the point at which the structure is at rest under dead load conditions. This would result in stress levels oscillating about the mean stress value. The decision was made to set the maximum stress at 28-ksi, resulting in a stress range of 12-ksi.

4.3.2 Determining Loads

After the test specimens were installed, the horizontal distance from the center of the loading box at the point of load application to the critical section at the base plate to pole wall connection was measured on each specimen. This measurement was necessary since different base plate thicknesses were used on the specimens. This distance was used to determine the value of the moment at the critical section due to the applied load at midspan. This is illustrated in Figure 4.1.

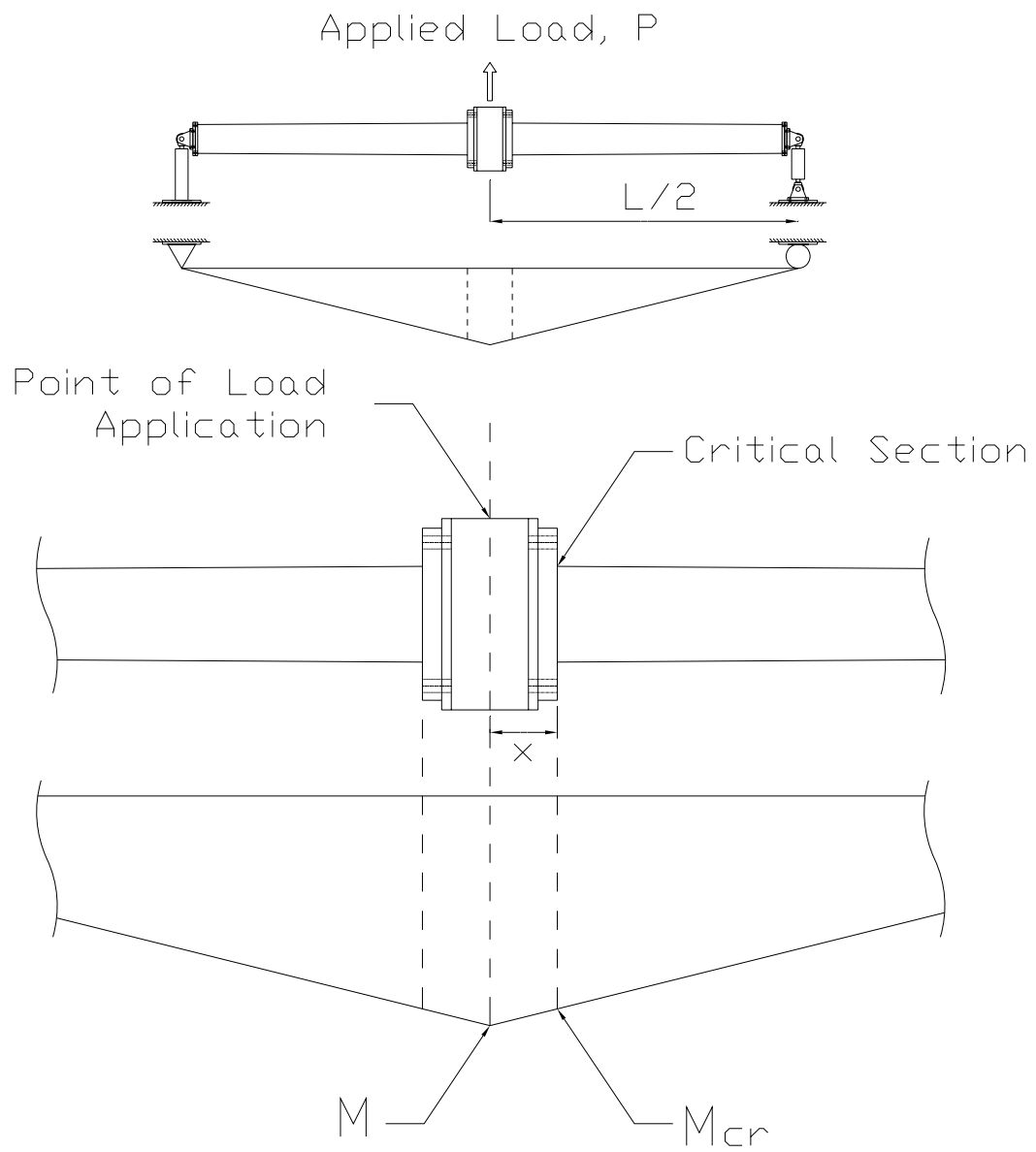


Figure 4.1 Determination of Moment at Critical Location

Using the measurements taken from the test specimens, the loads required to reach the desired minimum and maximum stresses were calculated utilizing the following three equations:

$$Mcr_i = \frac{P_i}{2} \cdot \left(\frac{L}{2} - x\right)$$

$$\sigma_i = \frac{Mcr_i \cdot c}{I}$$

$$P_i = \frac{2 \cdot \sigma_i \cdot I}{c \cdot \left(\frac{L}{2} - x\right)}$$

An example of the spreadsheet used to calculate the desired loads is shown in Figure 4.2. It is important to note that the average values of the two specimens being tested were used to determine the desired loads. The moment of inertia was calculated based on the assumption that any additional elements like the external collars or backing bars on the full-penetration welded specimens were not fully effective. This meant that only the mast-arm pole wall section at the base plate to pole wall connection was assumed to contribute to the section properties. This was done to ensure that all specimens tested in this testing program were tested under the same stress range for comparison of the fatigue performance under the Value Based Design Analysis Method. The calculated moments of inertia ranged from 65.73-in⁴ to 68.72-in⁴, with an average value of 66.99-in⁴. The distance from the neutral axis to the extreme tension fiber was assumed to be the radius of the pole wall section at the base plate to pole wall connection.

Specimen Names: 10-1.75-S-A,B

Specimen Dimensions

Test Length,L (ft): 16

Specimen A

Distance to weld from center,x (in): 6.924

Ave. Pole Diameter (in): 9.9375

Ave. wall Thickness (in): 0.184

Specimen B

Distance to weld from center,x (in): 6.912

Ave. pole Diameter (in): 9.9375

Ave. wall Thickness (in): 0.182

Average

Distance to weld from center,x (in): 6.918

Ave. pole Diameter (in): 9.9375

Ave. wall Thickness (in): 0.183

Calculated Properties:

$I \text{ (in}^4\text{)} = 66.72$

$C \text{ (in)} = 4.969$

Desired Stresses:

$\sigma_{\min} \text{ (ksi)} = 16$

$\sigma_{\max} \text{ (ksi)} = 28$

$\sigma_{\text{mean}} \text{ (ksi)} = 22$

stress range (ksi) = 12

Calculated Loads:

$P_{\min} \text{ (kips)} = 4.824$

$P_{\max} \text{ (kips)} = 8.442$

Figure 4.2 Calculation of Testing Loads

4.4 SETTING DEFLECTIONS

All tests were performed under deflection controlled conditions. This was done to ensure that, (1) dynamic loading effects under high frequency cyclic loading would not influence the stress experienced by the specimen at the critical section, and, (2) instability of the testing system under force control would be avoided.

4.4.1 Static Loading

In order to determine the deflections needed to reach the desired loads, the specimens were statically loaded under deflection controlled conditions to both the minimum and maximum desired loads and the deflections recorded. The process was repeated until the displacements needed to reach the desired loads converged. These converged displacement values were then taken as the minimum and maximum deflections needed to reach the desired loads.

4.5 DYNAMIC FATIGUE TESTING

4.5.1 Testing Frequency

After the minimum and maximum deflections were set, the testing frequency would be incrementally increased to the desired rate. A compensator was utilized to converge on the desired deflections to avoid overshooting when increasing the testing frequency. The typical testing frequency was 9 Hz; however, the first two tests were run at testing frequencies of 3.5 Hz and 4 Hz. The slower testing frequencies of the first two tests were due to excess internal vibrations experienced by the hydraulic pump when attempts were made to increase the testing frequencies further. The vibrations were subsequently eliminated by means of a retrofit of the hydraulic pump and the remaining tests were able to be tested at the higher testing frequency of 9 Hz.

4.5.2 Dynamic Loading Effects

As the testing frequency was increased, the loads required to reach the minimum and maximum deflections decreased. This decrease in loads confirmed that the system was being affected by dynamic loading effects under the high frequency cyclic loading. Even though the loads were decreasing, it was still evident that the critical section was experiencing the desired stress range since the desired deflections were being reached under the deflection controlled conditions.

4.5.3 Failure

Based on previous testing, it was expected that the traffic signal mast-arm test specimens specified for testing in this testing program would have improved fatigue performance. This improved fatigue performance would necessitate longer testing periods for each test. It was therefore necessary to define a point of failure that could be specified as an interlock limit for the cyclic loading controller that would stop the test even if the researcher was not present.

Specimen failure was initially set as a 5% reduction in the load required to reach either the specified minimum or maximum displacement. When this point of failure was reached during the first test, indications of fatigue cracks were unable to be found by visual inspection. The decision was then made to set specimen failure as a 10% reduction in load required to reach either the specified minimum or maximum displacement. When this point of failure was reached during the first test, a large fatigue crack had propagated a significant distance around the circumference of the mast-arm pole wall section as shown in Figure 4.3. This definition of failure was then judged to be adequate and subsequently applied to all the specimens tested in this testing program.



Figure 4.3 Fatigue Crack Propagation at Specified Point of Failure

4.5.4 Repair of Failed Specimen

In all cases, only one of the two specimens would fail. Since replicate specimens were not available for all specimen pairs, the failed specimen would have to be either repaired or rotated to resume the test until the second specimen reached failure. To repair the failed specimen, a groove was ground along the entire length of the fatigue crack and extended beyond the visible crack tips as shown in Figure 4.4. The area was then re-welded.

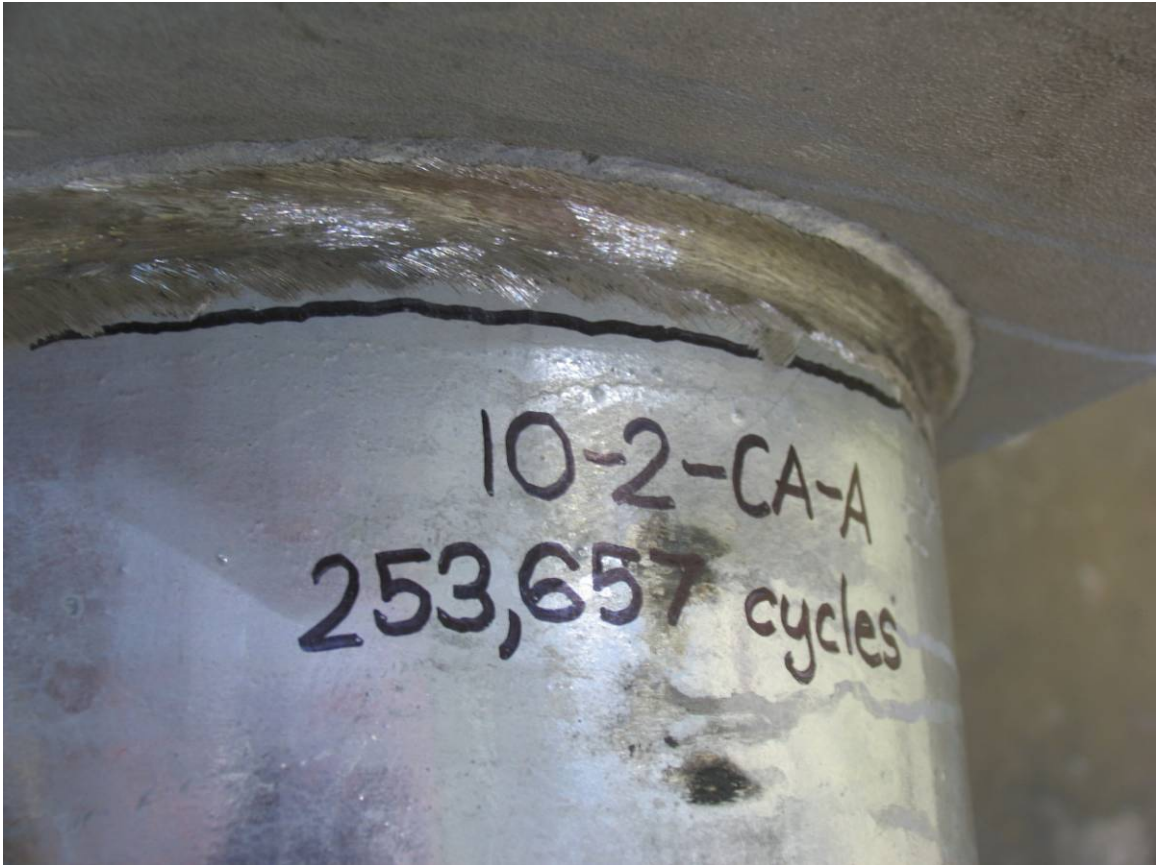


Figure 4.4 Repair of Failed Specimen

In some cases, the repaired specimen would fail again along the new weld and the repair would have to be made again. This became quite time consuming, so more often than not the specimens would instead be rotated 180°. After the rotation of the failed specimen, static tests would be repeated to converge upon new displacement values as described earlier. This would be done to confirm that the system stiffness did not change and that the desired stresses were being reached. The rotation of the failed specimen positioned the fatigue crack on the compression side for the remainder of the test. The positioning of the fatigue crack on the compression side eliminated any possible influence that the failed surface would have on the behavior of the system.

In several cases, the rotated failed specimen would fail in the rotated position. If a replicate specimen was available, it would be installed and the test continued. If a replicate specimen was not available, the test would be stopped and the specimen which had not failed would be considered a run-out. If a replicate specimen was installed, the static tests would again be repeated and the testing resumed.

CHAPTER 5

Results of Tensile Tests and Chemistry Analyses

In order to establish the material properties of the pole wall sections of the test specimens tested in this testing program, a series of tensile tests and chemistry analyses were performed. The specified steel was ASTM A595 Grade A steel.

5.1 TENSILE TESTING

5.1.1 Testing Process

A series of tensile tests were performed to confirm the yield strength and the tensile strength of the steel used to fabricate the pole wall sections of the test specimens. Tensile coupons were manufactured from pieces of steel removed from the pole wall sections of the test specimens after fatigue testing was completed. Four tensile coupons were manufactured, one from each of four randomly selected test specimens.

The four standard rectangular sheet-type tensile coupons were manufactured in accordance with ASTM A370. The reduced section was machined down to a width of 0.500-in and a length of 2.500-in to accommodate a gage length of 2.000-in. The reduced section width resulted in cross-sectional areas ranging from 0.091-in² to 0.093-in² for the four tensile coupons tested.

The tensile coupons were tested in a closed loop MTS machine under displacement control. The strain was measured with an extensometer with a 2-in gage length. During testing, the specimens were held at several intervals of constant displacement after yielding. This was done to determine the static yield strengths. Remarkably, three of the four specimens tested exhibited well-defined yield plateaus. This was unexpected because the material was expected to exhibit a behavior associated

with work hardening due to the cold working experienced during the fabrication process. The well-defined yield plateau behavior allowed the measurement of the static yield strengths. These specimens also exhibited an upper yield point. The fourth specimen exhibited behavior associated with work hardening and the yield strength was determined based on the 0.2 % offset method.

5.1.2 Testing Results

A plot showing the recorded behavior of the four specimens tested is shown in Figure 5.1. The specimens exhibiting the well-defined yield plateaus are shown in green, red, and, gold. In contrast, the specimen exhibiting behavior associated with work hardening is shown in blue.

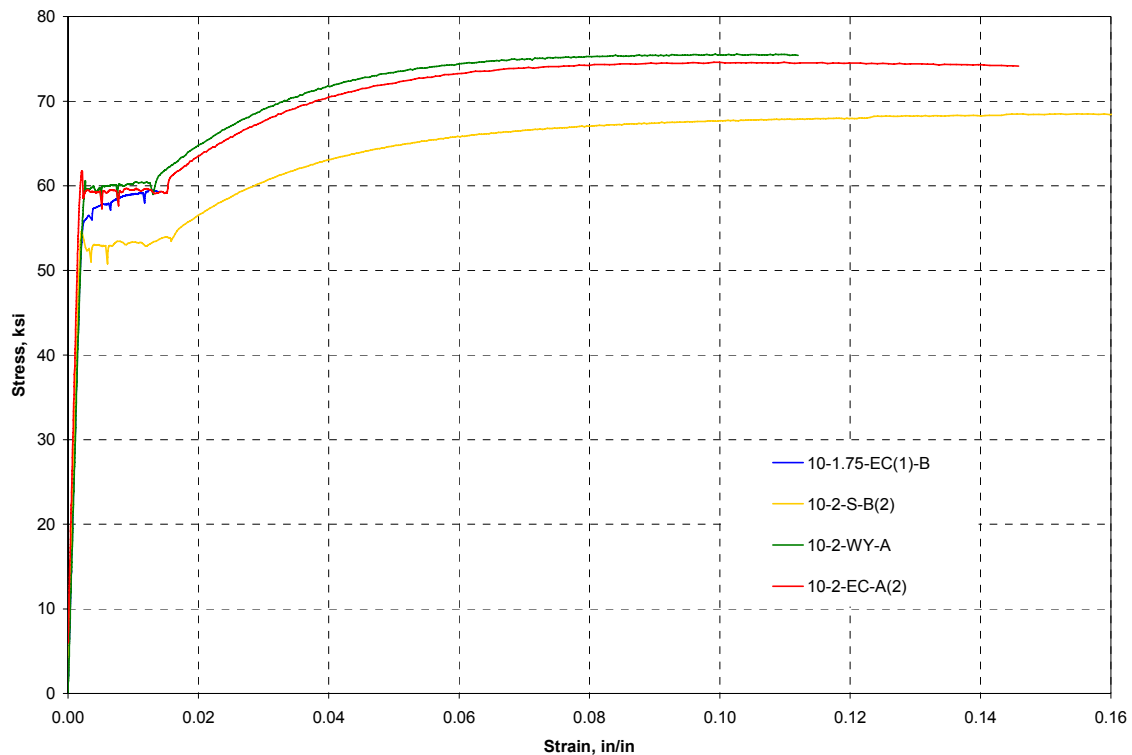


Figure 5.1 Tensile Coupon Testing Results

The plot shown in Figure 5.1 does not show the response to failure as the extensometer used to measure strain had to be removed prior to specimen failure to avoid damage. However, the load on the specimen was recorded to failure.

A plot showing the initial portion of the response of the specimen exhibiting behavior associated with work hardening along with a specimen exhibiting the well-defined yield plateau for comparison is shown in Figure 5.2. The 0.2 % offset line is also shown. The specimen did not exhibit a well-defined upper yield point or a constant yield plateau; the stress continued to increase with increasing strain, prompting the use of the 0.2 % offset method to determine the yield strength.

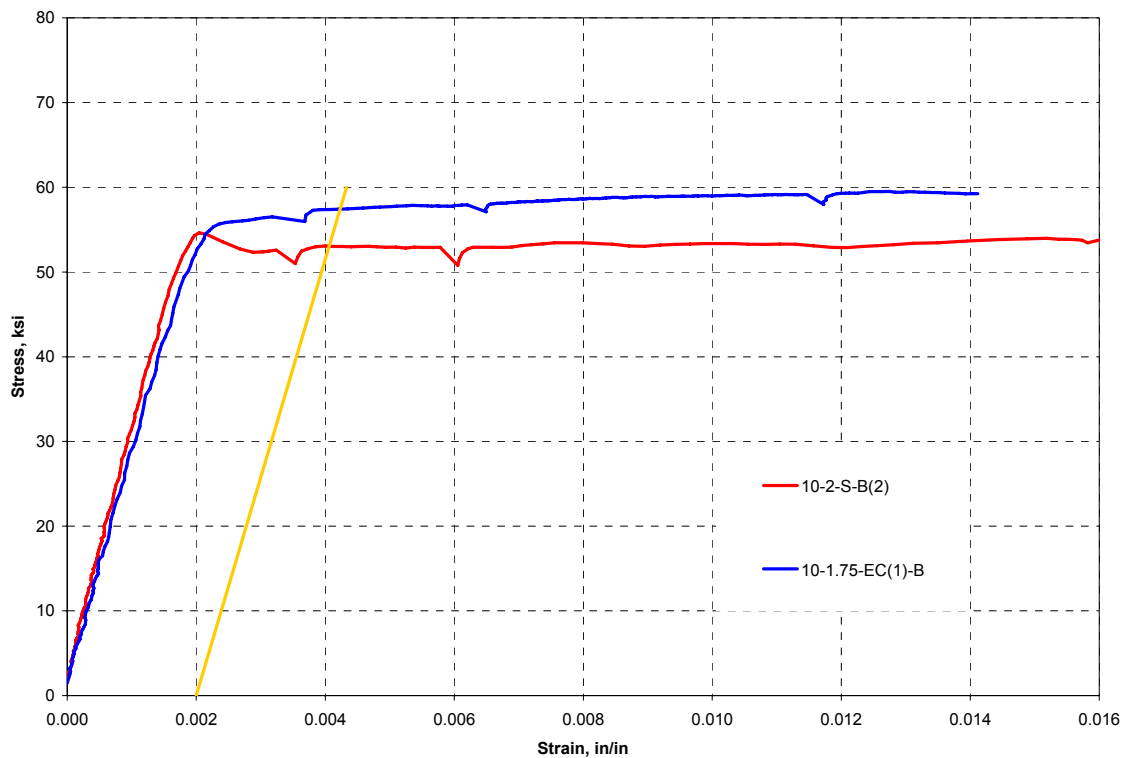


Figure 5.2 Yield Strength Determination by 0.2 % Offset Method

The results of the four tensile tests are shown in Table 5.1. In addition to the static yield strength, tensile strength, and gage length elongation values, the upper yield and dynamic yield values are also tabulated. The mill test reported values and the ASTM A595 Grade A minimum requirements are also included in the table.

Table 5.1 Tensile Coupon Testing Results

Specimen	Static Yield Strength [ksi]	Dynamic Yield [ksi]	Tensile Strength [ksi]	Elongation in 2-in. [%]	Upper Yield [ksi]
10-2-EC-A(2)	57.5	59.1	74.6	27.0	61.7
10-2-WY-A	58.6	59.2	75.8	26.0	60.6
10-2-S-B(2)	50.9	52.3	68.5	34.0	54.6
10-1.75-EC(1)-B	-	57.4 *	76.8	27.0	-
Mill Reported Values	56.2	-	70.7	-	-
ASTM A595 Grade A Minimum Requirements	-	55.0	65.0	23.0	-

* Dynamic Yield Strength determined by 0.2 % "offset method."

Comparison of the measured values to the ASTM A595 Grade A minimum requirements indicated that all the specimens tested met the minimum requirements with one exception, specimen 10-2-S-B(2). This specimen, with a yield strength of 52.3-ksi, did not reach the specified minimum yield strength value of 55-ksi, however, all other requirements were met.

The reduced yield strength of 52.3-ksi, when compared to the yield strengths of the other three specimens tested, was quite surprising since all the pole wall sections of the traffic signal mast-arm test specimens tested in this testing program were manufactured from the same heat of steel. It may have been due to a local variation in that particular heat of steel.

All the traffic signal mast-arm test specimens tested in this testing program were tested at a maximum stress of 28-ksi. This maximum stress value, the stress range achieved during testing, the yield strengths of the steel used to manufacture the pole wall sections, and, the maximum stress to yield strength ratio is presented in Table 5.2 Even though specimen 10-2-S-B(2) did not meet the minimum requirement for yield strength, the maximum nominal stress on the test specimen was only 55 % of the measured yield strength. The other three specimens had maximum stresses of just under 50 % of their respective measured yield strengths. The fatigue testing was therefore performed such that the specimens remained elastic.

Table 5.2 Comparison of the Tensile Coupon Testing Results and the Fatigue Testing Limits

Specimen	Stress Range [ksi]	Maximum Stress [ksi]	Yield Strength [ksi]	Max. Stress to Yield Strength Ratio
10-2-EC-A(2)	12	28	57.5	0.49
10-2-WY-A	12	28	58.6	0.48
10-2-S-B(2)	12	28	50.9	0.55
10-1.75-EC(1)-B	12	28	57.4	0.49

5.2 CHEMISTRY ANALYSIS

5.2.1 Analysis Procedure

A series of chemistry analyses were performed to confirm the chemical composition of the steel used to fabricate the pole wall sections of the test specimens. Samples were taken from pieces of steel removed from the pole wall sections of the test specimens after fatigue testing was completed. The samples were taken from the same specimens as the tensile coupons.

The chemistry analyses were performed by Chicago Spectro Service Laboratory, Inc. in Chicago, Illinois. The tests for carbon and sulfur were performed in accordance with ASTM E1019, and the tests for the other requested elements were performed in accordance with ASTM E415.

5.2.2 Analysis Results

The results of the chemistry analyses are presented in Table 5.3. The mill reported results as well as the ASTM A595 Grade A requirements are also presented. The presented results indicate that all the specimens tested met the requirements for ASTM A595 Grade A steel. It is important to note that the carbon contents of the four samples are essentially the same. Therefore, the four samples are most likely from the same heat, indicating that nothing out of the ordinary in the chemistry contributed to the lower strength of specimen 10-2-S-B(2).

Table 5.3 Chemistry Analyses Results

Composition by Product Analysis, %							
Elements	Mill Reported ^A	ASTM A595 Grade A Limits		Specimen Tested			
		Minimum	Maximum	10-2-EC-A(2)	10-2-WY-A	10-2-S-B(2)	10-1.75-EC(1)-B
Carbon	0.210	0.012	0.290	0.220	0.210	0.210	0.220
Manganese	0.800	0.260	0.940	0.670	0.680	0.660	0.660
Phosphorous	0.010	-	0.045	0.011	0.011	0.011	0.012
Sulfur	0.000	-	0.045	0.012	0.010	0.011	0.011
Silicon	0.010	^B	0.040	0.020	0.010	0.020	0.020
Copper	0.020	-	-	0.030	0.030	0.030	0.030
Chromium	0.020	-	-	0.020	0.020	0.020	0.020
Nickel	0.010	-	-	0.040	0.040	0.040	0.040
Molybdenum	-	-	-	0.010	0.010	0.010	0.010
Aluminum	-	^B	-	0.052	0.047	0.047	0.051

^A Composition by Heat Analysis, %

^B Silicon or silicon in combination with aluminum must be sufficient to ensure uniform mechanical properties. Their sum shall be greater than or equal to 0.020 %.

CHAPTER 6

Fatigue Test Results

The results of fatigue testing on the traffic signal mast-arm specimens tested over the course of this test program are presented in the following chapter. Following a brief discussion of the calculation of reported stresses, the results of the fatigue testing for each connection type will be presented.

6.1 TESTING PROGRAM OVERVIEW

A total of 10 pairs or 20 specimens were tested over the course of this test program. The nominal outside diameter of each specimen at the base plate connection was 10-in with a pole wall thickness of 0.1793-in (7 gauge). Sixteen of the specimens failed under fatigue loading; the remaining 4 specimens did not fail under fatigue loading and were considered run-outs. The specimens tested are listed in Table 6.1 along with the base plate thicknesses, connection details, and, cycles to failure.

In Table 6.1, the specimens that did not fail under fatigue loading have the number of cycles they accumulated shown in bold red text. As previously discussed, specimens that failed under fatigue loading would be rotated 180° and the test resumed. In some cases, the rotated failed specimen would fail in the rotated position before the replicate specimen being tested at the same time failed. These rotated failed specimens that failed in the rotated position, referred to as flipped specimens, are listed a second time in Table 6.1 with the specimens' names shown in bold green text. Additionally, the number of cycles accumulated to failure after being rotated is also shown. For example, specimen 10-3-S-B failed after 792,576 cycles and was then rotated. The specimen then accumulated an additional 376,291 cycles in the rotated position before failing again.

Table 6.1 Fatigue Test Results

Base Plate Thickness (in)	Connection Detail	Specimen Name	Cycles to Failure (10% Drop in Load)
1.75	Standard Socket	10-1.75-S-B	142,857
1.75	Standard Socket	10-1.75-S-B	134,197
1.75	Standard Socket	10-1.75-S-A	515,365
1.75	External Collar	10-1.75-EC-A(2)	2,345,896
1.75	External Collar	10-1.75-EC-A(2)	2,889,260
1.75	External Collar	10-1.75-EC-B(2)	5,755,111
1.75	External Collar	10-1.75-EC(1)-B	3,304,490
1.75	External Collar	10-1.75-EC(1)-B	2,382,309
1.75	External Collar	10-1.75-EC(1)-A	6,206,754
2	Standard Socket	10-2-S-B	165,998
2	Standard Socket	10-2-S-A	235,854
2	Standard Socket	10-2-S-A(2)	210,793
2	Standard Socket	10-2-S-A(2)	260,700
2	Standard Socket	10-2-S-B(2)	622,928
2	External Collar	10-2-EC-A(2)	3,939,099
2	External Collar	10-2-EC-B(2)	6,927,606
2	External Collar	10-2-EC(1)-A	5,384,143
2	External Collar	10-2-EC(1)-A	2,863,521
2	External Collar	10-2-EC(1)-B	8,247,664
2	Full-Penetration Weld	10-2-WY-A	4,997,925
2	Full-Penetration Weld	10-2-WY-B	7,527,441
2	California Socket	10-2-CA-A	253,657
2	California Socket	10-2-CA-B	310,352
3	Standard Socket	10-3-S-B	792,576
3	Standard Socket	10-3-S-B	376,291
3	Standard Socket	10-3-S-A	1,168,867

Some specimens were ultrasonically inspected after being fabricated to ensure an acceptable quality of work. These specimens' connection details are shown in bold blue text in Table 6.1.

6.2 CALCULATION OF REPORTED STRESSES

The results of the fatigue tests presented in this chapter follow the Value Based Design Analysis Method as described by previous researchers (Koenigs et al., 2003). In this method, the nominal stresses at the critical section are based on the applied load and the section properties of the mast-arm pole wall section at the base plate to pole wall connection. The additional elements like the external collars or backing bars are not included in the section properties.

The assumption is made that plane sections remain plane providing a linear strain distribution through the depth of the mast-arm cross section. Even though this assumption was shown by previous researchers to be slightly inaccurate as some local distortion does occur near the critical section, it was still used as it would have been increasingly difficult to quantify the amount of distortion and the exact stress distribution without using more rigorous analysis methods (Koenigs et al., 2003). Also, the assumption of plane sections remain plane would most likely be made by practicing engineers and this was taken into account when the section properties were calculated.

With the use of the Value Based Design Analysis Method, the results presented in this chapter are aimed at illustrating what modifications can be made to a standard design to improve the fatigue performance.

6.3 FATIGUE TEST RESULTS

The results of the fatigue testing for each connection type are presented in this section. Beginning with the socketed specimens, the presentation of the results will continue with the external collar specimens and the full-penetration welded specimens, concluding with the specimens that did not fail under fatigue loading.

6.3.1 Socketed Specimens

The results of the two socketed connections tested in this test program will be presented beginning with the standard design utilized by Valmont Industries and TXDOT and concluding with the standard design specified by CALTRANS.

6.3.1.1 *Standard Socketed Connection*

A total of 8 standard socketed connection specimens were tested in this test program. Two of the specimens had 1.75-in thick base plates, 4 of the specimens had 2-in thick base plates, and the remaining 2 specimens had 3-in thick base plates.



Figure 6.1 Typical Failure of the Standard Socketed Connection

The typical failure of the standard socketed connection specimens was a fatigue crack through the pole wall at the toe of the fillet weld. The fatigue crack initiated at the top of the test specimen, at the location of the extreme tension fiber, and propagated perpendicularly to the applied stress along the toe of the fillet weld. The typical failure is shown in Figure 6.1 with the extent of the crack propagation indicated. A more detailed view of the typical failure is shown in Figure 6.2. With the exception of two specimens, which were considered run-outs, all the standard socketed connection specimens failed in this manner.

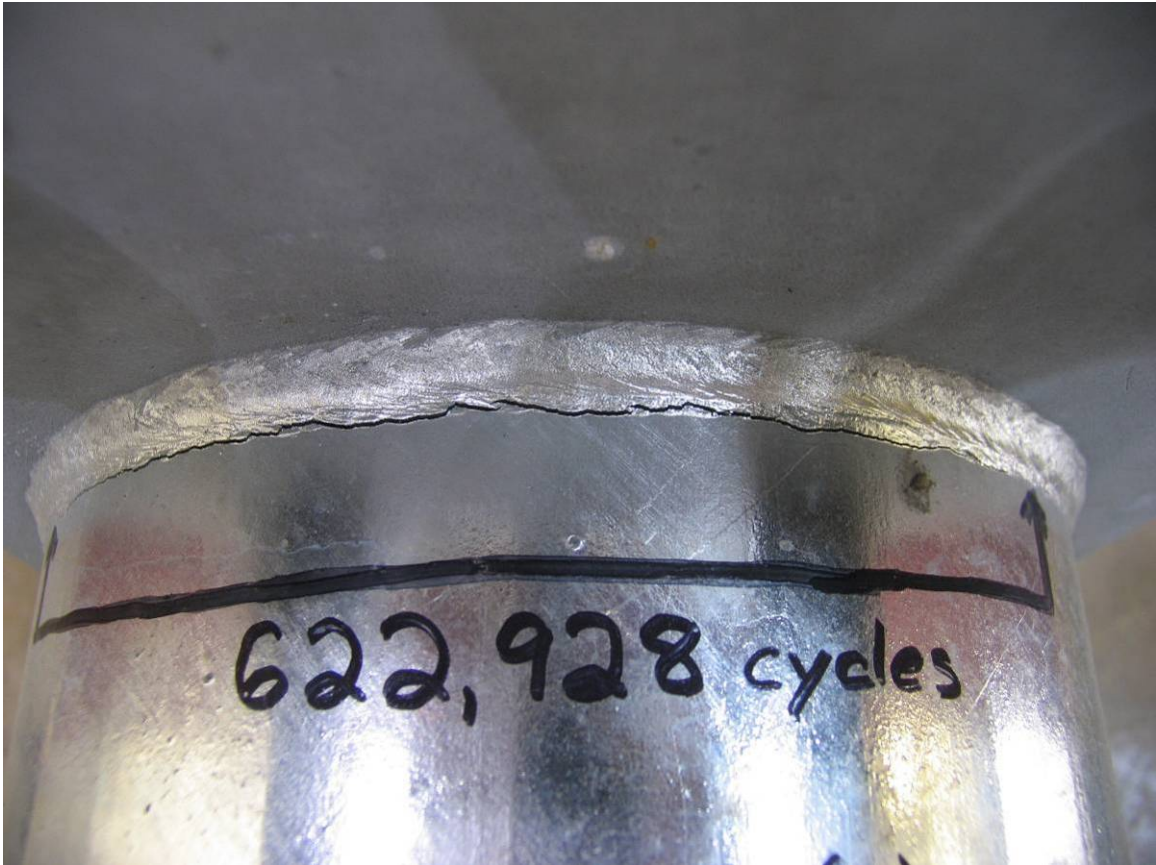


Figure 6.2 Detailed View of Failure Location

After testing, a cross section of a standard socketed connection specimen was cut to reveal the connection detail and weld profile. The cross section was ground, polished, and etched with a nitric acid solution to reveal the weld and the weld penetration as well as to highlight the fatigue crack. The etched cross section is shown in Figure 6.3. The fatigue crack can be seen through the pole wall at the toe of the fillet weld and is shown in more detail in Figure 6.4.

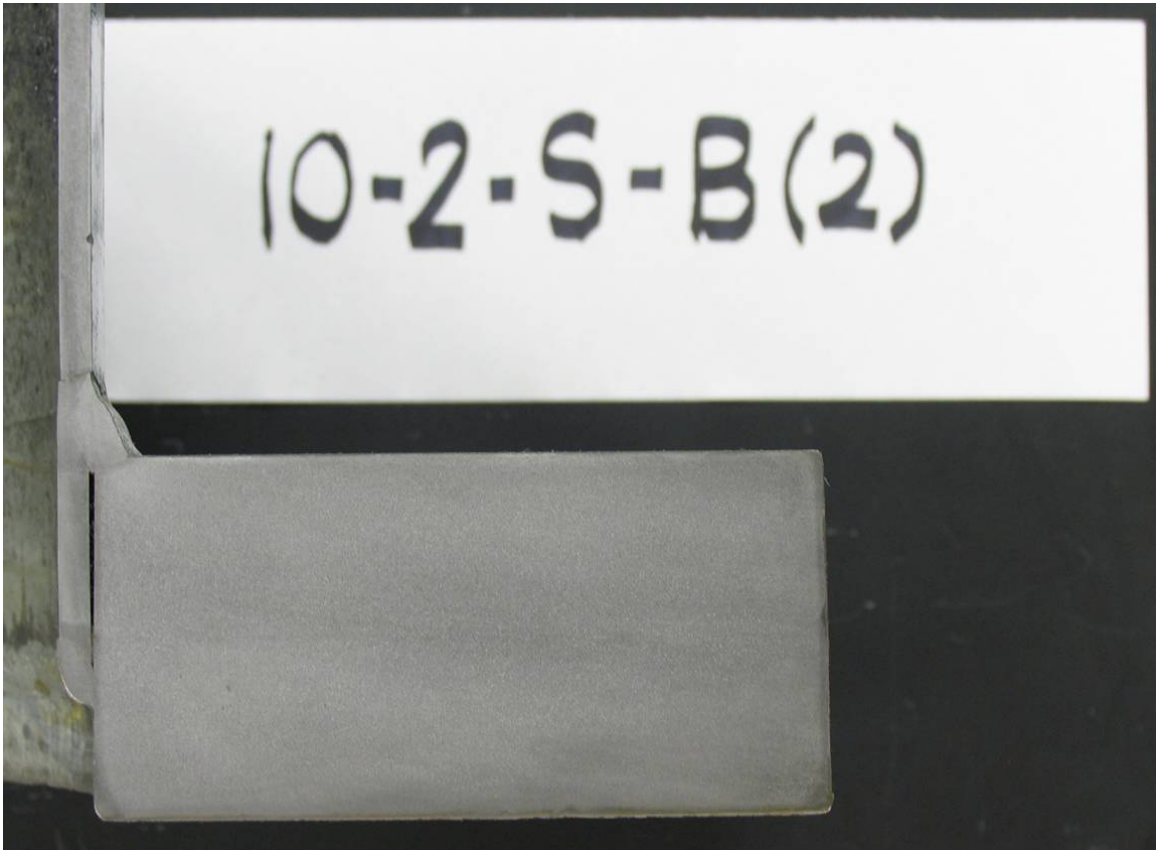


Figure 6.3 Etched Cross Section of a Standard Socketed Connection



Figure 6.4 Detailed View of Etched Failure Location

The results of the fatigue testing on the standard socketed connection specimens are summarized in Table 6.1 and are also shown graphically in Figure 6.5. The specimens with 1.75-in thick base plates are shown in red, the specimens with 2-in thick base plates are shown in blue, and the specimens with 3-in thick base plates are shown in green. Specimens that were rotated to continue testing and failed in the rotated position are shown with no fill while run-out specimens are indicated with an arrow.

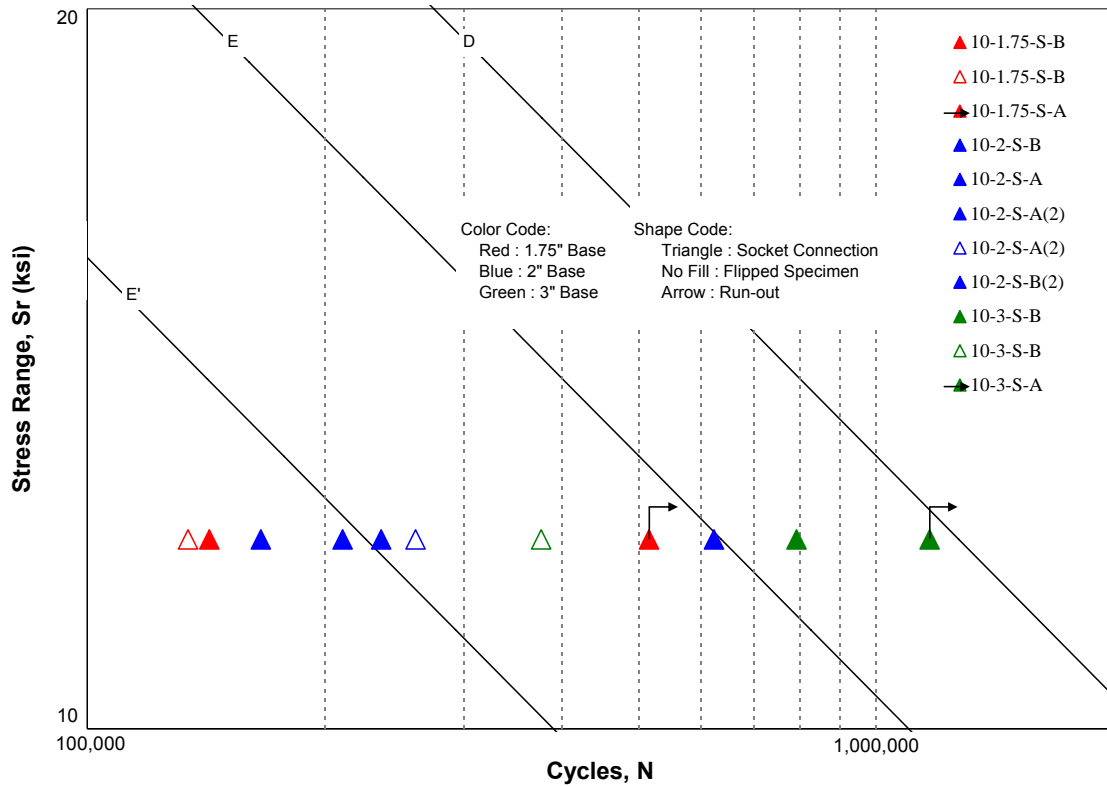


Figure 6.5 Standard Socketed Connection Fatigue Test Results

6.3.1.2 California Weld Profile

Two California weld profile socketed connection specimens were tested in this test program. Both of the specimens had 2-in thick base plates. The typical failure was identical to the standard socketed connection specimens with a fatigue crack through the pole wall at the toe of the fillet weld. The fatigue crack initiated at the top of the test specimen, at the location of the extreme tension fiber, and propagated perpendicularly to the applied stress along the toe of the fillet weld. The typical failure is shown in Figure 6.6 with the extent of the crack propagation indicated.



Figure 6.6 Typical Failure of the California Weld Profile Socketed Connection

The results of the fatigue testing on the California weld profile socketed connection specimens are summarized in Table 6.1 and are also shown graphically in Figure 6.7.

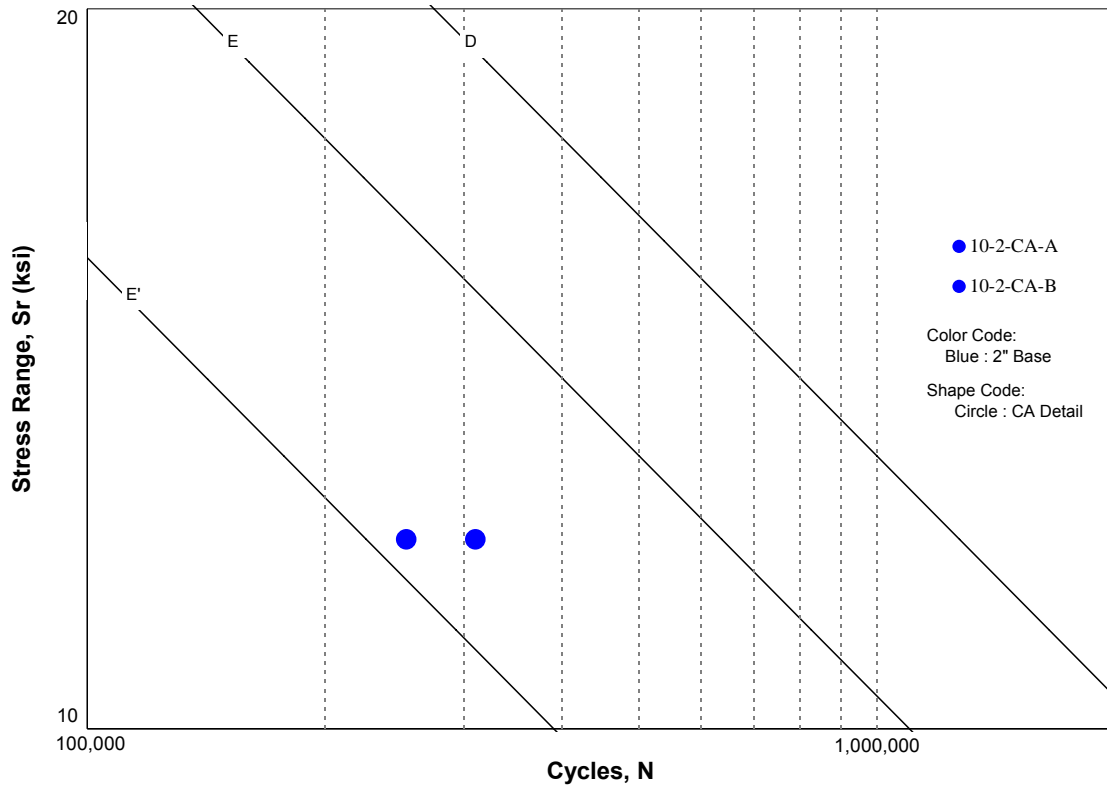


Figure 6.7 California Weld Profile Socketed Connection Fatigue Test Results

6.3.2 External Collar Specimens

A total of 8 external collar specimens were tested in this test program. Four of the specimens had 1.75-in thick base plates and the remaining 4 specimens had 2-in thick base plates.

6.3.2.1 *Typical Failure of External Collar Specimens*

The typical failure of the external collar specimens was a fatigue crack through the external collar and the pole wall at the toe of the base plate to external collar weld. The fatigue crack initiated at the top of the test specimen, at the location of the extreme tension fiber, and propagated perpendicularly to the applied stress along the toe of the weld. The typical failure is shown in Figure 6.8 with the extent of the crack propagation indicated. A more detailed view of the typical failure is shown in Figure 6.9.



Figure 6.8 Typical Failure of the External Collar Specimens

With the exception of two specimens, which were considered run-outs, and one other specimen, which failed in a different manner, all the external collar specimens failed in this manner.

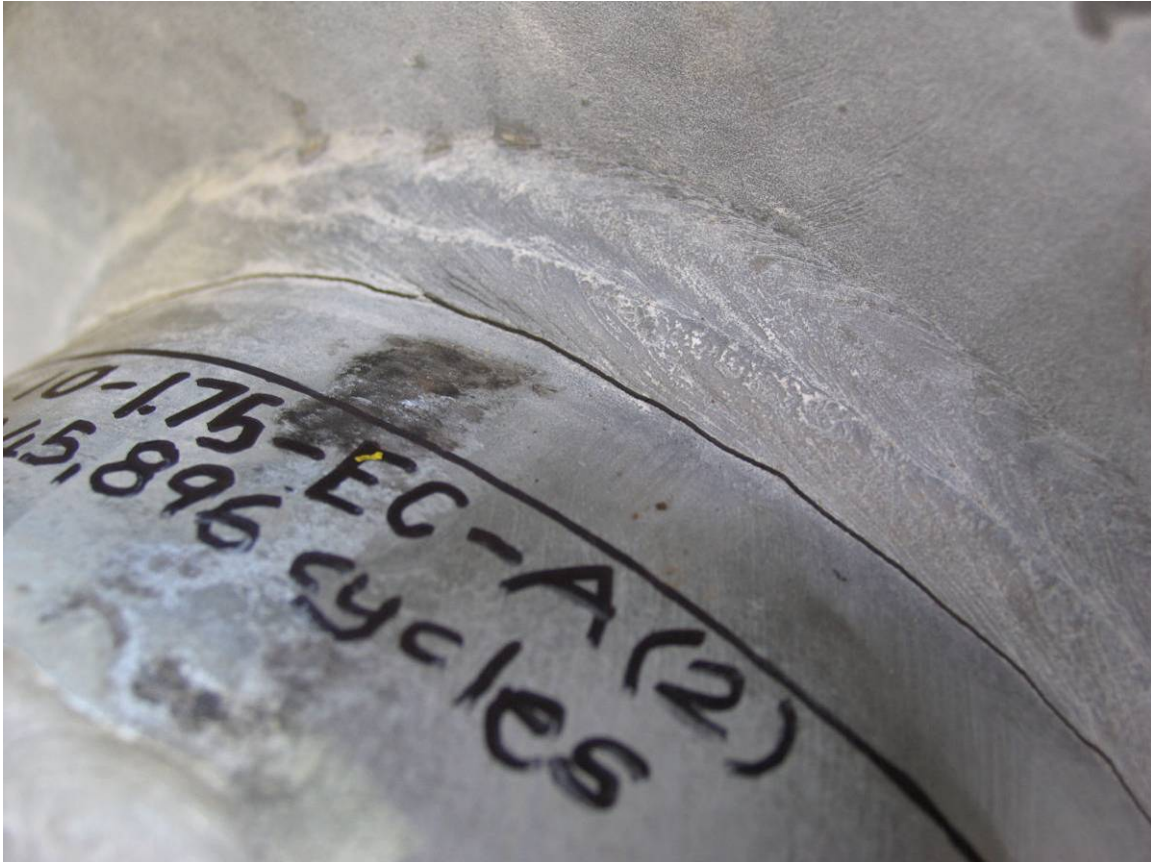


Figure 6.9 Detailed View of Failure Location

After testing, a cross section of an external collar specimen was cut to reveal the connection detail and weld profile. The cross section was ground, polished, and etched with a nitric acid solution to reveal the weld and the weld penetration as well as to highlight the fatigue crack. The etched cross section is shown in Figure 6.10. The fatigue crack can be seen through the external collar at the toe of the weld and continuing through the pole wall. The fatigue crack is shown in more detail in Figure 6.11. The

fatigue crack initiated at the external collar to base plate reinforcing weld (1) and propagated through the external collar (2). Once the external collar was cracked, another fatigue crack initiated at the fusion line of the weld in the pole wall (3) and propagated through (4).

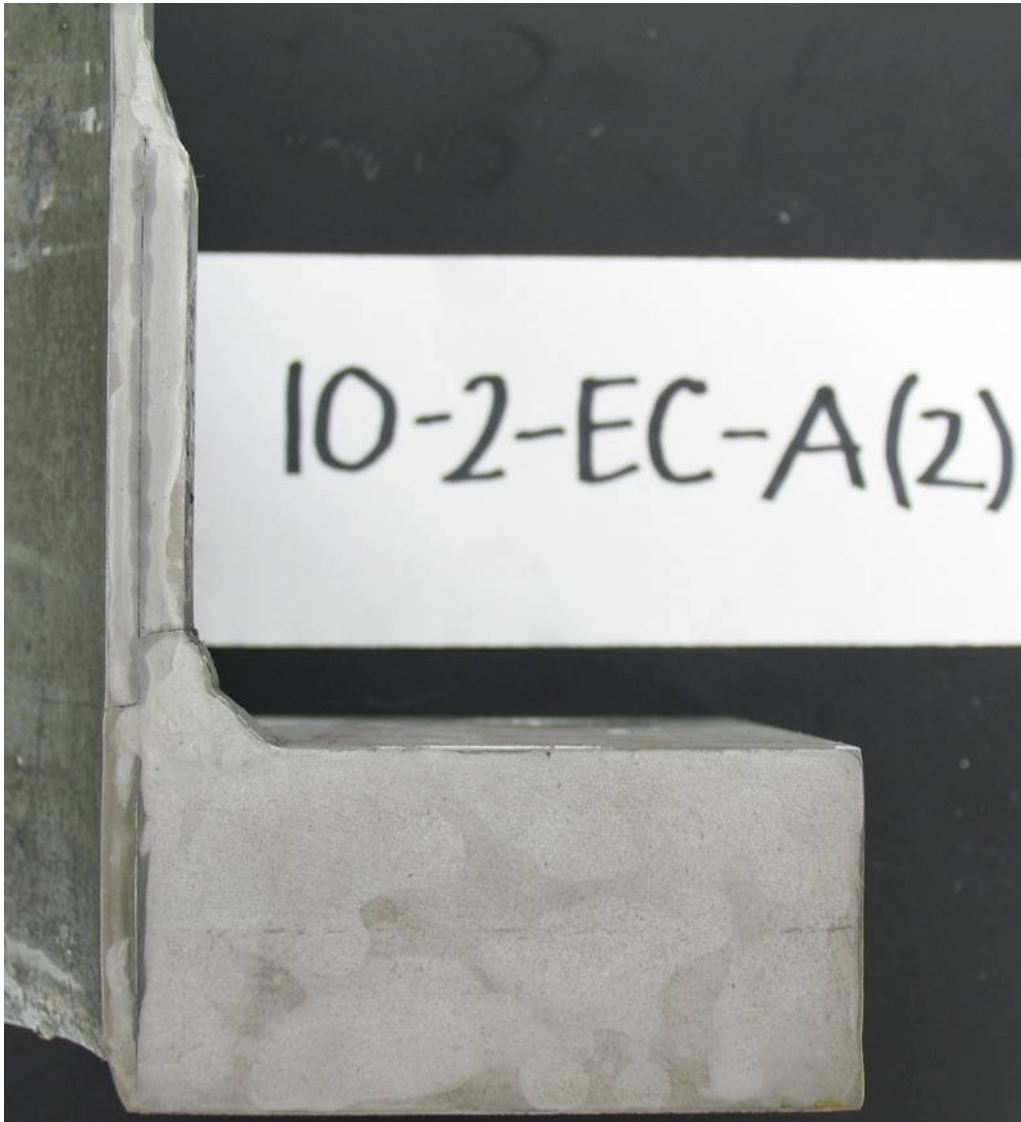


Figure 6.10 Etched Cross Section of an External Collar Specimen

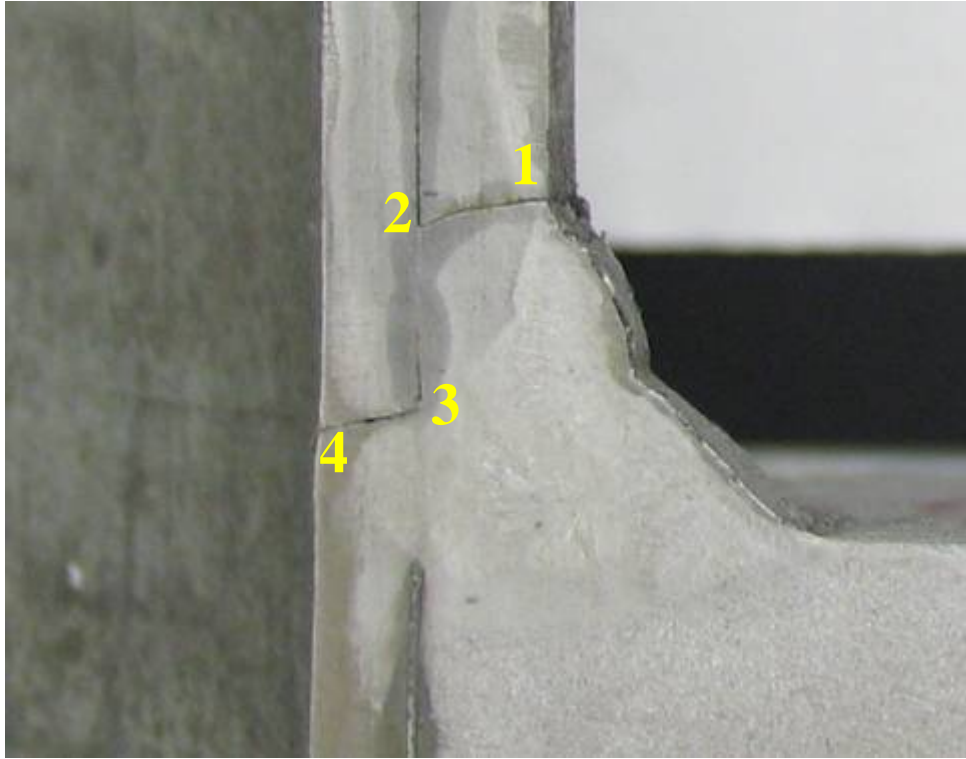


Figure 6.11 Detailed View of Etched Failure Location

6.3.2.2 *Exception to Typical Failure of External Collar Specimens*

The exception to the typical failure, excluding the two specimens that were considered run-outs, occurred in specimen 10-2-EC-B(2) and is shown in Figure 6.12. Two fatigue cracks developed, one at the toe of the external collar to pole wall fillet weld at the maximum dimension of the external collar, and the other, at the top of the specimen at the top of the external collar to pole wall fillet weld at the minimum dimension of the external collar.

The fatigue crack at the toe of the external collar to pole wall fillet weld is shown in more detail in Figure 6.13 with the extent of crack propagation indicated. Even though the point of fatigue crack initiation was not at the extreme tension fiber, sufficient stress was applied to both initiate and propagate the fatigue crack along the weld toe. The fatigue crack propagated perpendicularly to the applied stress, moving away from the toe of the fillet weld through the pole wall as the weld turned to follow the scalloped edge of the external collar.



Figure 6.12 Exception to Typical Failure

The fatigue crack at the top of the specimen at the top of the external collar to pole wall fillet weld is shown in more detail in Figure 6.14 with the extent of crack propagation indicated. The fatigue crack initiated at the top of the test specimen, at the location of the extreme tension fiber, and propagated perpendicularly to the applied stress along the top of the weld and through the external collar as the weld turned to follow the scalloped edge of the external collar.

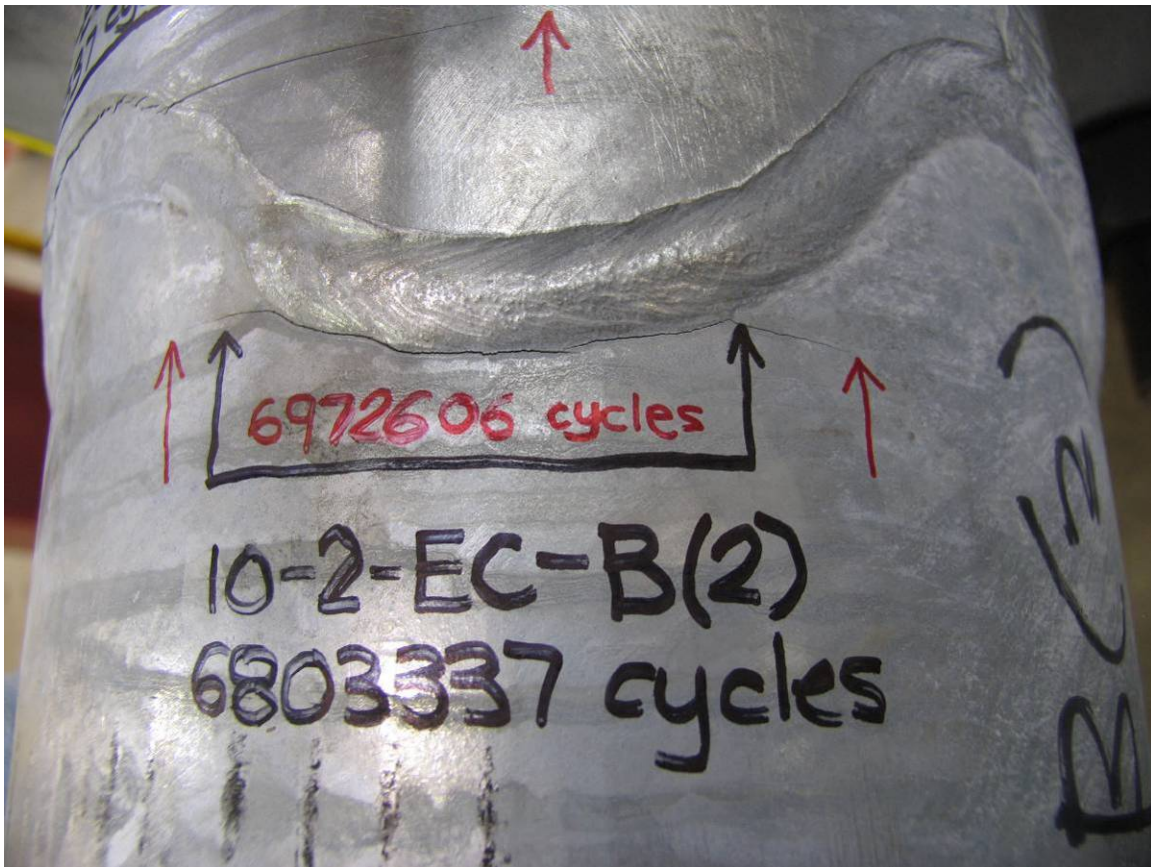


Figure 6.13 Fatigue Crack at External Collar Maximum Dimension



Figure 6.14 Fatigue Crack at External Collar Minimum Dimension

After testing, a cross section of the external collar specimen was cut to reveal the connection detail and weld profile. The cross section was taken through the top of the specimen as tested at the location of the collar minimum dimension, ground, polished, and etched with a nitric acid solution to reveal the weld and the weld penetration as well as to highlight the fatigue crack. The etched cross section is shown in Figure 6.15. The fatigue crack can be seen through the root of the fillet weld at the top of the external collar and then cracking through the pole wall at the root of the base plate to external collar weld after cracking through the base of the weld.

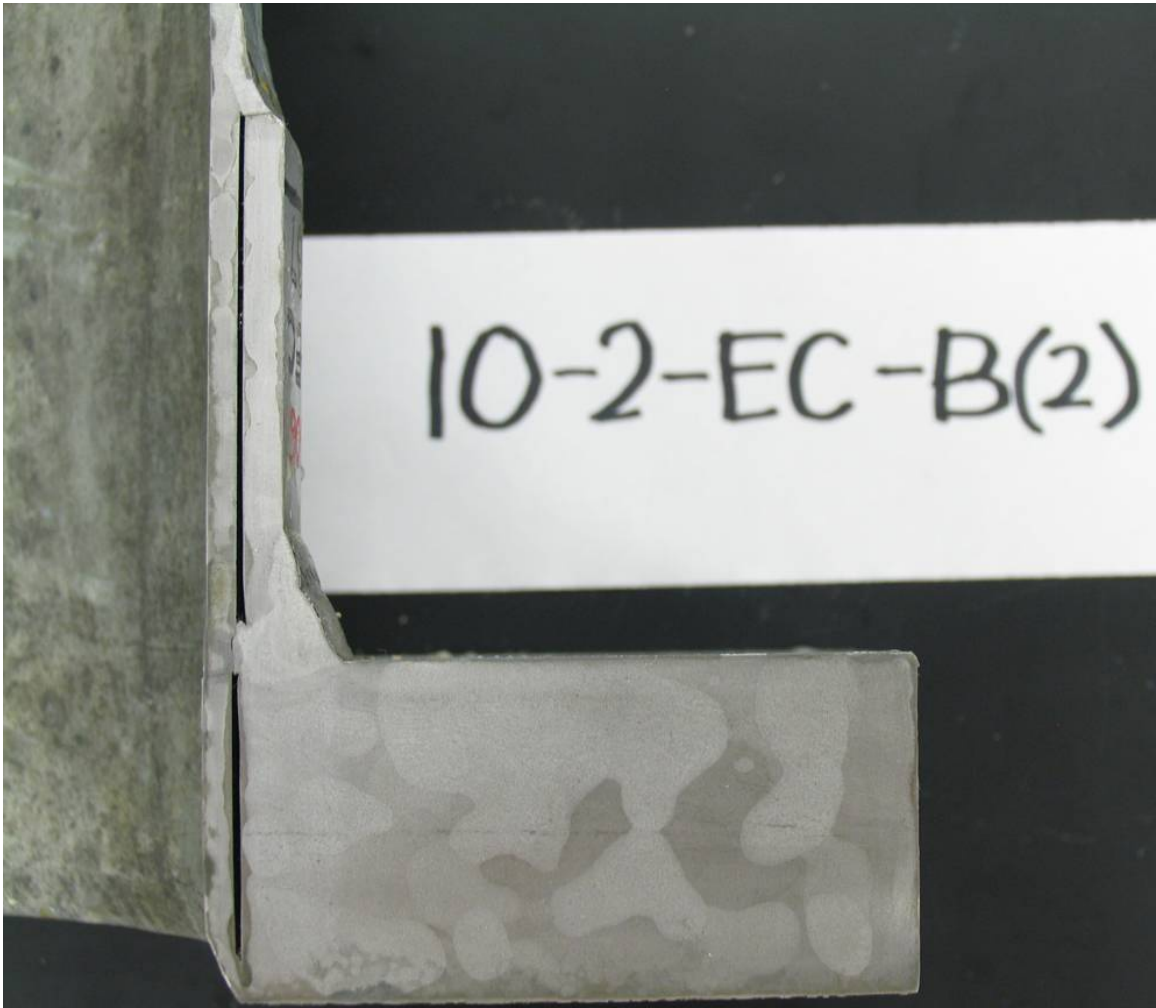


Figure 6.15 Etched Cross Section of an External Collar Specimen

The fatigue crack through the fillet weld at the top of the external collar is shown in more detail in Figure 6.16 while the fatigue crack through the pole wall is highlighted in Figure 6.17. It is thought that the fatigue crack initiated at the fillet weld at the top of the external collar and propagated along the base of the base plate to external collar weld and, finally, propagated through the pole wall.

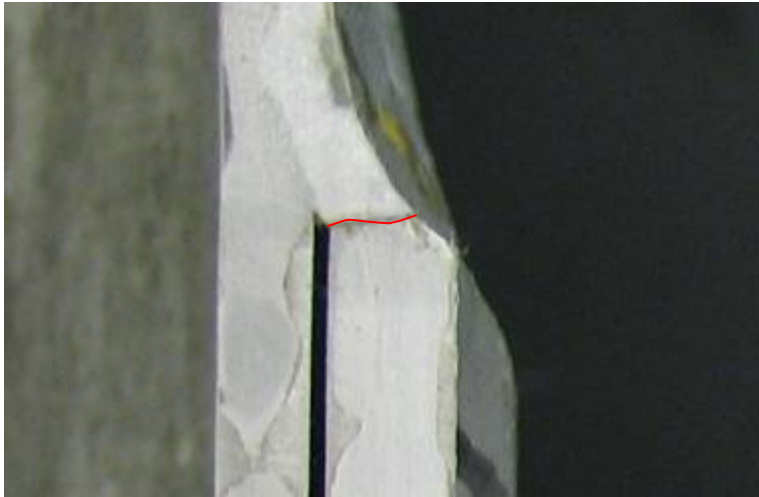


Figure 6.16 Fatigue Crack at Top of External Collar

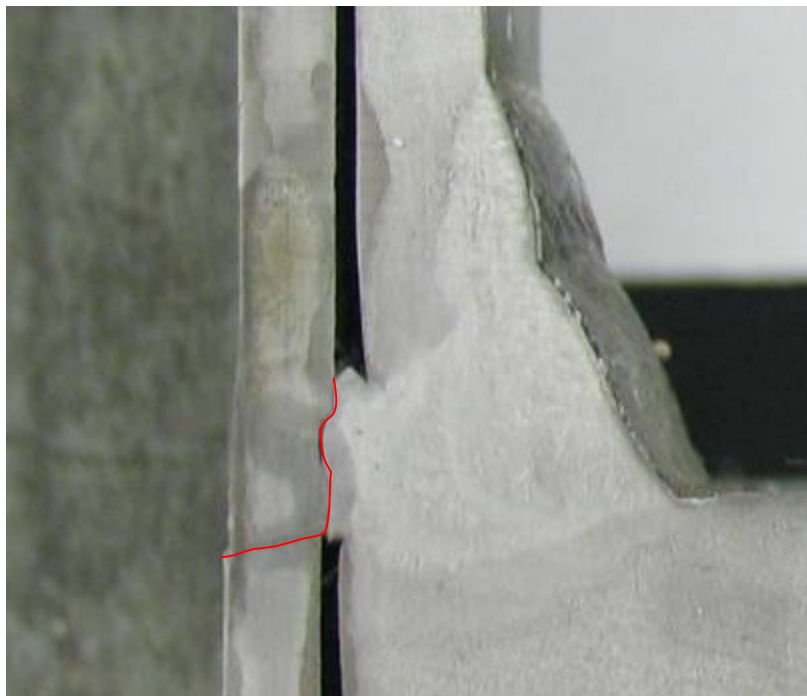


Figure 6.17 Fatigue Crack Through Pole Wall

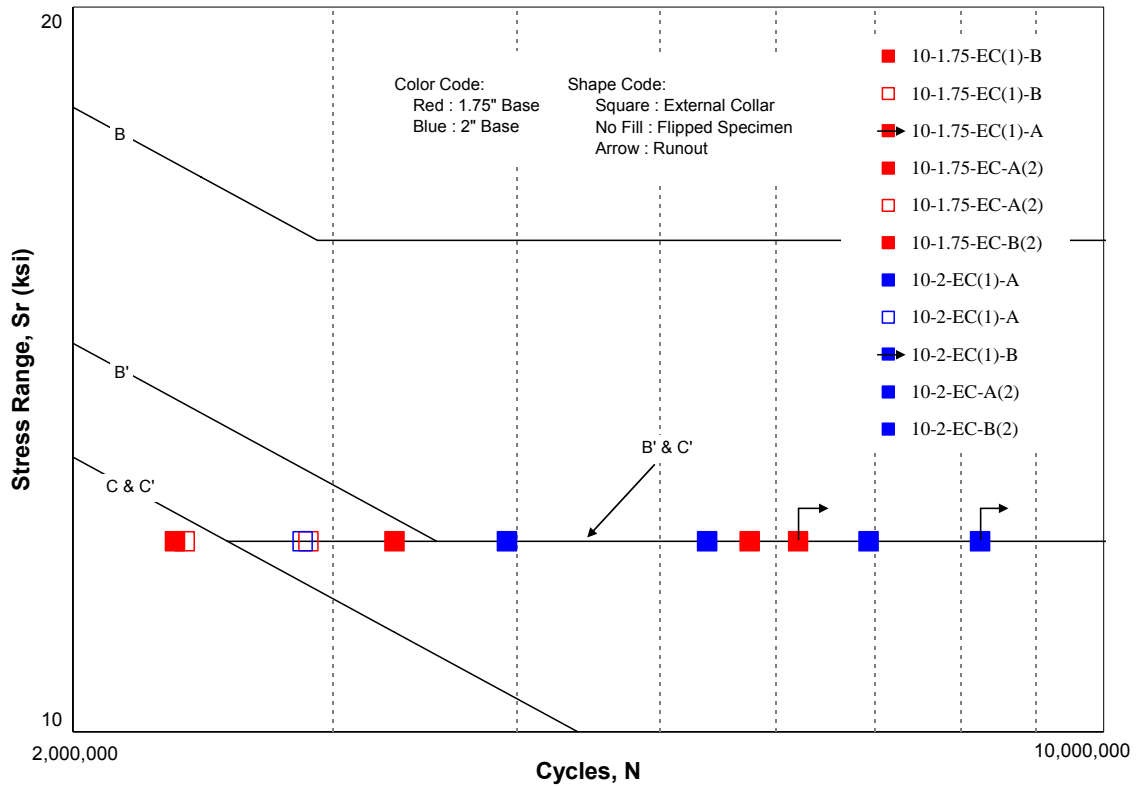


Figure 6.18 External Collar Specimens Fatigue Test Results

The results of the fatigue testing on the external collar specimens are summarized in Table 6.1 and are also shown graphically in Figure 6.18. The specimens with 1.75-in thick base plates are shown in red and the specimens with 2-in thick base plates are shown in blue. Specimens that were rotated to continue testing and failed in the rotated position are shown with no fill while run-out specimens are indicated with an arrow. Specimen 10-2-EC-B(2), which failed in the atypical manner at 6,927,606 cycles, exhibited the best fatigue performance when compared to the specimens that failed in the typical manner. This improved fatigue behavior is most likely attributable to the failure mode; the cause of which, unfortunately, being unknown.

6.3.3 Full-Penetration Welded Specimens

Two full-penetration welded specimens were tested in this test program. Both of the specimens had 2-in thick base plates. The typical failure was similar to the socketed connection specimens with a fatigue crack through the pole wall at the toe of the base plate to pole wall weld. The fatigue crack initiated at the top of the test specimen, at the location of the extreme tension fiber, and propagated perpendicularly to the applied stress along the toe of the full-penetration weld. The typical failure is shown in Figure 6.19 with the extent of the crack propagation indicated.

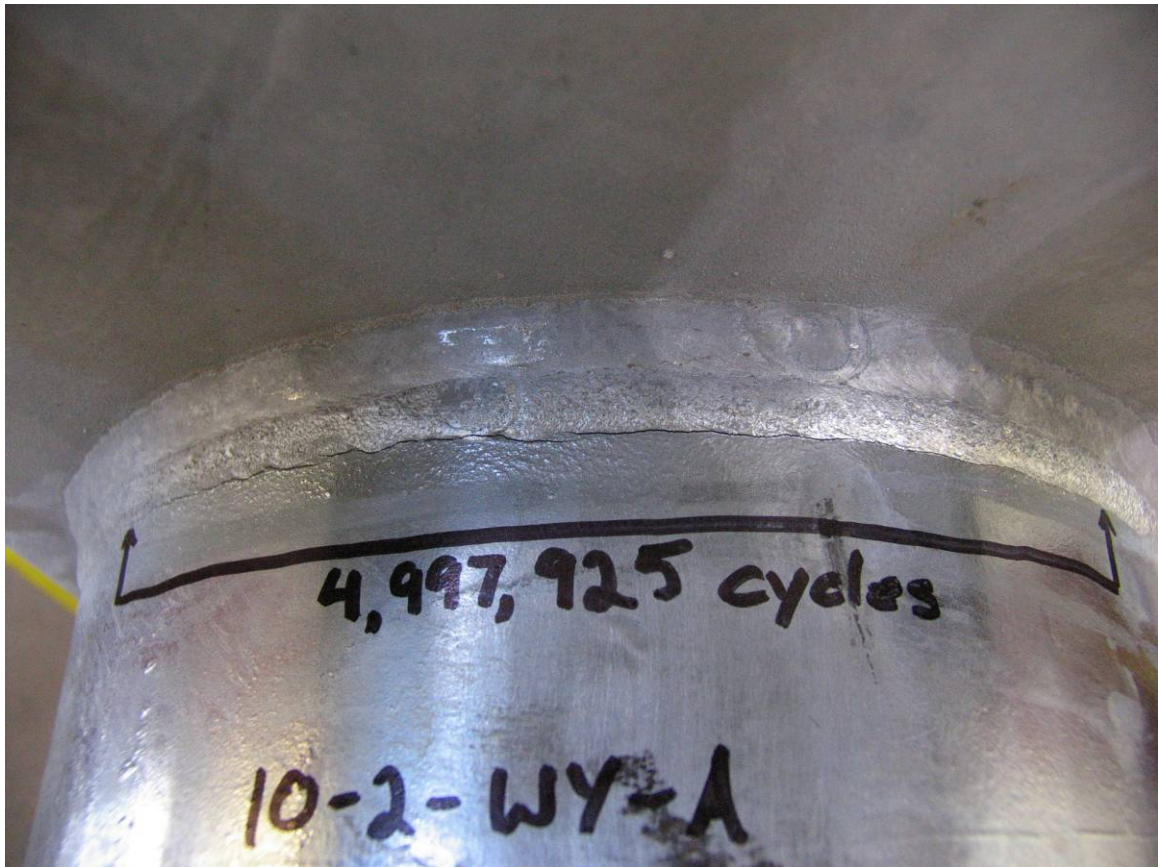


Figure 6.19 Typical Failure of the Full-Penetration Welded Specimens

After testing, a cross section of a full-penetration welded specimen was cut to reveal the connection detail and weld profile. The cross section was ground, polished, and etched with a nitric acid solution to reveal the weld and the weld penetration as well as to highlight the fatigue crack. The etched cross section is shown in Figure 6.20. The fatigue crack can be seen through the pole wall at the toe of the weld and is shown in more detail in Figure 6.21.

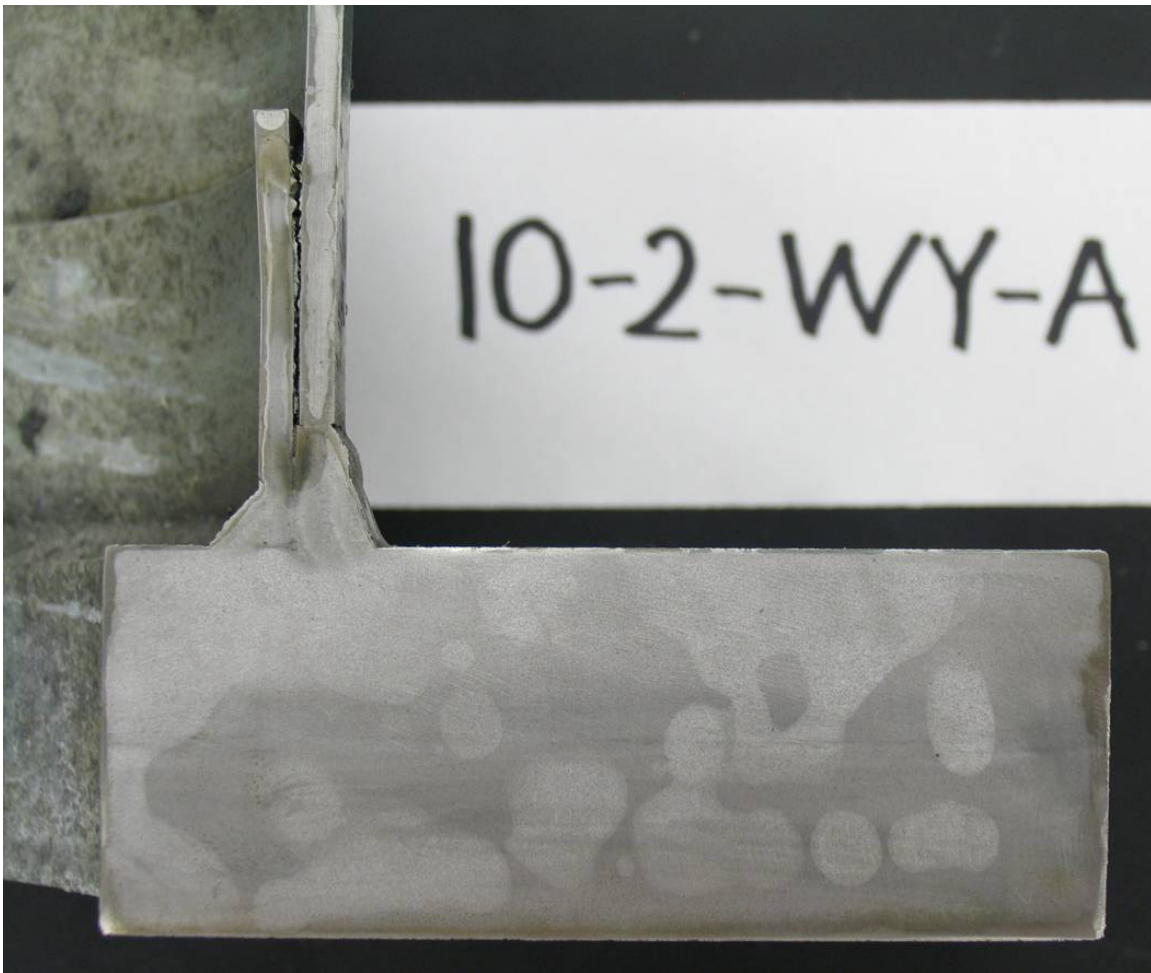


Figure 6.20 Etched Cross Section of a Full-Penetration Welded Specimen

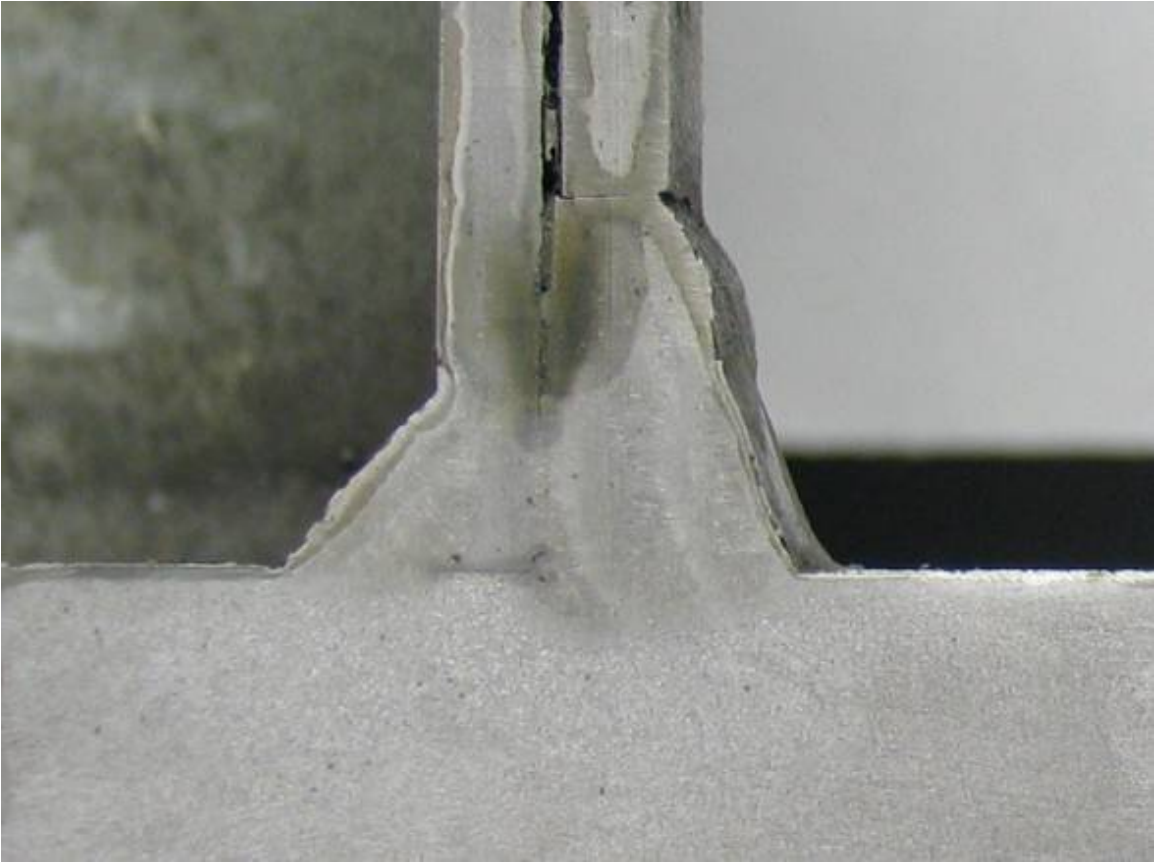


Figure 6.21 Detailed View of Etched Failure Location

The results of the fatigue testing on the full-penetration welded specimens are summarized in Table 6.1 and are also shown graphically in Figure 6.22.

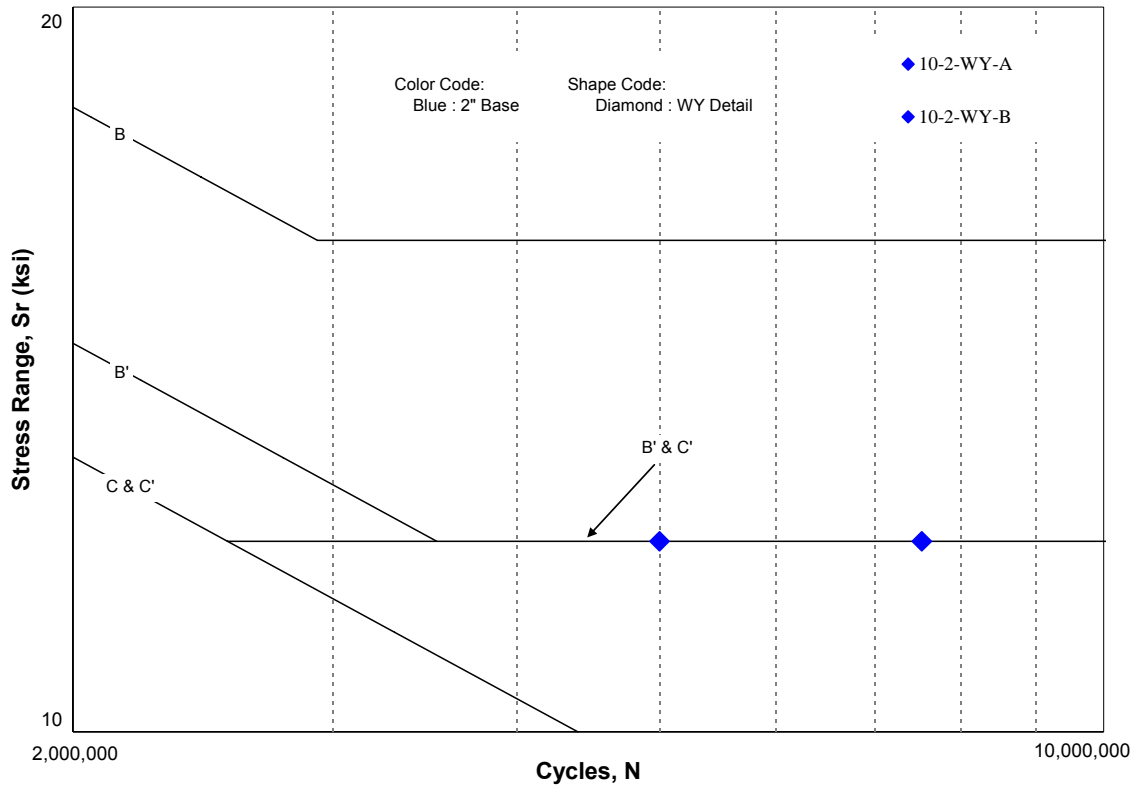


Figure 6.22 Full-Penetration Welded Specimens Fatigue Test Results

6.3.4 Run-Out Specimens

A total of 4 specimens tested over the course of this test program did not fail under fatigue loading and were considered run-outs. Two of the specimens were standard socketed connection specimens and the other two specimens were external collar specimens.

6.3.4.1 Standard Socketed Connection Run-Out Specimens

The two standard socketed connection specimens that did not fail under fatigue loading had different base plate thicknesses; one specimen had a base plate thickness of 1.75-in and the other specimen had a base plate thickness of 3-in. In both cases, fatigue cracks were not observed when testing had stopped. There was, however, a marked difference between the specimens that did not fail under fatigue loading and those that did. In both specimens that did not fail under fatigue loading, it was observed that the toe of the base plate to pole wall fillet weld had been ground smooth during manufacturing before galvanizing. This can be seen in Figure 6.23 and in further detail in Figure 6.24.



Figure 6.23 Base Plate to Pole Wall Fillet Weld on Run-Out Specimen

It is thought that the fillet welds were made larger than specified and subsequently ground down to comply with the specified size. The other standard socketed connection specimens did not have a smooth weld toe as shown in Figure 6.2



Figure 6.24 Detailed View of Base Plate to Pole Wall Fillet Weld

6.3.4.2 External Collar Run-Out Specimens

The two standard external collar specimens that did not fail under fatigue loading had different base plate thicknesses; one specimen had a base plate thickness of 1.75-in and the other specimen had a base plate thickness of 2-in. In both cases, fatigue cracks were not observed when testing had stopped. No difference between the specimens that did not fail under fatigue loading and those that did was observed.

CHAPTER 7

Discussion of Fatigue Test Results

The results of the fatigue testing are discussed in this chapter. The discussion examines the influence of the test specimen design variables in the order presented earlier. The influence on the fatigue performance of varying the base plate thickness for certain connection types will first be discussed. This will be followed by a discussion of the influence of varying the weld type used and adding external collars. Additionally, the influence on the fatigue performance of the fully effective behavior of the external collar will briefly be discussed.

7.1 INFLUENCE OF DESIGN VARIABLES

7.1.1 Base Plate Thickness

The base plate thickness was varied for two of the connection types tested; the standard socketed connection and the external collar connection. Three base plate thicknesses were tested with standard socketed connections; 1.75-in, 2-in, and 3-in. Two base plate thicknesses were tested with external collar connections; 1.75-in and 2-in.

7.1.1.1 *Standard Socketed Connection Specimens*

The results of the fatigue testing of the standard socketed connection specimens are plotted in Figure 7.1. All eight specimens tested were subjected to a stress range of 12-ksi at the base plate to pole wall weld; the only difference between the specimens was the base plate thicknesses.

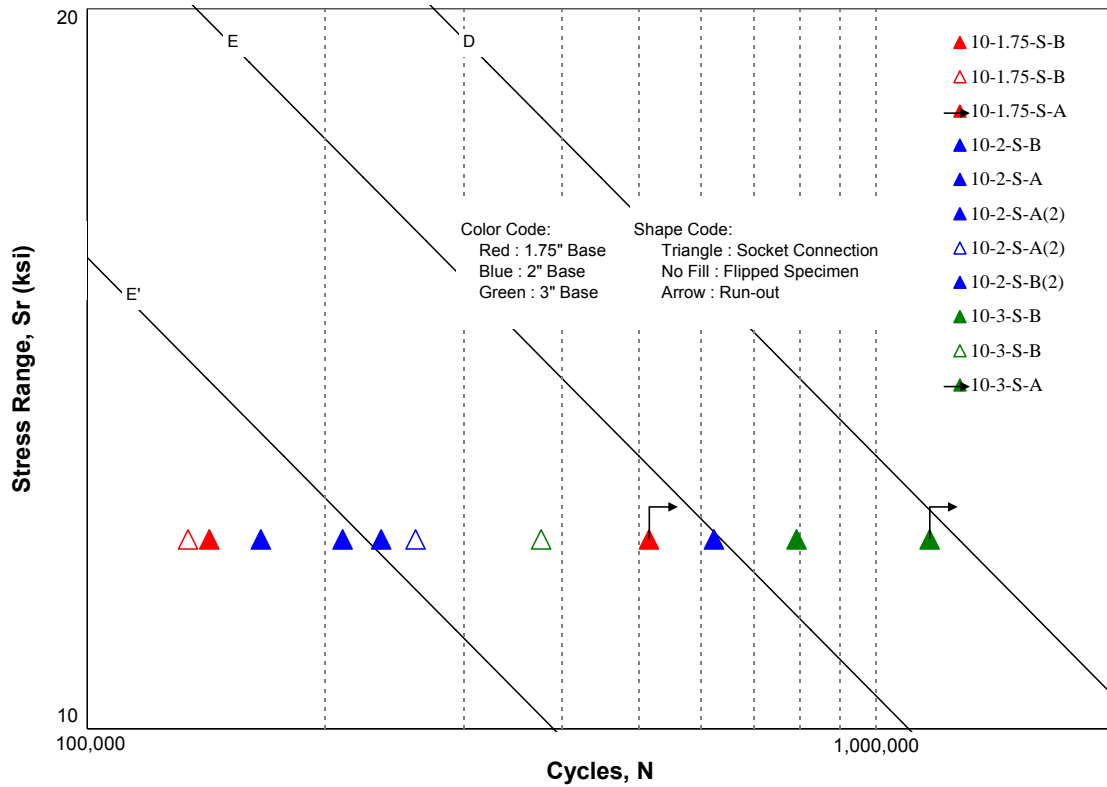


Figure 7.1 Standard Socketed Connection Fatigue Test Results

To illustrate the influence that varying the base plate thickness had on the fatigue performance of the standard socketed connection specimens, the average of the number of cycles to failure under fatigue loading for specimens having the same base plate thickness was determined. Averages were calculated for (1) all specimens excluding both flipped and run-out specimens, (2) all specimens including flipped specimens only, (3) all specimens including run-out specimens only, and, (4) all specimens including both flipped and run-out specimens. These averages are shown in Table 7.1. Two groups of specimens had run-outs; the specimens with base plate thicknesses of 1.75-in and the specimens with base plate thicknesses of 3-in. All three groups had flipped specimens.

**Table 7.1 Average Number of Cycles to Failure
(Standard Socketed Connection Specimens)**

Base Plate Thickness (in)	Connection Detail	Average Number of Cycles to Failure (10% Drop in Load)			
		Failures	Failures + Flipped	Failures + Run-Outs	Failures + Flipped + Run-Outs
1.75	Standard Socket	142,857	138,527	329,111	264,140
2	Standard Socket	308,893	299,255	N/A	N/A
3	Standard Socket	792,576	584,434	980,722	779,245

The inclusion of only the flipped specimens reduces the averages for all three groups of standard socketed connection specimens. The resulting averages are thought to be accurate since the flipped specimens provide another representative fatigue life evaluation. Including only the run-out specimens increases the averages for all three groups. This is not surprising since the run-out specimens performed significantly better than those that failed. The averages including both the flipped and run-out specimens are again slightly lower than including only the run-out specimens. This is again thought to be accurate when compared to the averages of including only the run-out specimens. It is important to note that both the averages including the run-out specimens could be considered a lower bound mean since the fatigue life of the run-out specimens would be larger than the recorded number of cycles.

The average numbers of cycles to failure for the three groups of standard socketed connection specimens with varying base plate thicknesses including only the flipped specimens shown in Table 7.1 are plotted in Figure 7.2. The AASHTO fatigue stress category curves are also shown. The influence of varying the base plate thicknesses is clear, with the fatigue performance improving as the base plate thickness increases.

The fatigue provisions of the 2001 AASHTO Highway Signs, Luminaires and Traffic Signal Specifications classifies the fatigue details of cantilevered support structures by stress category, only considering the type of weld used and the loading condition. For fillet welded tube to transverse plate connections, a standard socketed connection, the fatigue stress category is E'. This classification ignores element sizes like the base plate thickness. From the plot shown in Figure 7.2, the group of specimens with a base plate thickness of 1.75-in did not reach category E' while the group of specimens with a base plate thickness of 2-in performed better than category E'. Furthermore, the group of specimens with a base plate thickness of 3-in almost reached category E. This indicates that the AASHTO stress category classification is not accurate and that increasing the base plate thickness for socketed connections will increase the fatigue performance.

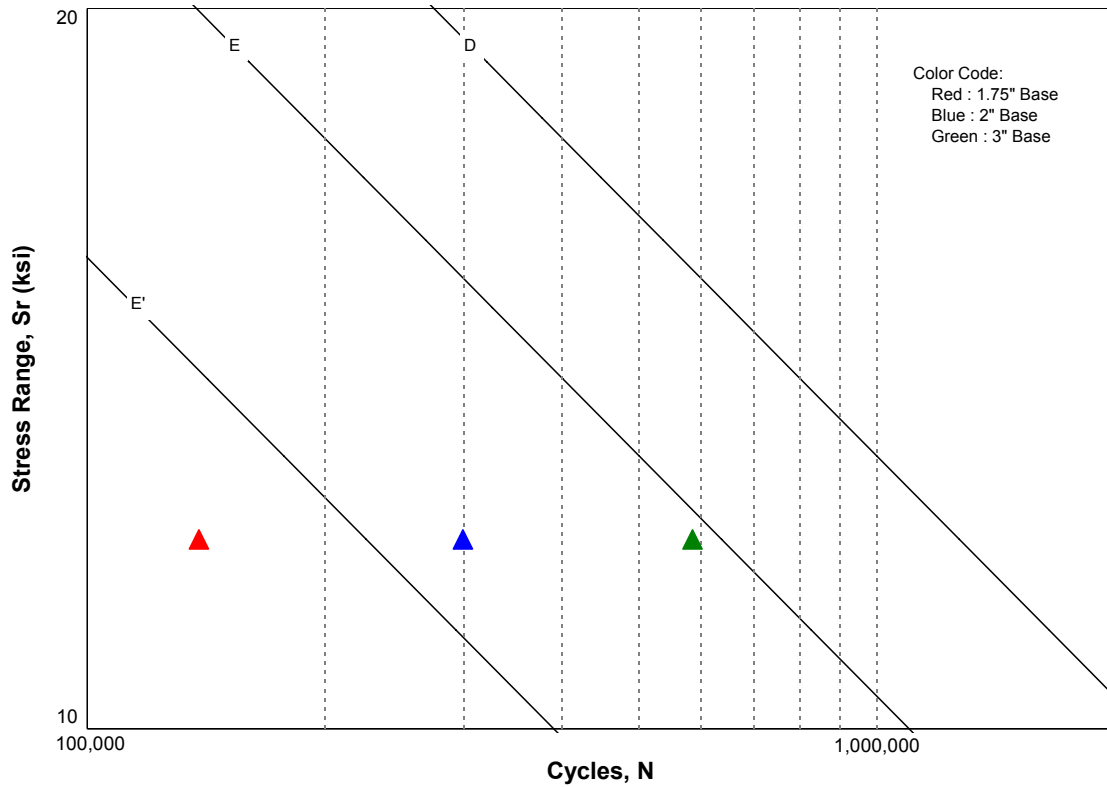


Figure 7.2 Influence of Base Plate Thickness on Fatigue Performance (Standard Connection Specimens)

7.1.1.2 External Collar Specimens

The results of the fatigue testing of the external collar specimens are plotted in Figure 7.3. All eight specimens tested were subjected to a stress range of 12-ksi at the base plate to pole wall weld; the only difference between the specimens being the base plate thicknesses.

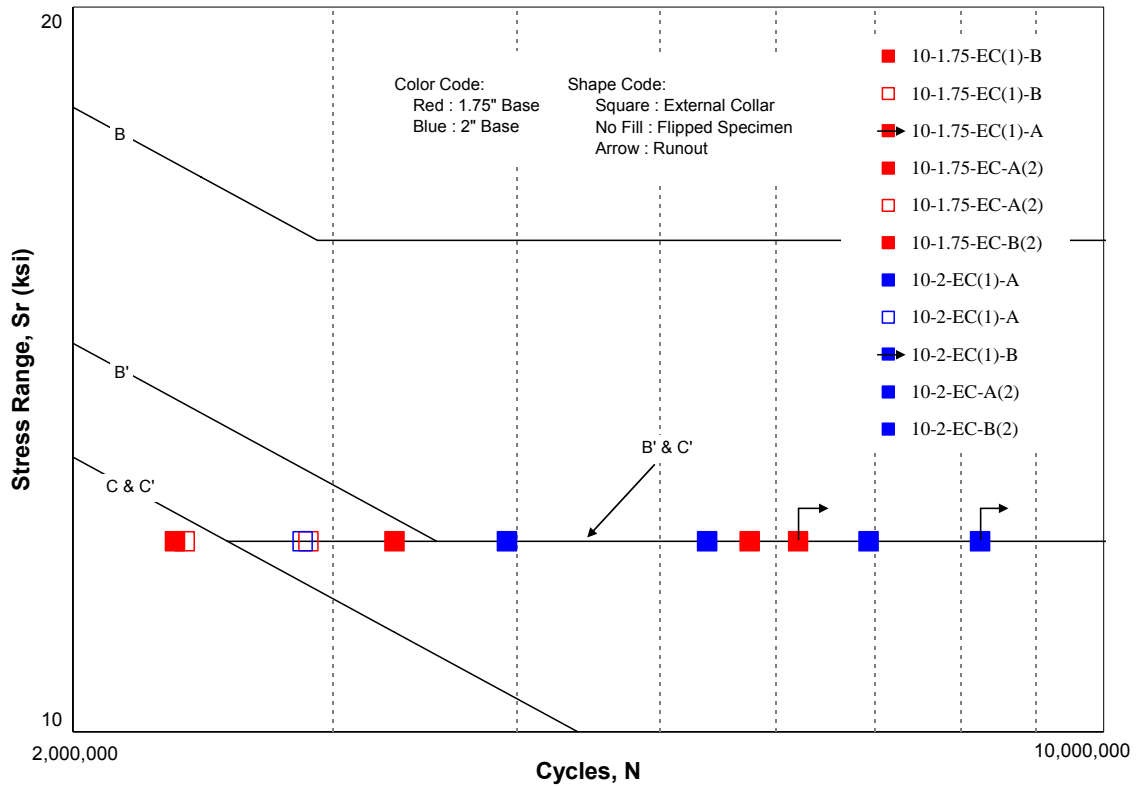


Figure 7.3 External Collar Specimens Fatigue Test Results

To illustrate the influence that varying the base plate thickness had on the fatigue performance of the external collar specimens, the average of the number of cycles to failure under fatigue loading for specimens having the same base plate thickness was determined. Averages were calculated in the same way as was done with the standard socketed connection specimens and are shown in Table 7.2. Both groups of specimens with base plate thicknesses of 1.75-in and 2-in had run-outs and flipped specimens.

**Table 7.2 Average Number of Cycles to Failure
(External Collar Specimens)**

Base Plate Thickness (in)	Connection Detail	Average Number of Cycles to Failure (10% Drop in Load)			
		Failures	Failures + Flipped	Failures + Run-Outs	Failures + Flipped + Run-Outs
1.75	External Collar	3,801,832	3,335,413	4,403,063	3,813,970
2	External Collar	5,416,949	4,778,592	6,124,628	5,472,407

The inclusion of only the flipped specimens reduces the averages for the two groups of external collar specimens. The resulting averages are thought to be accurate since the flipped specimens provide another representative fatigue life evaluation. Including only the run-out specimens increases the averages for both groups. This is not too surprising since the run-out specimens performed better than those that failed. The averages including both the flipped and run-out specimens are again slightly lower than including only the run-out specimens. This is again thought to be accurate when compared to the averages of including only the run-out specimens. It is again important to note that both the averages including the run-out specimens could be considered a lower bound mean since the fatigue life of the run-out specimens would be larger than the recorded number of cycles.

The average numbers of cycles to failure for the two groups of external collar specimens with varying base plate thicknesses including only the flipped specimens are plotted in Figure 7.4. The AASHTO fatigue stress category curves are also shown. The influence of varying the base plate thicknesses is clear, as was the case with the standard socketed connection specimens, with the fatigue performance improving as the base plate thickness increases.

The fatigue provisions of the 2001 AASHTO Highway Signs, Luminaires and Traffic Signal Specifications do not have an explicit fatigue detail classification for the external collar connection. However, both groups of external collar specimens reach fatigue stress category C' with the group of external collar specimens with 2-in thick base plates exceeding category B'. For the current discussion, the fatigue stress category of the external collar connection is not as important as the observation that the fatigue performance of the external collar specimens is improved with increased base plate thicknesses.

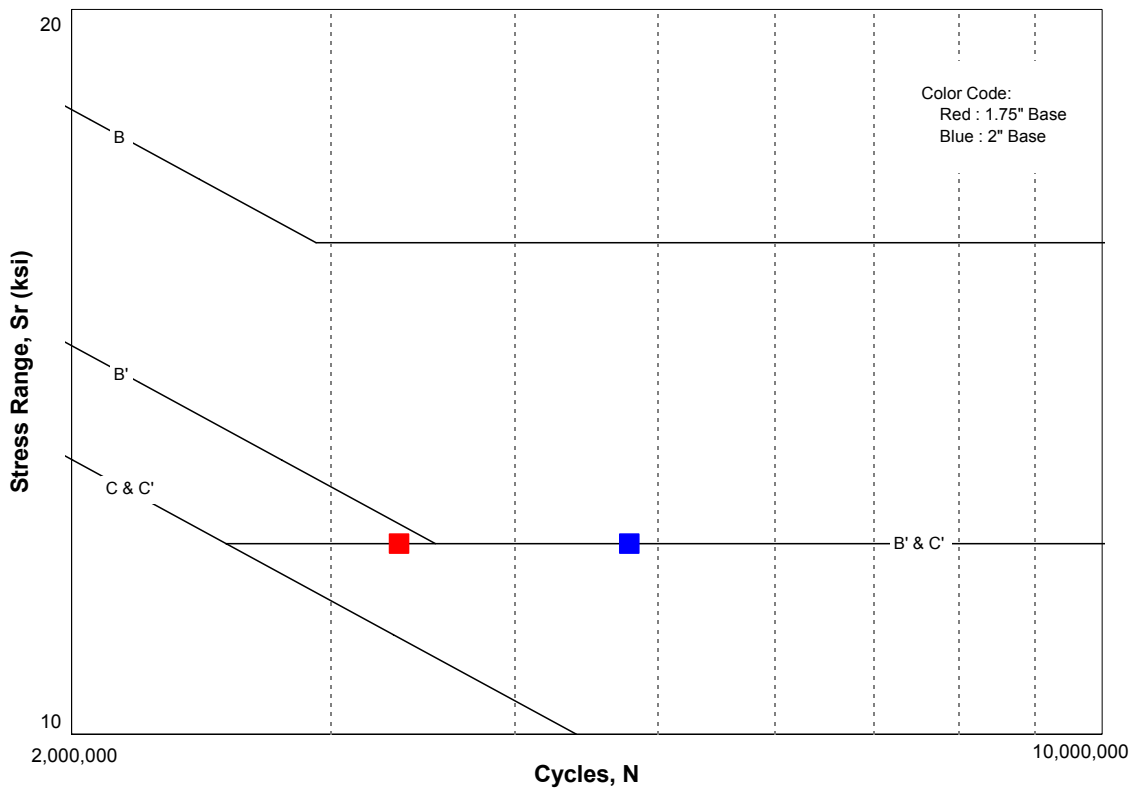


Figure 7.4 Influence of Base Plate Thickness on Fatigue Performance (External Collar Specimens)

7.1.2 Weld Type

The weld type used to make the connection between the mast-arm pole section and the base plate was varied in three groups of specimens. In order to eliminate any other test variable, the base plate thickness was 2-in for each group of specimens. The three groups of specimens were the standard socketed connection specimens, the California weld profile socketed connection specimens, and the full-penetration welded specimens.

To illustrate the influence that varying the weld type used had on the fatigue performance of the test specimens, the average of the number of cycles to failure under fatigue loading for each of the three groups of test specimens was determined. In taking the averages, shown in Table 7.3, the flipped specimens were included. Only the standard socketed connection group had flipped specimens while none of the three groups had run-outs.

**Table 7.3 Average Number of Cycles to Failure
(Different Weld Types)**

Base Plate Thickness (in)	Connection Detail	Average Number of Cycles to Failure (10% Drop in Load)
2	Standard Socket	299,255
2	California Socket	282,005
2	Full-Penetration Weld	6,262,683

The average numbers of cycles to failure for the three groups of test specimens with varying weld types are plotted in Figure 7.5. The AASHTO fatigue stress category curves are also shown. The influence of varying the weld type used is quite clear when comparing the two groups of socketed connection specimens to the group of full-

penetration welded specimens. The full-penetration welded specimens group's fatigue life was over 20 times that of both the groups of socketed connection specimens.

The difference in fatigue performance is remarkable but should not be attributed to the full-penetration weld alone. One must note that the full-penetration welded specimens had smaller internal holes in their base plates. This change resulted in stiffer base plates. The increased fatigue performance of the full-penetration welded specimens could, therefore, be a result of a combination of both the weld type and the stiffened base plates.

No appreciable difference between the fatigue performances of the two groups of socketed connection specimens was seen. The two groups of socketed connection specimens differed only by the geometry of the base plate to pole wall fillet weld used on either group.

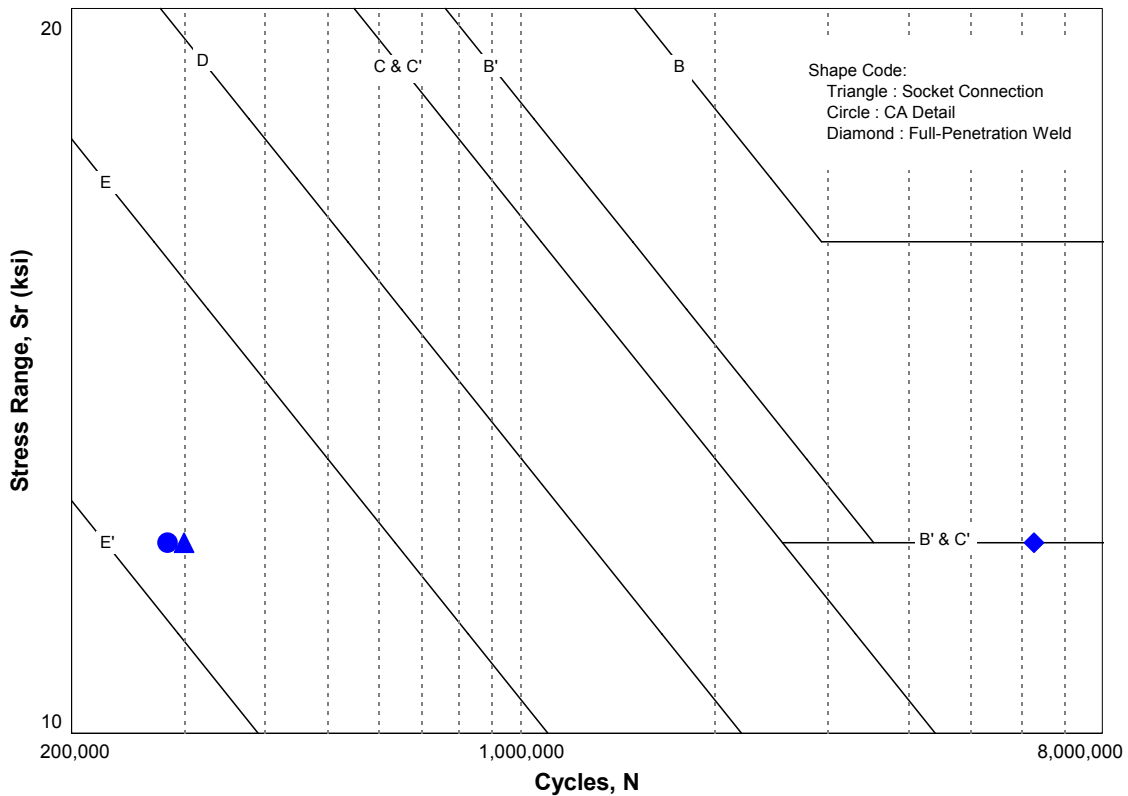


Figure 7.5 Influence of Weld Type on Fatigue Performance

The fatigue provisions of the 2001 AASHTO Highway Signs, Luminaires and Traffic Signal Specifications classify both groups of socketed connection specimens as fatigue stress category E'. This classification is accurate for the two groups of socketed connection specimens tested since both groups exceed category E', however, both groups had specimens with 2-in thick base plates. The group of full-penetration welded specimens far exceeded the fatigue stress category classification of E' assigned to full-penetration groove welded tube to transverse plate connections. This indicates that the AASHTO stress category might underestimate the fatigue performance of full-penetration welded tube to transverse plate connections. (The 2006 Interim to the 2001

AASHTO Highway Signs, Luminaires and Traffic Signal Specifications classifies the full-penetration welded specimens tested in this testing program as fatigue stress category E. This change in classification is due to the inclusion of full-penetration welded tube to transverse plate connections with a backing ring attached to the plate with a continuous fillet weld around interior face of backing ring to fatigue stress category E. Even with this change, the AASHTO specification still underestimates the fatigue performance of full-penetration welded tube to transverse plate connections).

7.1.3 External Stiffeners

In order to fully assess the influence of adding external stiffeners in the form of external collars to socketed connection specimens, two approaches will be presented. The first examines the addition of the external collar by the Value Based Design Analysis Method where the fatigue life of the external collar specimens is shown without considering the change in section properties as a result of adding the external collar. The second examines the addition of the external collar by assuming the external collar is fully effective and contributes to the specimen's section properties.

7.1.3.1 External Collar Specimens

By the Value Based Design Analysis Method, the contribution of the external collar is only to the fatigue performance of the specimen and is not considered when determining the stress range that the specimen was subjected to. The external collar will, therefore, be considered as an element that only affects the fatigue performance of the socketed connection to which it was added. Two groups of specimens were chosen to illustrate the fatigue performance contribution of the external collar, the standard socketed connection specimens and the external collar specimens. In order to eliminate any other test variable, the base plate thickness was 2-in for each group of specimens.

**Table 7.4 Average Number of Cycle to Failure
(External Collar Contribution)**

Base Plate Thickness (in)	Connection Detail	Average Number of Cycles to Failure (10% Drop in Load)
2	Standard Socket	299,255
2	External Collar	4,778,592

The average of the number of cycles to failure under fatigue loading for both groups of specimens was determined to quantify the contribution of the external collar. In taking the averages, shown in Table 7.4, both the specimens that were considered run-outs were not included while the flipped specimens were included. The group of external collar specimens had run-outs while both groups had flipped specimens.

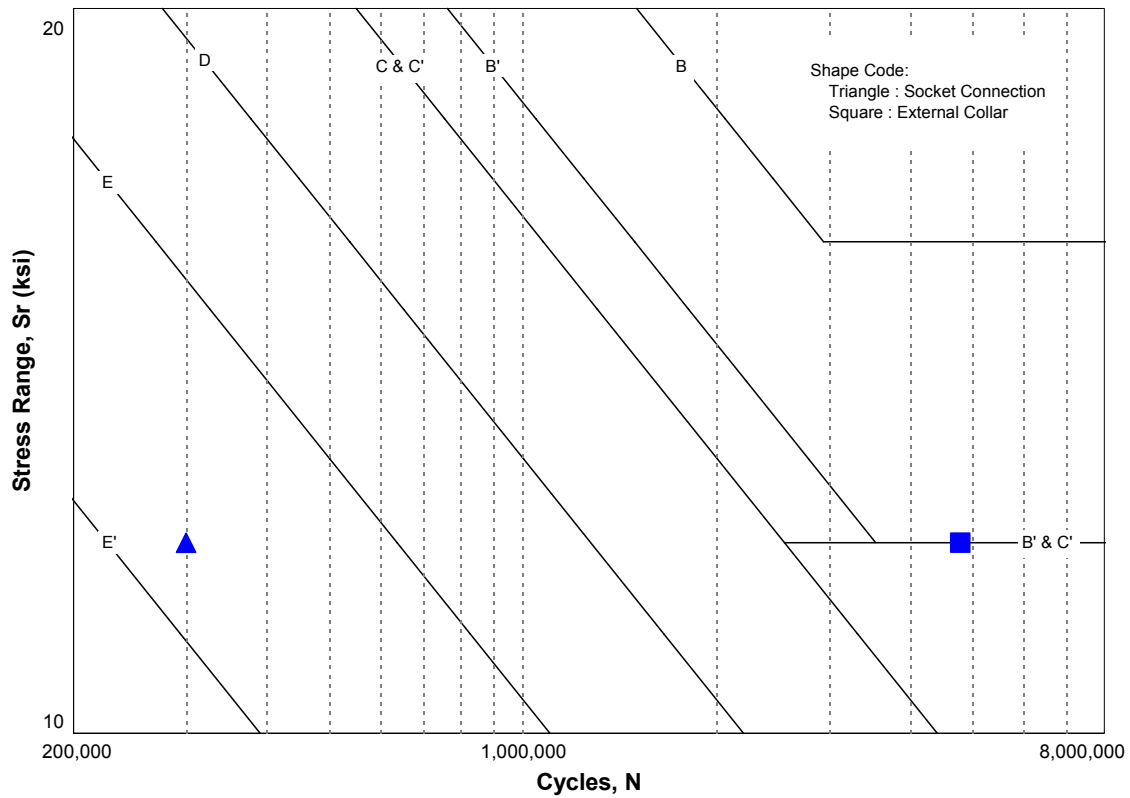


Figure 7.6 Contribution of the External Collar to Fatigue Performance

The average numbers of cycles to failure for the two groups of specimens chosen to illustrate the fatigue performance contribution of the external collar are plotted in **Error! Reference source not found.** The AASHTO fatigue stress category curves are also shown.

The contribution of the external collar to the fatigue performance of the socketed connection specimens is clear, with the fatigue performance improving drastically with the addition of the external collar. The external collar connection specimens group's

fatigue life was nearly 16 times that of the group of standard socketed connection specimens.

Since the addition of the external collar was the only difference between these two groups of specimens, the contribution of this additional element to the fatigue performance of the socketed connection is clearly indicated by the Value Based Design Analysis Method.

7.1.3.2 Fully Effective Behavior of External Collar

Previous researchers have shown that the external collar is not fully effective (Koenigs et al., 2003). It would, therefore, be a bad assumption to rely on the external collar to contribute to the section properties of a cantilevered mast-arm structure when calculating the stress range for design purposes. However, since the degree of effectiveness of the external collar is not known, several locations were chosen on the external collar connection for calculating the stress range to illustrate the uncertainty accompanying this particular design. The group of external collar specimens with 2-in thick base plates was chosen for this illustration.

In addition to the base plate to pole wall connection, three locations were chosen to calculate the stress range experienced by the external collar connection. These three locations are shown in Figure 7.7 and are, as numbered, (1) the external collar to pole wall fillet weld at the collar minimum dimension at the top of the mast-arm, (2) the external collar to pole wall fillet weld at the collar maximum dimension at approximately 45° from the top of the mast-arm, and, (3) the base plate to external collar connection at the top of the mast-arm.

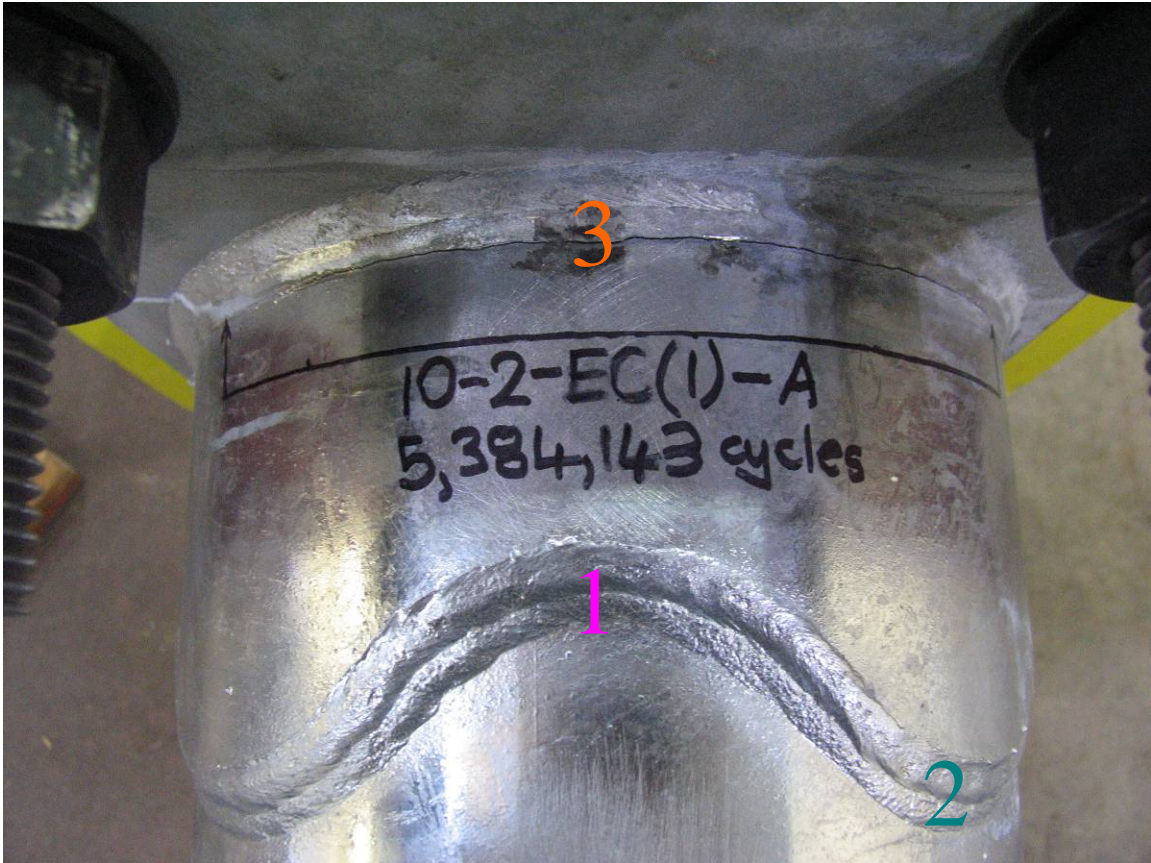


Figure 7.7 Additional Locations for Stress Range Calculation

The calculated stress ranges experienced at the four locations described above along with the average numbers of cycles to failure for the group of external collar specimens with 2-in base plates is shown in Figure 7.8. For comparison, the average number of cycles to failure for the group of standard socketed specimens with 2-in base plates is also shown.

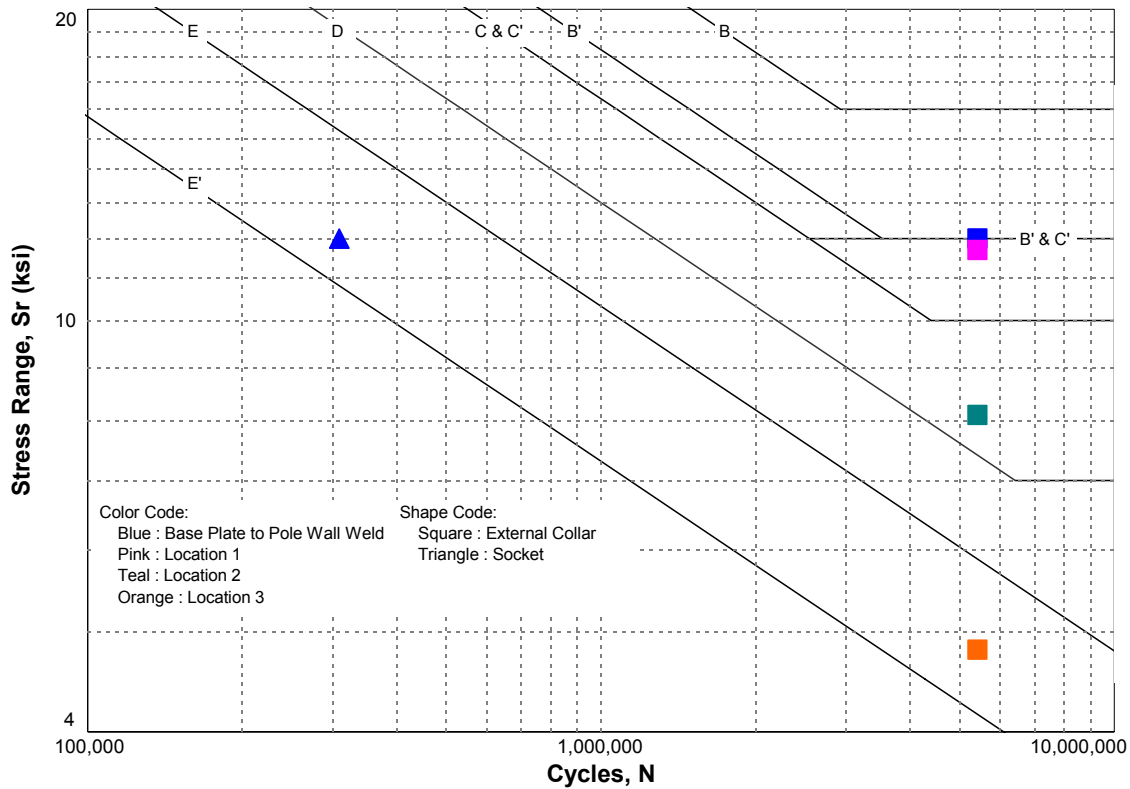


Figure 7.8 Influence of Stress Range Calculation Location on Fatigue Category

The result for the stress range of 12-ksi calculated under the assumption that the external collar does not contribute to the section properties of the mast-arm is shown in blue. The results for the stress range calculated at the external collar to pole wall fillet weld at both the collar minimum and maximum dimension, locations 1 and 2, are shown in pink and teal respectively. The stress ranges calculated at these two locations were 11.7-ksi and 8.1-ksi. In both cases, at the external collar to pole wall connection, the contribution of the external collar to the section properties was ignored. The result for the stress range calculated under the assumption that the external collar is fully effective, at location 3, is shown in orange. This stress range was calculated to be 4.8-ksi.

As mentioned before, the fatigue provisions of the 2001 AASHTO Highway Signs, Luminaires and Traffic Signal Specifications do not have an explicit fatigue detail classification for the external collar connection. However, the three additional locations chosen to calculate the stress range experienced by the external collar connection could be classified separately.

The base plate to external collar weld could be classified as an E' detail considering that both fillet welded and full-penetration groove welded tube to transverse plate connections are classified as stress category E' details. Since the weld used is a partial-penetration groove weld, the stress category E' classification might be appropriate. This classification diminishes the impact of the external collar as the socketed connection specimens tested were also classified as stress category E'. As is indicated by the fatigue provision, nothing is gained by adding the external collar. However, as was shown before, the fatigue life drastically increased.

For both the external collar to pole wall connection locations, the fatigue classification is not explicit. However, if fatigue stress category E' is chosen, both locations will exceed this category. This exceedance of the fatigue stress category E' goes some way to indicate the influence of the external collar, but is not as dramatic as was the case when the external collar was ignored when calculating the section properties.

In comparing the case of assumed fully effective external collar behavior to the socketed connection, nothing seems to be gained by the addition of the external collar since both fall into fatigue stress category E'. This similar categorization ignores the dramatic increase in fatigue life of the external collar specimens.

CHAPTER 8

Base Plate Stiffness

In order to better identify the overall characteristic of the mast-arm test specimen that contributed to the test specimen's fatigue performance, a numerical evaluation of all the test specimens tested in this testing program was undertaken. In addition to the test specimens tested in this testing program, specimens from the previous research undertaken at the University of Texas and high-mast test specimens tested concurrently to this testing program were also included.

8.1 MOTIVATION FOR NUMERICAL EVALUATION

During research evaluating the fatigue performance of high-mast lighting structures conducted concurrently with this testing program at the University of Texas, the researcher observed that the stiffness of the pair of specimens could be related to the fatigue performance of the specimens. The test setup used was similar to the one utilized in this testing program only on a larger scale. The researcher determined the paired specimen stiffness, shown in Table 8.1, by dividing the load range undergone during testing by the total test deflection. The load range was simply the difference between the maximum and minimum loads that produced the stress range desired during testing. The total test deflection was twice the testing amplitude. The researcher then compared the paired specimen stiffness to the average fatigue life of the specimens being tested as shown in Figure 8.1. The researcher observed that, in general, as the paired specimen stiffness increased, the fatigue life improved.

Table 8.1 High-Mast Paired Specimen Stiffness (Courtesy of Craig Rios)

Specimen Set	Average Number of Cycles to Failure	Maximum Load (kips)	Minimum Load (kips)	Load Range (kips)	Testing Amplitude (in)	Total Deflection (in)	Paired Specimen Stiffness (kips/in)
24-1.5-8-S-A,B	13,193	34.820	15.827	18.993	0.352	0.704	26.979
24-2-8-S-A,B	46,772	36.505	16.593	19.912	0.310	0.619	32.168
24-2-8-WY-A,B	133,809	36.804	16.729	20.075	0.289	0.577	34.792
24-3-8-S-A,B	147,550	36.589	16.631	19.958	0.271	0.542	36.823
24-2-8-SB-A,B	634,186	36.106	16.412	19.694	0.225	0.450	43.764
24-1.5-12-S-A,B	27,977	36.299	16.500	19.799	0.314	0.628	31.527
24-2-12-S-A,B	143,214	36.216	16.462	19.754	0.279	0.557	35.465

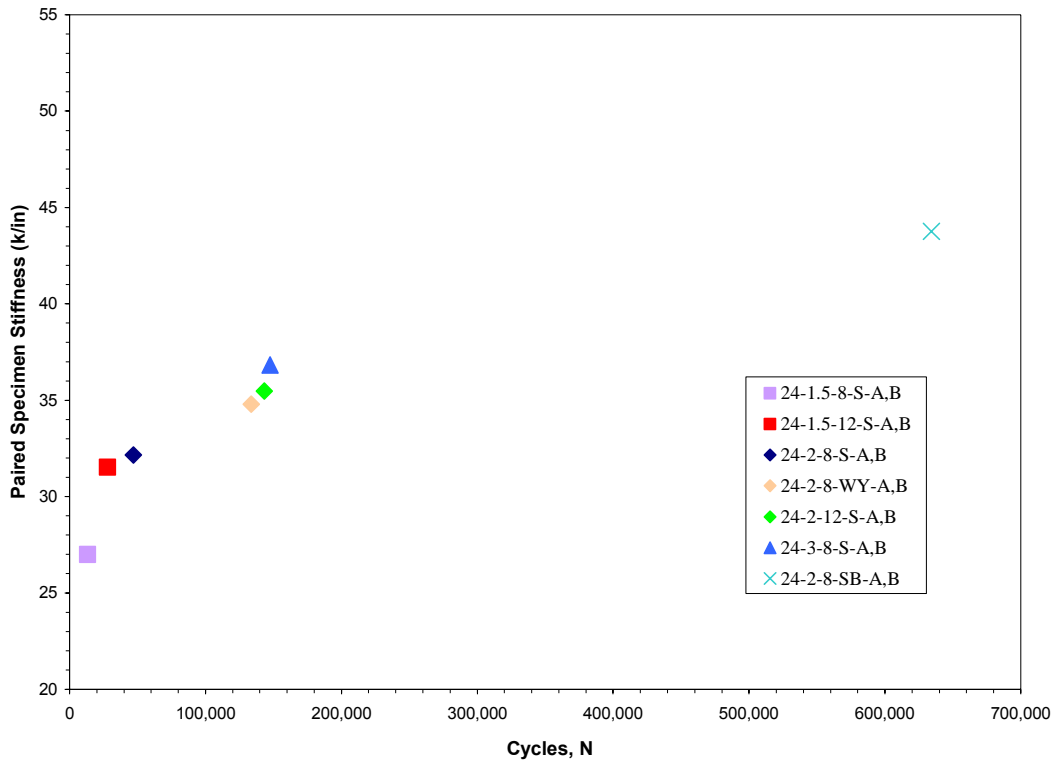
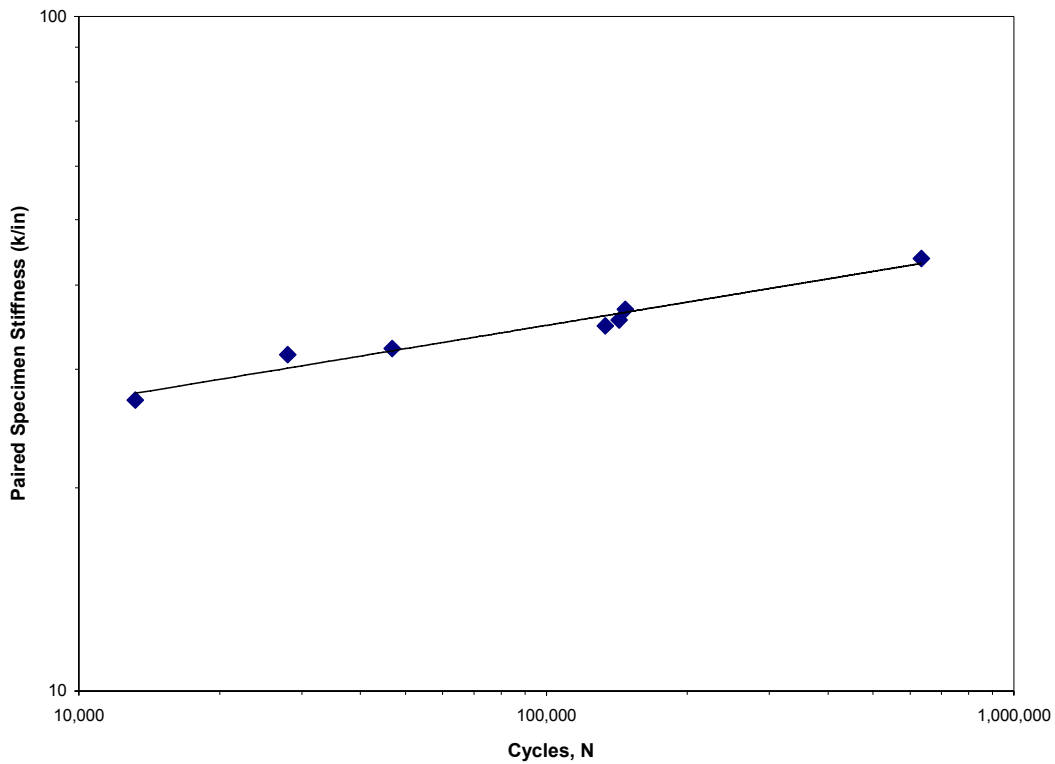


Figure 8.1 High-Mast Paired Specimen Stiffness (Courtesy of Craig Rios)



**Figure 8.2 High-Mast Paired Specimen Stiffness [Logarithmic Scale]
(Courtesy of Craig Rios)**

This general relationship between the paired specimen stiffness and the fatigue life of the high-mast specimens motivated the researcher to further evaluation of the data and the logarithmic plot shown in Figure 8.2 was created. As can be seen, a general straight-line relationship was observed.

8.2 NUMERICAL EVALUATION

The relationship between paired specimen stiffness and fatigue life observed by the researcher evaluating the fatigue performance of high-mast lighting specimens led to a search for a similar relationship in the mast-arm specimens tested in this testing program.

8.2.1 Further Refinement of Numerical Evaluation

As the relationship between paired specimen stiffness and fatigue life for the mast-arm specimens tested in this testing program was being evaluated, it became evident that further refinement of the relationship was necessary. The relationship observed was judged to be both insufficient when other geometric variables such as pole diameter were varied as well as unspecific when it came to evaluating what component specifically contributed to the fatigue performance of mast-arm type structures.

The observation was made that, in general, two components contributed to the paired specimen stiffness: (1) the mast-arm pole section and (2) the mast-arm base plate connection. Since the mast-arm pole section was essentially the same for each mast-arm specimen tested, it was decided to focus on the mast-arm base plate connection as the component that determined the fatigue performance. The question of what effect, if any, the base plate to loading box connection had on the fatigue performance of the mast-arm base plate connection was considered during this evaluation. The conclusion was made that the specimens were installed and connected in a fairly similar manner each time and that the effect, if any, that the base plate to loading box connection had on the fatigue performance of the mast-arm base plate connection would be fairly consistent throughout and, therefore, would not be separately evaluated.

8.2.2 Determination of Base Plate Rotational Stiffness

The base plate rotational stiffness was determined based on the assumption that the total deflection undergone during testing was made up of two components, (1) the deflection of the mast-arm pole section, and (2) the deflection due to the rotation of the base plate connection. The total deflection undergone during testing was known and the deflection of the mast-arm pole section could be calculated based on a fixed tapered beam model with a point load at the end. This analysis was done using the area moment method

described in section 2.5 of the Design of Welded Structures published by the James F. Lincoln Arc Welding Foundation (Blodgett, 1966). The tapered mast-arm was modeled using 100 straight round sections. An example is shown in Appendix A. The deflection due to the rotation of the base plate connection would then be the difference between the total deflection undergone during testing and the calculated mast-arm pole section deflection. The rotational stiffness of the base plate connection, shown in Table 8.2, would then be calculated by dividing the moment at the connection by the rotation undergone; the rotation simply being the deflection due to the rotation divided by the specimen length. The mast-arm pole section stiffness, the load range divided by the deflection of the mast-arm pole section, is also shown.

Table 8.2 Base Plate Rotational Stiffness

Specimen	Load Range (kips)	Δ_{test} (in)	Δ_{mast} (in)	Δ_{bp} (in)	k_{mast} (k/in)	k_{bp} (k-in)
10-2-S-A,B	1.815	0.339	0.233	0.106	7.78	126,864
10-2-CA-A,B	1.792	0.315	0.234	0.081	7.66	164,659
10-1.75-S-A,B	1.809	0.338	0.235	0.103	7.71	130,582
10-2-S-A,B(2)	1.796	0.318	0.234	0.084	7.68	158,357
10-3-S-A,B	1.819	0.277	0.229	0.048	7.95	272,412
10-1.75-EC-A,B(2)	1.809	0.292	0.234	0.058	7.72	233,810
10-1.75-EC(1)-A,B	1.826	0.296	0.234	0.062	7.82	217,960
10-2-EC-A,B(2)	1.844	0.288	0.232	0.056	7.96	242,439
10-2-WY-A,B	1.859	0.299	0.232	0.067	8.01	206,156
10-2-EC(1)-A,B	1.819	0.278	0.232	0.046	7.82	295,666

8.2.3 Base Plate Rotational Stiffness Normalization

In order to allow for a non-dimensional base plate rotational stiffness that would facilitate in the comparison of test data outside of the scope of this testing program, a normalized base plate rotational stiffness was determined. The normalized base plate rotational stiffnesses for the test specimens included in this testing program are shown in Figure 8.3. The specimen pairs are arranged from the worst average fatigue performance to the best. The normalization was achieved by multiplying the calculated base plate rotational stiffness by the pole wall thickness and dividing by the product of the calculated mast-arm stiffness, the area enclosed by the mast-arm pole section at the base plate connection, and, the nominal diameter of the pole section as shown in the following equation:

$$k_{normalized} = \frac{k_{bp} \cdot t}{k_{mast} \cdot A_o \cdot d_o}$$

Adding the pole wall thickness and the nominal diameter would allow for comparison with other test data, including the concurrent high-mast research data.

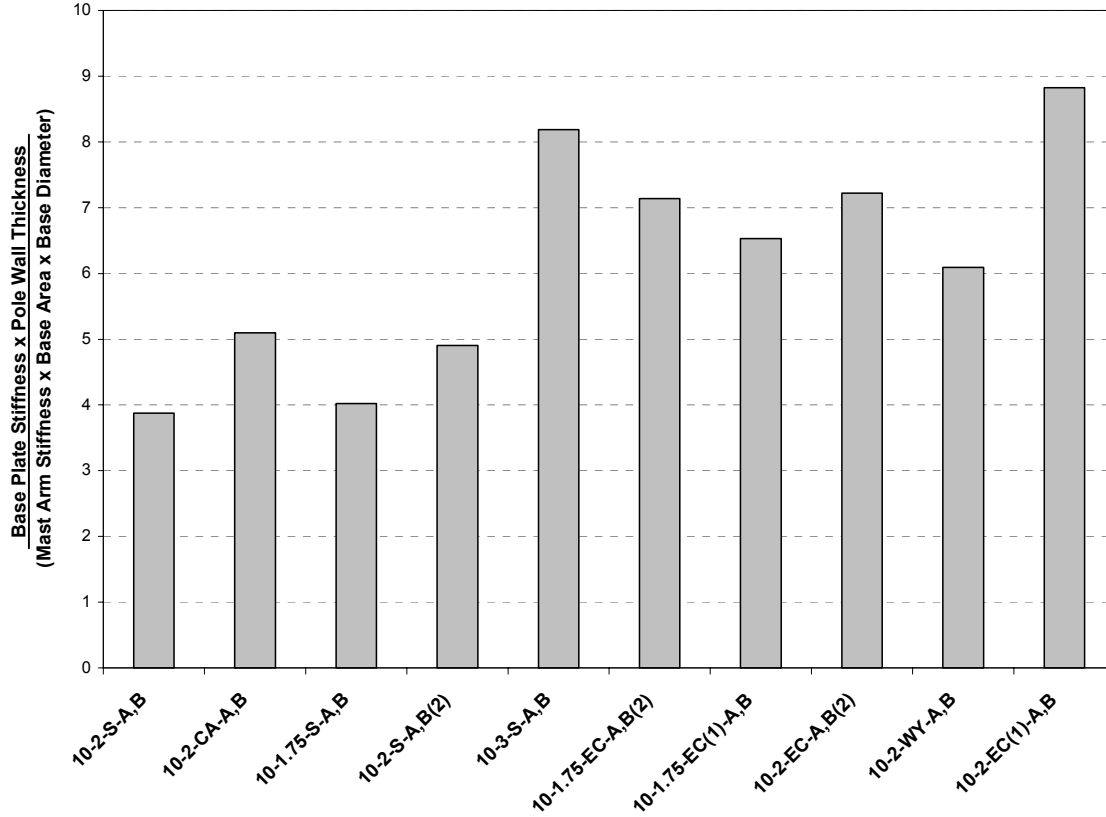


Figure 8.3 Normalized Base Plate Rotational Stiffness

8.3 COMPARISON WITH EXISTING DATA

The decision was made to compare the fatigue performance of the specimens tested in this testing program utilizing the normalized base plate rotational stiffness to both the concurrent high-mast fatigue research as well as the previous research conducted at the University of Texas. This was done to evaluate whether or not the base plate rotational stiffness could be isolated as one of the major contributors to the fatigue performance of mast-arm type structures. The fatigue performance of the specimens being compared was also normalized by utilizing the fatigue life coefficient, A , to allow for comparison with tests conducted at varying stress ranges.

The base plate rotational stiffness along with the fatigue life coefficient for each pair of specimens compared is presented in both Table 8.3 and Table 8.4. The data used for comparison for the specimens tested in this testing program as well as the concurrent high-mast data is presented in Table 8.3 while the data from the previous research conducted at the University of Texas is presented in Table 8.4. The stress range is presented in the second column with the fatigue life of each specimen (excluding flipped specimens but including run-outs) presented in the third and fourth columns. The average and logarithmic average is presented in the fifth and sixth columns. The logarithmic average was determined by the following equation:

$$N_{log} = 10^{\left(\frac{\log(N_A) + \log(N_B)}{2} \right)}$$

The fatigue life coefficients are presented in columns seven through ten with the normalized base plate rotational stiffness completing the table in column eleven. The fatigue life coefficient was determined by the following equation:

$$A_i = \frac{N_i \cdot S_r^3}{10^8}$$

The average fatigue life coefficient is compared to the normalized base plate rotational stiffness in Figure 8.4. It can be seen that a relationship does indeed exist between the fatigue performance and the base plate rotational stiffness. It could be inferred that somehow increasing the base plate rotational stiffness would improve the fatigue performance of mast-arm type structures.

Table 8.3 Normalized Base Plate Rotational Stiffness Data Including Concurrent High-Mast Research

Specimen Pair	Stress Range (ksi)	N _A	N _B	N _{avg}	N _{log}	A _{min}	A _{max}	A _{avg}	A _{log}	k _{bp} t/(k _{mast} A _o d _o)
10-1.75-S-A,B	12.0	515,365	142,857	329,111	271,337	2.5	8.9	5.7	4.7	4.02
10-2-S-A,B	12.0	235,854	165,998	200,926	197,867	2.9	4.1	3.5	3.4	3.87
10-2-S-A,B(2)	12.0	210,793	622,928	416,861	362,366	3.6	10.8	7.2	6.3	4.91
10-3-S-A,B	12.0	1,168,867	792,576	980,722	962,505	13.7	20.2	16.9	16.6	8.19
10-1.75-EC-A,B(2)	12.0	2,345,896	5,755,111	4,050,504	3,674,356	40.5	99.4	70.0	63.5	7.14
10-1.75-EC(1)-A,B	12.0	6,206,754	3,304,490	4,755,622	4,528,814	57.1	107.3	82.2	78.3	6.53
10-2-CA-A,B	12.0	253,657	310,352	282,005	280,576	4.4	5.4	4.9	4.8	5.10
10-2-WY-A,B	12.0	4,997,925	7,527,441	6,262,683	6,133,644	86.4	130.1	108.2	106.0	6.09
10-2-EC-A,B(2)	12.0	3,939,099	6,927,606	5,433,353	5,223,842	68.1	119.7	93.9	90.3	7.22
10-2-EC(1)-A,B	12.0	5,384,143	8,247,664	6,815,904	6,663,828	93.0	142.5	117.8	115.2	8.82
24-1.5-12-S-A,B	12.0	27,977	27,977	27,977	27,977	0.5	0.5	0.5	0.5	1.53
24-2-12-S-A,B	12.0	143,214	143,214	143,214	143,214	2.5	2.5	2.5	2.5	2.11
24-3-12-TX-A,B	12.0	236,154	327,487	281,821	278,096	4.1	5.7	4.9	4.8	3.09
24-2-8-WY-A,B	12.0	133,809	133,809	133,809	133,809	2.3	2.3	2.3	2.3	1.93
24-1.5-8-S-A,B	12.0	13,193	13,193	13,193	13,193	0.2	0.2	0.2	0.2	1.24
24-2-8-S-A,B	12.0	46,772	46,772	46,772	46,772	0.8	0.8	0.8	0.8	1.57
24-3-8-S-A,B	12.0	147,550	147,550	147,550	147,550	2.5	2.5	2.5	2.5	2.17
24-2-8-SB-A,B	12.0	785,058	483,314	634,186	615,979	8.4	13.6	11.0	10.6	5.47

Table 8.4 Normalized Base Plate Rotational Stiffness Data from Previous Research (Phases 1 and 2)

Specimen Pair	Stress Range (ksi)	N _A	N _B	N _{avg}	N _{log}	A _{min}	A _{max}	A _{avg}	A _{log}	$k_{bp}t/(k_{mast}A_o d_o)$
10VALuA,B	12.0	249,446	453,948	351,697	336,505	4.3	7.8	6.0	5.8	2.42
10VALuC,D	6.3	2,072,592	6,856,881	4,464,737	3,769,817	5.1	17.0	11.1	9.3	2.70
10VAL3x1/4A,B	11.6	476,269	696,326	586,298	575,881	7.5	10.9	9.2	9.0	3.13
10VAL3x3/8A,B	12.0	386,253	410,410	398,332	398,148	6.7	7.1	6.9	6.9	2.76
10VAL6x3/8A,B	12.0	242,728	653,392	448,060	398,242	4.2	11.3	7.8	6.9	2.08
10TXuA,B	6.1	2,199,343	2,816,706	2,508,025	2,488,956	5.0	6.4	5.7	5.7	3.68
10TXuC,D	12.0	177,596	194,694	186,145	185,949	3.1	3.4	3.2	3.2	2.78
10TXuE,F	11.8	320,915	141,155	231,035	212,835	2.3	5.3	3.8	3.5	2.63
10TX3x1/4A,B	12.1	616,136	416,146	516,141	506,362	7.4	11.0	9.2	9.0	3.13
10TX3x3/8A,B	12.0	473,735	657,716	565,726	558,196	8.3	11.5	9.9	9.7	3.94
10TX6x3/8A,B	11.9	783,857	783,857	783,857	783,857	13.2	13.2	13.2	13.2	3.76
VALNuA,B	11.9	389,428	265,540	327,484	321,572	4.5	6.6	5.6	5.5	2.67
VALNuGA,B	11.6	183,132	151,679	167,406	166,665	2.4	2.9	2.6	2.6	2.65
VALNuPRA,B	11.6	4,557,126	4,557,126	4,557,126	4,557,126	72.0	72.0	72.0	72.0	2.94
VALN6x3/8@45C,D	6.4	6,066,817	6,066,817	6,066,817	6,066,817	15.7	15.7	15.7	15.7	3.23
VALNCoIA,B	11.9	4,245,460	2,363,152	3,304,306	3,167,439	39.8	71.5	55.7	53.4	3.64
VALNu2A,B	11.9	5,144,528	1,683,127	3,413,828	2,942,600	28.3	86.5	57.4	49.5	4.97
VALNICA,B	14.1	227,030	227,030	227,030	227,030	6.3	6.3	6.3	6.3	3.40
VALN6x3/8@45A,B	18.0	238,515	161,843	200,179	196,474	9.5	13.9	11.7	11.5	4.48
VALNURA(#4),B(#1)	12.1	1,776,724	950,670	1,363,697	1,299,645	16.9	31.6	24.3	23.1	7.39
VALNWA,B	17.6	422,400	422,400	422,400	422,400	23.2	23.2	23.2	23.2	3.44

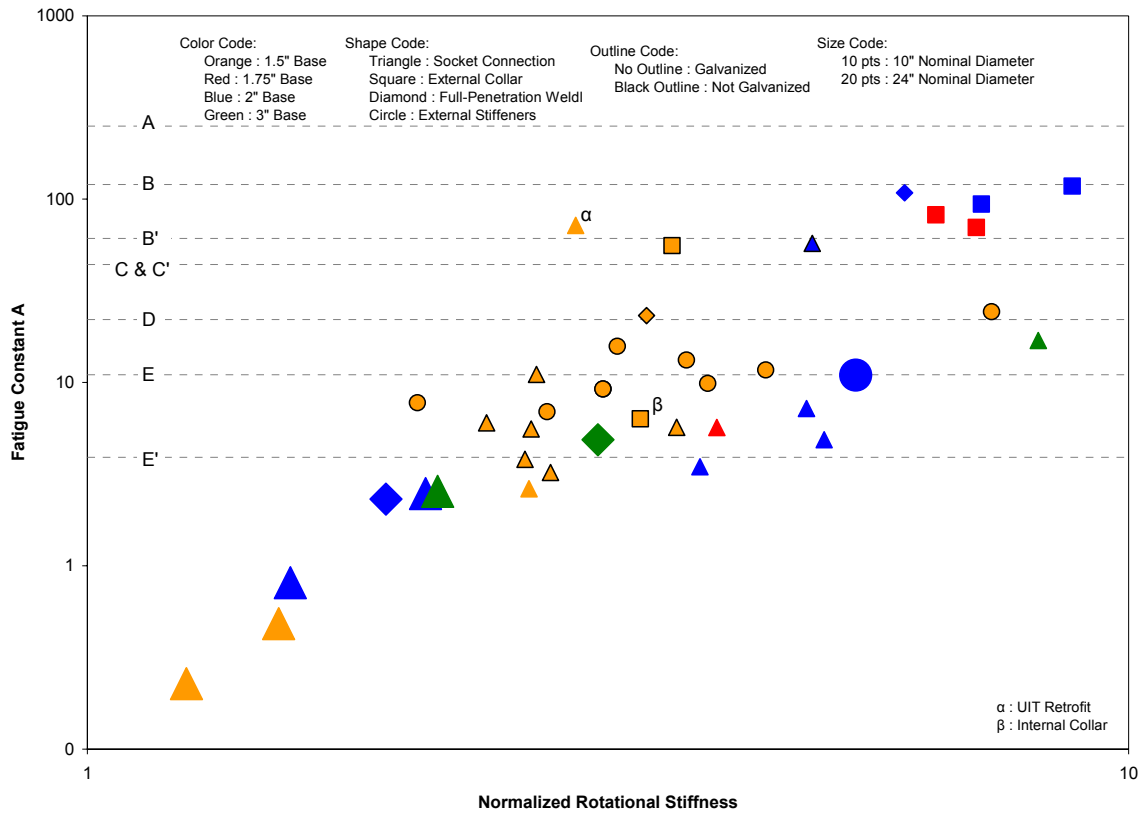


Figure 8.4 Normalized Base Plate Rotational Stiffness Including Concurrent High-Mast Research and Previous Research

CHAPTER 9

Conclusions and Recommended Research

9.1 CONCLUSIONS

Based on the results of the fatigue tests performed during this testing program, the following conclusions can be made:

- The test results indicate that the thickness of the base plate has an influence on the fatigue performance of traffic signal mast-arm base plate to pole wall connections. This base plate thickness effect was observed in both the standard socketed connection specimens as well as the external collar connection specimens. The effect that varying the base plate thickness has on the fatigue performance is not represented in the current specifications, as the base plate thickness is not included as a design variable in the fatigue provisions.
- No appreciable difference in the fatigue performance was observed when comparing the California weld profile socketed connection specimens to the standard socketed connection specimens. The only difference between the two sets of specimens was the specified geometry of the base plate to pole wall fillet welds

- The fatigue performance of standard socketed connections could be improved by smoothing the weld profile by grinding as was seen in the two run-out specimens. Even though this was not an intentional inclusion in this testing program, the performance of these two specimens confirms that smooth weld profiles improve the fatigue performance of fillet welded socketed connections. Caution, however, must be taken when smoothing welds as part of the mast-arm section could be removed, decreasing the section properties.
- The fatigue performance of the full-penetration welded connection specimens was significantly better than the standard socketed connection specimens. The current specifications underestimate the fatigue performance of full-penetration welded base plate to pole wall connections by classifying this detail as either a fatigue stress category E or E' detail, depending on how the backing bar is connected to the base plate. The test results indicate that a classification of fatigue stress category B' is possible with a minimum base plate thickness of 2-in. The increased cost of manufacturing a full-penetration welded connection could be justified considering the improved fatigue performance which was over 20 times that of standard socketed connection.
- The test results indicate that the addition of an external collar to a socketed connection dramatically improves the fatigue performance. Employing the Value Based Design Analysis Method led to a possible classification of the full-penetration welded connection as a fatigue stress category B' detail. This possible classification does not hold true when the external collar is included in the section properties calculation; the stress range

reduces as a result of increased section properties and the full-penetration welded connection drops down to fatigue stress category E', the same category as the standard socketed connection detail. The classification by fatigue stress category is not that important as the observation that under the same in-service loads, traffic signal mast-arms with external collar connection details will have improved fatigue performance than those with standard socketed connection details.

- Even though the decision was made to galvanize all the test specimens in this testing program to ensure a more representative fatigue life evaluation when compared to in-service conditions, the negative effect of galvanizing on fatigue performance remains quite remarkable. This is particularly evident when a comparison is made between two groups of standard socketed connection specimens with 2-in thick base plates. One group was tested by previous researchers at the University of Texas and was not galvanized and one group was tested in this testing program and was galvanized. The group of specimens that was not galvanized performed over 10 times better than the group of specimens that was galvanized under fatigue loading.
- The numerical evaluation presented earlier indicated that a possible relationship exists between base plate rotational stiffness and fatigue performance. The base plate rotational stiffness could be increased by increasing the thickness, increasing the width compared to the pole diameter, adding additional bolts, or changing the bolt location. It is certain that many more options exist for increasing the base plate rotational stiffness.

9.2 RECOMMENDED RESEARCH

In light of the results of the fatigue tests performed during this testing program, the following continued research is recommended:

- Since the diameter was a constant for all the mast-arm specimens tested in this testing program, it is recommended that testing be done on specimens with different diameters. While the test results indicated possible fatigue stress categorization for certain connection details, such as fatigue stress category B' for a full-penetration welded connection with a 2-in base plate, it would be of interest to determine whether or not that same categorization would be valid for a larger diameter mast-arm with both the same connection type and base plate thickness.
- While only round specimens were included in this testing program, it is certain that mast-arm poles of varying cross-sectional shapes are in use throughout the United States. It would be of great value to gather fatigue performance data on commonly used mast-arm poles that are not round to be both better informed and able to make recommendations as to which shapes should be avoided or embraced.
- The test results indicate that both base plate thickness and connection type, among other variables, have a significant effect on the fatigue performance of mast-arms. It is recommended that testing be done on specimens that use a combination of these variables. The resulting specimens could have even greater improved fatigue performance than what was shown in this testing program.

- The improved fatigue performance of the full-penetration welded connection could be as a result of a combination of both the weld and a stiffer base plate due to having a smaller hole in the plate when compared to the standard socketed connection. It is recommended that a study be done that investigates the effect of relative base plate hole size on fatigue performance of full-penetration welded connections.
- In light of the findings of the numerical evaluation, it is recommended that testing be done on specimens with both relatively wider base plates and varying bolt numbers and locations. The results of such a study would provide a clearer understanding of what affects the fatigue performance of base plate to pole wall connections.
- Since galvanizing is shown to significantly impede the fatigue performance of welded connections, it is recommended that a study be undertaken to determine the cause.

APPENDIX A

Mast-Arm Deflection Calculation Example

List of symbols used in the mast-arm deflection calculation example and the definitions:

ℓ_{total}	total length (in)
$d_o(\ell=t_{bp})$	measured outside diameter at the base plate to pole wall connection (in)
t	measured pole wall thickness (in)
taper	specimen taper (in/ft)
t_{bp}	measured base plate thickness (in)
t_{ep}	end plate thickness (in)
ℓ_{mast}	length of pole wall section (in)
$\ell_{support}$	measured distance from the outside edge of the end plate to the support pin (in)
s	segment length = $\ell_{mast}/100$ (in)
E	modulus of elasticity (ksi)
P_{max}	maximum load applied to specimen pair (kips)
P_{min}	minimum load applied to specimen pair (kips)
P	support reaction = $[P_{max} + P_{min}]/2$ (kips)
x_j	distance from support reaction to center of segment = $\ell_{support} + [\text{segment number} \cdot s] - [s/2]$ (in)
amp	testing amplitude (in)
Δ_{test}	total test deflection = $2 \cdot \text{amp}$ (in)
$d_o(\ell=x_j)$	outside diameter at $x_j = d_o(\ell=t_{bp}) - [(\ell_{mast} + \ell_{support} - x_j) \cdot (\text{taper}/12)]$ (in)
$d_i(\ell=x_j)$	inside diameter at $x_j = d_o(\ell=x_j) - 2t$ (in)
I_j	moment of inertia at $x_j = [\pi/64] \cdot [(d_o(\ell=x_j))^4 - (d_i(\ell=x_j))^4]$ (in ⁴)
M_j	moment at $x_j = P \cdot x_j$ (kip-in)
Δ_{mast}	mast-arm pole deflection = $[s/E] \cdot \sum M_j x_j / I_j$ (in)
k_{mast}	mast-arm pole stiffness = P/Δ_{mast} (kip/in)
k_{bp}	base plate rotational stiffness = $[P \cdot (\ell_{mast} + \ell_{support}) \cdot \ell_{mast}]/[\Delta_{test} - \Delta_{mast}]$ (kip-in)
Δ_{bp}	deflection due to base plate rotation = $[P \cdot (\ell_{mast} + \ell_{support}) \cdot \ell_{mast}]/k_{bp}$ (in)
A_o	area enclosed by mast-arm pole at base plate connection = $[\pi/4] \cdot (d_o(\ell=t_{bp}))^2$ (in ²)

Specimen Pair

10-2-S-A,B

Specimen Measurements

ℓ_{total}	86.75	in	$\Sigma M_j x_j / I_j$	8057.0	ksi
$d_o(\ell=t_{bp})$	9.9375	in	Δ_{mast}	0.2334	in
t	0.183	in	k_{mast}	7.78	kip/in
taper	0.14	in/ft	k_{sys}	5.35	kip/in
t_{bp}	2	in	k_{bp}	126864	kip-in
t_{ep}	0.75	in	Δ_{bp}	0.1060	in
ℓ_{mast}	84	in			
$\ell_{support}$	4.25	in			
s	0.84	in	A_o	77.56	in ²
check	87.83	in	k_{bp}/k_{mast}	16317	in ²
E	29000	ksi	$k_{bp}/(k_{mast}A_o)$	210	in ² /in ²
P_{max}	8.467	kip	$k_{bp}t/(k_{mast}A_o d_o)$	3.87	in ³ /in ³
P_{min}	4.838	kip			
P	1.8145	kip			
amp	0.1697	in			
Δ_{test}	0.3394	in			

segment	x_j	$d_o(\ell=x_j)$	$d_i(\ell=x_j)$	I_j	M_j	$M_j x_j / I_j$
1	4.67	8.962	8.596	48.7	8.5	0.8
2	5.51	8.972	8.606	48.8	10.0	1.1
3	6.35	8.982	8.616	49.0	11.5	1.5
4	7.19	8.992	8.626	49.1	13.0	1.9
5	8.03	9.002	8.636	49.3	14.6	2.4
6	8.87	9.011	8.645	49.5	16.1	2.9
7	9.71	9.021	8.655	49.6	17.6	3.4
8	10.55	9.031	8.665	49.8	19.1	4.1
9	11.39	9.041	8.675	50.0	20.7	4.7
10	12.23	9.051	8.685	50.1	22.2	5.4
11	13.07	9.060	8.694	50.3	23.7	6.2
12	13.91	9.070	8.704	50.5	25.2	7.0
13	14.75	9.080	8.714	50.6	26.8	7.8
14	15.59	9.090	8.724	50.8	28.3	8.7
15	16.43	9.100	8.734	51.0	29.8	9.6
16	17.27	9.109	8.743	51.1	31.3	10.6
17	18.11	9.119	8.753	51.3	32.9	11.6
18	18.95	9.129	8.763	51.5	34.4	12.7
19	19.79	9.139	8.773	51.6	35.9	13.8
20	20.63	9.149	8.783	51.8	37.4	14.9
21	21.47	9.158	8.792	52.0	39.0	16.1

22	22.31	9.168	8.802	52.2	40.5	17.3
23	23.15	9.178	8.812	52.3	42.0	18.6
24	23.99	9.188	8.822	52.5	43.5	19.9
25	24.83	9.198	8.832	52.7	45.1	21.2
26	25.67	9.207	8.841	52.8	46.6	22.6
27	26.51	9.217	8.851	53.0	48.1	24.1
28	27.35	9.227	8.861	53.2	49.6	25.5
29	28.19	9.237	8.871	53.4	51.2	27.0
30	29.03	9.247	8.881	53.5	52.7	28.6
31	29.87	9.256	8.890	53.7	54.2	30.1
32	30.71	9.266	8.900	53.9	55.7	31.8
33	31.55	9.276	8.910	54.1	57.2	33.4
34	32.39	9.286	8.920	54.2	58.8	35.1
35	33.23	9.296	8.930	54.4	60.3	36.8
36	34.07	9.305	8.939	54.6	61.8	38.6
37	34.91	9.315	8.949	54.8	63.3	40.4
38	35.75	9.325	8.959	54.9	64.9	42.2
39	36.59	9.335	8.969	55.1	66.4	44.1
40	37.43	9.345	8.979	55.3	67.9	46.0
41	38.27	9.354	8.988	55.5	69.4	47.9
42	39.11	9.364	8.998	55.6	71.0	49.9
43	39.95	9.374	9.008	55.8	72.5	51.9
44	40.79	9.384	9.018	56.0	74.0	53.9
45	41.63	9.394	9.028	56.2	75.5	56.0
46	42.47	9.403	9.037	56.4	77.1	58.1
47	43.31	9.413	9.047	56.5	78.6	60.2
48	44.15	9.423	9.057	56.7	80.1	62.4
49	44.99	9.433	9.067	56.9	81.6	64.6
50	45.83	9.443	9.077	57.1	83.2	66.8
51	46.67	9.452	9.086	57.3	84.7	69.0
52	47.51	9.462	9.096	57.4	86.2	71.3
53	48.35	9.472	9.106	57.6	87.7	73.6
54	49.19	9.482	9.116	57.8	89.3	76.0
55	50.03	9.492	9.126	58.0	90.8	78.3
56	50.87	9.501	9.135	58.2	92.3	80.7
57	51.71	9.511	9.145	58.4	93.8	83.1
58	52.55	9.521	9.155	58.5	95.4	85.6
59	53.39	9.531	9.165	58.7	96.9	88.1
60	54.23	9.541	9.175	58.9	98.4	90.6
61	55.07	9.550	9.184	59.1	99.9	93.1

62	55.91	9.560	9.194	59.3	101.4	95.7
63	56.75	9.570	9.204	59.5	103.0	98.3
64	57.59	9.580	9.214	59.7	104.5	100.9
65	58.43	9.590	9.224	59.8	106.0	103.5
66	59.27	9.599	9.233	60.0	107.5	106.2
67	60.11	9.609	9.243	60.2	109.1	108.9
68	60.95	9.619	9.253	60.4	110.6	111.6
69	61.79	9.629	9.263	60.6	112.1	114.3
70	62.63	9.639	9.273	60.8	113.6	117.1
71	63.47	9.648	9.282	61.0	115.2	119.9
72	64.31	9.658	9.292	61.2	116.7	122.7
73	65.15	9.668	9.302	61.3	118.2	125.5
74	65.99	9.678	9.312	61.5	119.7	128.4
75	66.83	9.688	9.322	61.7	121.3	131.3
76	67.67	9.697	9.331	61.9	122.8	134.2
77	68.51	9.707	9.341	62.1	124.3	137.1
78	69.35	9.717	9.351	62.3	125.8	140.1
79	70.19	9.727	9.361	62.5	127.4	143.0
80	71.03	9.737	9.371	62.7	128.9	146.0
81	71.87	9.746	9.380	62.9	130.4	149.1
82	72.71	9.756	9.390	63.1	131.9	152.1
83	73.55	9.766	9.400	63.3	133.5	155.1
84	74.39	9.776	9.410	63.5	135.0	158.2
85	75.23	9.786	9.420	63.7	136.5	161.3
86	76.07	9.795	9.429	63.9	138.0	164.4
87	76.91	9.805	9.439	64.0	139.6	167.6
88	77.75	9.815	9.449	64.2	141.1	170.7
89	78.59	9.825	9.459	64.4	142.6	173.9
90	79.43	9.835	9.469	64.6	144.1	177.1
91	80.27	9.844	9.478	64.8	145.6	180.3
92	81.11	9.854	9.488	65.0	147.2	183.6
93	81.95	9.864	9.498	65.2	148.7	186.8
94	82.79	9.874	9.508	65.4	150.2	190.1
95	83.63	9.884	9.518	65.6	151.7	193.4
96	84.47	9.893	9.527	65.8	153.3	196.7
97	85.31	9.903	9.537	66.0	154.8	200.0
98	86.15	9.913	9.547	66.2	156.3	203.4
99	86.99	9.923	9.557	66.4	157.8	206.7
100	87.83	9.933	9.567	66.6	159.4	210.1

APPENDIX B

Measured Dimensions of Test Specimens

Table B.1 General Dimensions – Socketed Connections and Full-Penetration Welded Connections

Specimen	Length (in)	Base Plate Thickness (in)				Pole Wall Thickness (in)				Pole Outside Diameter at Base (in)		
		1	2	3	Avg.	1	2	3	Avg.	1	2	Avg.
10-1.75-S-A	86.75	1.779	1.785	1.769	1.778	0.183	0.186	0.184	0.184	9.969	9.906	9.938
10-1.75-S-B	86.50	1.759	1.780	1.764	1.768	0.181	0.182	0.183	0.182	9.781	9.750	9.766
10-2-S-A	86.75	2.027	2.056	2.027	2.037	0.184	0.184	0.183	0.184	9.938	9.938	9.938
10-2-S-B	86.63	2.023	2.035	2.020	2.026	0.181	0.184	0.184	0.183	9.844	9.844	9.844
10-2-S-A(2)	86.75	2.027	2.025	2.028	2.027	0.179	0.181	0.184	0.181	9.875	9.938	9.906
10-2-S-B(2)	86.75	2.034	2.040	2.032	2.035	0.184	0.148	0.182	0.171	9.938	9.906	9.922
10-3-S-A	86.75	3.040	3.039	3.063	3.047	0.183	0.185	0.181	0.183	9.875	9.938	9.906
10-3-S-B	86.69	3.030	3.014	3.025	3.023	0.183	0.181	0.181	0.182	9.719	9.688	9.703
10-2-CA-A	86.75	2.012	2.024	2.028	2.021	0.185	0.184	0.180	0.183	9.906	9.906	9.906
10-2-CA-B	86.75	2.030	2.032	2.023	2.028	0.180	0.178	0.183	0.180	9.875	9.969	9.922
10-2-WY-A	86.75	2.000	2.018	2.003	2.007	0.183	0.185	0.191	0.186	9.969	10.000	9.984
10-2-WY-B	86.63	1.990	2.016	2.030	2.012	0.185	0.183	0.188	0.185	9.969	10.031	10.000

Table B.1 General Dimensions – Socketed Connections and Full-Penetration Welded Connections (Continued)

Specimen	Weld Dimension on Pole Wall (in)				Weld Dimension on Base Plate (in)				Weld Throat Dimension (in)			
	1	2	3	Avg.	1	2	3	Avg.	1	2	3	Avg.
10-1.75-S-A	0.438	0.438	0.438	0.438	0.219	0.313	0.313	0.281	-	-	-	-
10-1.75-S-B	0.375	0.375	0.375	0.375	0.313	0.313	0.313	0.313	-	-	-	-
10-2-S-A	0.438	0.438	0.406	0.427	0.313	0.219	0.281	0.271	-	-	-	-
10-2-S-B	0.375	0.375	0.375	0.375	0.312	0.312	0.250	0.291	-	-	-	-
10-2-S-A(2)	0.375	0.375	0.375	0.375	0.250	0.250	0.250	0.250	-	-	-	-
10-2-S-B(2)	0.438	0.438	0.438	0.438	0.281	0.250	0.250	0.260	-	-	-	-
10-3-S-A	0.500	0.500	0.500	0.500	0.313	0.281	0.250	0.281	-	-	-	-
10-3-S-B	0.375	0.375	0.375	0.375	0.219	0.250	0.188	0.219	-	-	-	-
10-2-CA-A	0.438	0.500	0.500	0.479	0.375	0.375	0.344	0.365	0.250	0.250	0.313	0.271
10-2-CA-B	0.500	0.438	0.563	0.500	0.344	0.313	0.344	0.333	0.313	0.250	0.250	0.271
10-2-WY-A	0.625	0.688	0.688	0.667	0.250	0.250	0.250	0.250	-	-	-	-
10-2-WY-B	0.625	0.625	0.688	0.646	0.250	0.250	0.281	0.260	-	-	-	-

Table B.2 General Dimensions – External Collar Connections

Specimen	Length (in)	Base Plate Thickness (in)				Pole Wall Thickness (in)			
		1	2	3	Avg.	1	2	3	Avg.
10-1.75-EC(1)-A	86.69	1.785	1.776	1.757	1.773	0.181	0.183	0.185	0.183
10-1.75-EC(1)-B	86.56	1.775	1.779	1.773	1.776	0.183	0.181	0.184	0.183
10-1.75-EC-A(2)	86.69	1.762	1.760	1.761	1.761	0.183	0.183	0.183	0.183
10-1.75-EC-B(2)	86.75	1.767	1.769	1.767	1.768	0.183	0.181	0.182	0.182
10-2-EC(1)-A	86.69	2.032	2.036	2.027	2.032	0.184	0.183	0.183	0.183
10-2-EC(1)-B	86.69	2.025	2.024	2.035	2.028	0.183	0.179	0.180	0.181
10-2-EC-A(2)	86.63	2.014	2.021	2.015	2.017	0.186	0.185	0.187	0.186
10-2-EC-B(2)	86.63	2.018	2.021	2.018	2.019	0.183	0.181	0.186	0.183

120

Table B.2 General Dimensions – External Collar Connections (*Continued*)

Specimen	Collar Thickness (in)				Pole Inside Diameter at Base (in)		
	1	2	3	Avg.	1	2	Avg.
10-1.75-EC(1)-A	0.254	0.256	0.257	0.256	9.625	9.625	9.625
10-1.75-EC(1)-B	0.254	0.254	0.252	0.253	9.594	9.625	9.609
10-1.75-EC-A(2)	0.256	0.254	0.257	0.256	9.594	9.563	9.578
10-1.75-EC-B(2)	0.246	0.246	0.246	0.246	9.563	9.625	9.594
10-2-EC(1)-A	0.249	0.252	0.250	0.250	9.625	9.625	9.625
10-2-EC(1)-B	0.252	0.249	0.253	0.251	9.563	9.625	9.594
10-2-EC-A(2)	0.249	0.247	0.251	0.249	9.625	9.625	9.625
10-2-EC-B(2)	0.249	0.258	0.257	0.255	9.563	9.625	9.594

Table B.2 General Dimensions – External Collar Connections (Continued)

Specimen	Weld Dimension at Base Plate (in)							
	On Pole Wall				On Base Plate			
	1	2	3	Avg.	1	2	3	Avg.
10-1.75-EC(1)-A	0.750	0.688	0.688	0.708	0.313	0.313	0.313	0.313
10-1.75-EC(1)-B	0.625	0.625	0.625	0.625	0.281	0.281	0.313	0.292
10-1.75-EC-A(2)	0.750	0.750	0.688	0.729	0.344	0.438	0.375	0.385
10-1.75-EC-B(2)	0.688	0.750	0.750	0.729	0.281	0.406	0.375	0.354
10-2-EC(1)-A	0.563	0.563	0.500	0.542	0.250	0.344	0.313	0.302
10-2-EC(1)-B	0.625	0.625	0.625	0.625	0.344	0.313	0.344	0.333
10-2-EC-A(2)	0.688	0.688	0.625	0.667	0.531	0.500	0.469	0.500
10-2-EC-B(2)	0.875	0.750	0.750	0.792	0.406	0.313	0.344	0.354

Table B.2 General Dimensions – External Collar Connections (Continued)

Specimen	Weld Dimension at Top of Collar (in)							
	On Pole Wall				On Collar			
	1	2	3	Avg.	1	2	3	Avg.
10-1.75-EC(1)-A	0.625	0.563	0.500	0.563	0.219	0.281	0.219	0.240
10-1.75-EC(1)-B	0.500	0.500	0.438	0.479	0.250	0.250	0.250	0.250
10-1.75-EC-A(2)	0.500	0.531	0.500	0.510	0.219	0.250	0.219	0.229
10-1.75-EC-B(2)	0.500	0.594	0.406	0.500	0.219	0.156	0.250	0.208
10-2-EC(1)-A	0.625	0.563	0.563	0.583	0.250	0.250	0.188	0.229
10-2-EC(1)-B	0.500	0.500	0.500	0.500	0.219	0.219	0.281	0.240
10-2-EC-A(2)	0.563	0.563	0.563	0.563	0.188	0.188	0.219	0.198
10-2-EC-B(2)	0.625	0.625	0.563	0.604	0.188	0.188	0.188	0.188

Table B.2 General Dimensions – External Collar Connections (Continued)

Specimen	Collar Maximum Dimension (in)			Collar Minimum Dimension (in)		
	1	2	Avg.	1	2	Avg.
10-1.75-EC(1)-A	5.250	5.125	5.188	3.160	3.050	3.105
10-1.75-EC(1)-B	5.188	5.125	5.156	3.188	3.125	3.156
10-1.75-EC-A(2)	5.125	5.063	5.094	3.125	3.125	3.125
10-1.75-EC-B(2)	5.000	5.250	5.125	3.250	3.250	3.250
10-2-EC(1)-A	5.125	5.250	5.188	3.250	3.188	3.219
10-2-EC(1)-B	5.125	5.125	5.125	3.250	3.125	3.188
10-2-EC-A(2)	5.125	5.125	5.125	3.250	3.125	3.188
10-2-EC-B(2)	5.125	5.125	5.125	3.125	3.188	3.156

REFERENCES

1. American Association of State Highway and Transportation Officials, Standard Specifications for Structural Supports for Highway Signs, Luminaires and Traffic Signals. Fourth Edition. Washington, D.C.: AASHTO, 2001.
2. American Association of State Highway and Transportation Officials, Standard Specifications for Structural Supports for Highway Signs, Luminaires and Traffic Signals. Interim Edition. Washington, D.C.: AASHTO, 2006.
3. Albert, Matthew N. “Field Testing of Cantilevered Traffic Signal Structures under Truck-Induced Gust Loads.” M.S. Thesis, Department of Civil Engineering, The University of Texas at Austin, May 2006.
4. ASTM Specification A370 “Standard Test Methods and Definitions for Mechanical Testing of Steel Products.”
5. ASTM Specification A595 “Standard Specification for Steel Tubes, Low-Carbon or High-Strength Low-Alloy, Tapered for Structural Use.”
6. Blodgett, Omer W. Design of Welded Structures. Cleveland, OH: The James F. Lincoln Arc Welding Foundation, June 1966.
7. Dexter, R. J., and Ricker, M. J. NCHRP Report 469: Fatigue-Resistant Design of Cantilevered Signal, Sign, and Light Supports. Washington, D.C.: Transportation Research Board – National Research Council, 2002.
8. Duraisamy, Ramadevi. “Finite Element Study of Mast-Arm Socket Welded Connections.” M.S. Thesis, Department of Civil Engineering, The University of Texas at Austin, December 2005.
9. Kaczinski, M. R., Dexter, R. J., and Van Dien, J. P. NCHRP Report 412: Fatigue-Resistant Design of Cantilevered Signal, Sign and Light Supports. Washington, D.C.: Transportation Research Board – National Research Council, 1998.
10. Koenigs, Mark T. “Fatigue Resistance of Traffic Signal Mast-Arm Connection Details.” M.S. Thesis, Department of Civil Engineering, The University of Texas at Austin, May 2003.
11. Koenigs, Mark T., Botros, Tamer A., Freytag, Dylan, and Frank, Karl H. Fatigue Strength of Signal Mast-Arm Connections. Research Report 4178-2. Center for Transportation Research, Bureau of Engineering Research, The University of Texas at Austin, August 2003.

12. nyc.gov. "City Lights Design Competition." 5 January 2004. <<http://www.nyc.gov/html/ddc/home.html>>. Path: Design; 2004 City Lights; Competition; Brief Written History.
13. South, Jeffrey M. Fatigue Analysis of Overhead Sign and Signal Structures. Physical Research Report No. 115. Illinois Department of Transportation, Bureau of Materials and Physical Research, May 1994.
14. Union Metal: Poles for a Safer America. Union Metal Corporation. 4 June 2007. <<http://www.unionmetal.com/products/trafficcontrol.asp>>.
15. Williams, Barry. "Four-way Traffic Signals Save Money, Preserve Historic Atmosphere." American City & County. March 1995: 49.

VITA

Thomas Henry Anderson was born in Bloemfontein, South Africa on February 8, 1983, to Hendrik Johannes Anderson and Marlene Louise Anderson. After completing his work at Guymon High School, Guymon, Oklahoma in 2001, he enrolled at Oklahoma State University in Stillwater, Oklahoma. He received a Bachelor of Science in Civil Engineering from Oklahoma State University in May of 2005, and graduated *summa cum laud*. He enrolled in the graduate program at The University of Texas at Austin in August of 2005.

Permanent Address: 3406-A Tom Green St.
 Austin, TX 78705
 messeji@gmail.com

This thesis was typed by the author.